SGP-TR-167

Inferring Immobile and In-situ Water Saturation from Laboratory and Field Measurements

Rodolfo P. Belen Jr.

June 2000

Financial support was provided through the
Stanford Geothermal Program under
Department of Energy Grant No. DE-FG07-95ID13370
and No. DE-FG07-99ID13763,
and by the Department of Petroleum Engineering,
Stanford University

Abstract

Analysis of experimental data and numerical simulation results of dynamic boiling experiments revealed that there is an apparent correlation between the immobile water saturation and the shape of the steam saturation profile. An elbow in the steam saturation profile indicates the sudden drop in steam saturation that marks the transition from steam to two-phase conditions inside the core during boiling. The immobile water saturation can be inferred from this elbow in the steam saturation profile. Based on experimental results obtained by Satik (1997), the inferred immobile water saturation of Berea sandstone was found to be about 0.25, which is consistent with results of relative permeability experiments reported by Mahiya (1999). However, this technique may not be useful in inferring the immobile water saturation of less permeable geothermal rocks because the elbow in the steam saturation profile is less prominent.

Models of vapor and liquid-dominated geothermal reservoirs that were developed based on Darcy's law and material and energy conservation equations proved to be useful in inferring the in-situ and immobile water saturations from field measurements of cumulative mass production, discharge enthalpy, and downhole temperature. Knowing rock and fluid properties, and the difference between the stable initial, T_o, and dry-out, T_d, downhole temperatures, the in-situ and immobile water saturations of vapor-dominated reservoirs can be estimated. On the other hand, the in-situ and immobile water saturations, and the change in mobile water content of liquid-dominated reservoirs can be inferred from the cumulative mass production, Δm, and enthalpy, h', data. Comparison with two-phase, radial flow, numerical simulation results confirmed the validity and usefulness of these models.

Acknowledgments

This research was conducted with financial support through the Stanford Geothermal Program under the US Department of Energy Grant No. DE-FG07-95ID13370.

To Prof. Roland Horne for his guidance, encouragement, support and great sense of humor.

To Stefan Finsterle and Malou Guerrero for their patience with me in learning TOUGH2 and iTOUGH2.

To Huda Nassori and Kewen Li for their patience with me in the laboratory.

Contents

List of Tables

List of Figures

Chapter 1

1. Introduction

Relative permeability is important in describing the flow of two-phase steam in geothermal reservoirs and in performing geothermal reservoir engineering calculations. Presently, however, relative permeability relations for steam and liquid water are not completely understood. Permeability relations are normally adopted from field data or from nitrogen and water flow experiments.

The experimental determination of steam and liquid water relative permeabilities is a central target of the Stanford Geothermal Program. Flow-through experiments on Berea sandstones were performed by Ambusso (1996), Satik (1998) and Mahiya (1999) using X-ray computer tomography to determine the steam saturation profiles. In a different approach, numerical simulation was used by Guerrero et al. (1998) to infer relative permeabilities of Berea sandstones, based on temperature, pressure, and steam saturation data obtained from dynamic boiling experiments performed by Satik (1997).

All of these earlier studies used Berea sandstone in order to capitalize on its higher permeability relative to geothermal rocks, which enabled the experiments to be performed in reasonable time. This study aimed to extend the understanding to low permeability geothermal rocks by determining only the endpoint saturations of the relative permeability curves. The endpoint or irreducible or immobile saturation of a certain phase is the saturation at which that phase becomes mobile in multiphase flow.

Combining information about the endpoint saturations from the “slow” geothermal rock experiments with information about the general shape of the relative permeability curves from the “faster” sandstone rock experiments could then define the steam-liquid water relative permeability behavior completely.

Furthermore, knowledge of the immobile and in-situ water saturation will provide a better understanding of the adsorption characteristics and fluid storage capacities of geothermal rocks. This will be valuable in estimating the size of the available geothermal resource accurately and in evaluating geothermal reservoir performance.

The objective of this study was to determine the endpoint saturation of the steam and liquid water relative permeability curves by inference from pressure, temperature and saturation data obtained from past dynamic boiling experiments conducted by Satik (1997) using Berea sandstone rocks.

In addition, the study developed models of both vapor and liquid-dominated geothermal reservoirs to allow inference of the in-situ and immobile water saturation from field measurements of cumulative mass production, discharge enthalpy, and downhole temperature.

Chapter 2

2. Inferring Immobile Water Saturation from Laboratory Measurements

This study analyzed results of past dynamic boiling experiments performed by Satik (1997) using Berea sandstone rocks. The intent was to investigate the feasibility of inferring the immobile water saturation from experimental pressure, temperature and saturation data. Using numerical simulation, this study also evaluated the feasibility of extending the technique to geothermal rocks.

2.1. Experimental Design

In 1996 and 1997, Satik performed a series of boiling experiments using Berea sandstone cores. The objective of the study was to further the understanding of the boiling process in porous media and ultimately to obtain capillary functions and relative permeability relations for steam and liquid water. The dynamic boiling experiments involved the heating of a rock saturated with liquid water and observing the boiling process by continuous measurement of pressure, temperature, heat flux and steam saturation within the core. The X-ray CT scanner was used to visualize the boiling process and to determine the three-dimensional fluid distributions within the rock.

These experiments are analogous to drainage experiments in oil and water systems, in which oil, the nonwetting fluid, is injected into a rock saturated with water, the wetting fluid, to displace the water from the rock. However, in the case of the boiling experiments, steam produced by heating the water-saturated rock displaces the liquid water from the rock.

The experimental apparatus consisted of a core holder housing the Berea sandstone core, a data acquisition system, a vacuum pump, a water pump and a balance (Figure 2-1).

The core was insulated with a fiber blanket to minimize heat losses. The heater was attached to the end of the core that was closed to fluid flow. The other end was connected to a water reservoir placed on a balance that was used to monitor the amount of water displaced from the core during the boiling process. Pressure, temperature and heat flux were measured in the core using pressure transducers, thermocouples and heat flux sensors respectively and were recorded automatically in a data acquisition system.

The core was first dried and then vacuumed to remove air inside the pore spaces. The core was then scanned at 1-cm intervals to obtain dry-core CT values to be used in computing the steam saturations. The core was then saturated with deaerated water and then scanned again at the same locations to obtain wet-core CT values. The heater was then turned on and pressure, temperature and heat flux were measured continuously during each heating step until steady-state conditions were reached. Steady state had been reached when no more water flowed out of the core and when pressure, temperature and heat flux measurements had stabilized. At the same time, the core was scanned again to obtain CT values that were used to calculate the steam saturation distribution. The heating rate was increased and the procedure was repeated. Different experiments were performed in which the core was mounted vertically and horizontally.

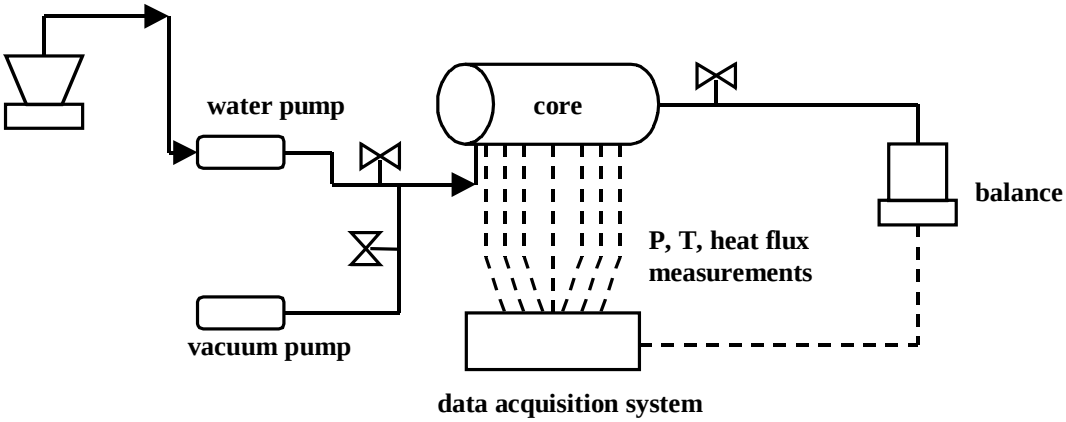

Figure 2-1: Experimental set-up of boiling experiments (Satik 1997).

Properties of the Berea sandstone core used in the boiling experiments are summarized in Table 2-1.

Table 2-1: Properties of Berea sandstone core.

Porosity	22%
Permeability	600 md
Length	43 cm
Diameter	5.04 cm

2.2. Results of Boiling Experiments

In all the boiling experiments, steady-state steam saturation, temperature and pressure profiles indicated a progressive boiling process with the formation of distinct regions of steam, two-phase and liquid water. The profiles at earlier time and lower heat flux have the characteristics of a two-phase region followed by a single-phase liquid zone while at later time and higher heat flux the profiles indicate a two-phase region between single

phase steam and liquid water regions. Figures 2-2 to 2-4 illustrate the steam saturation, temperature and pressure profiles of a vertical boiling experiment performed by Satik (1997) showing the formation of steam, two-phase and liquid regions within the core as the heat flux was increased.

The sudden drop in the steam saturation near the heater end of the core marks the transition from steam to two-phase conditions. This drop is designated in this study as the "elbow" in the steam saturation profile.

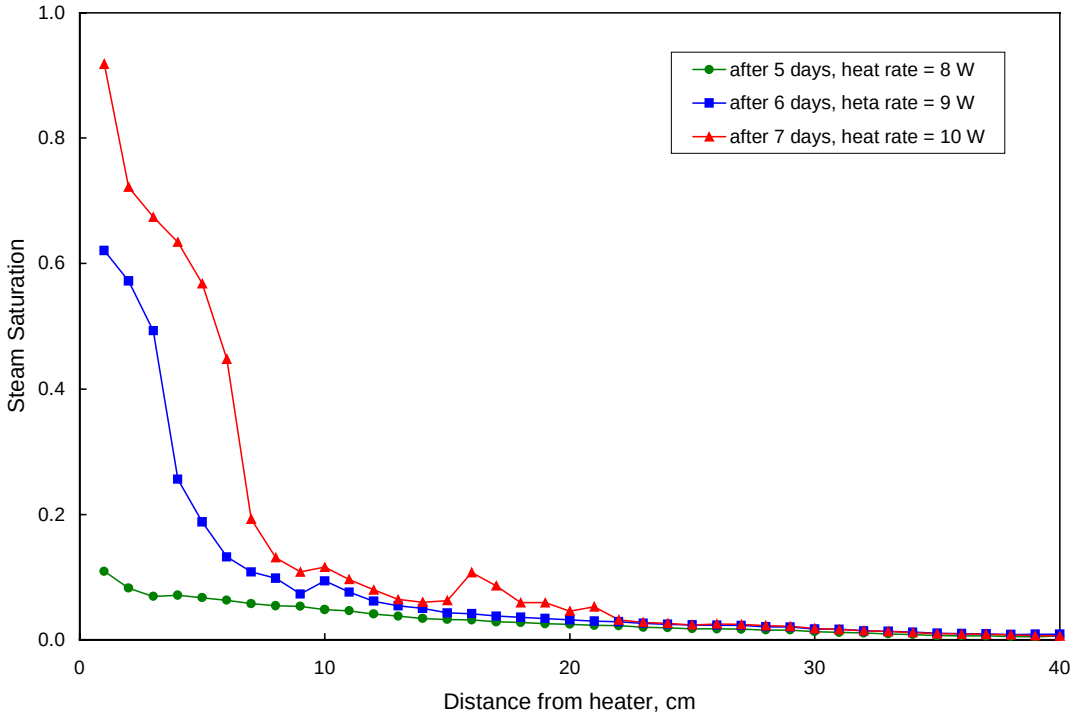

Figure 2-2: Steam saturation profile of vertical boiling experiment (Satik, Spring 1997).

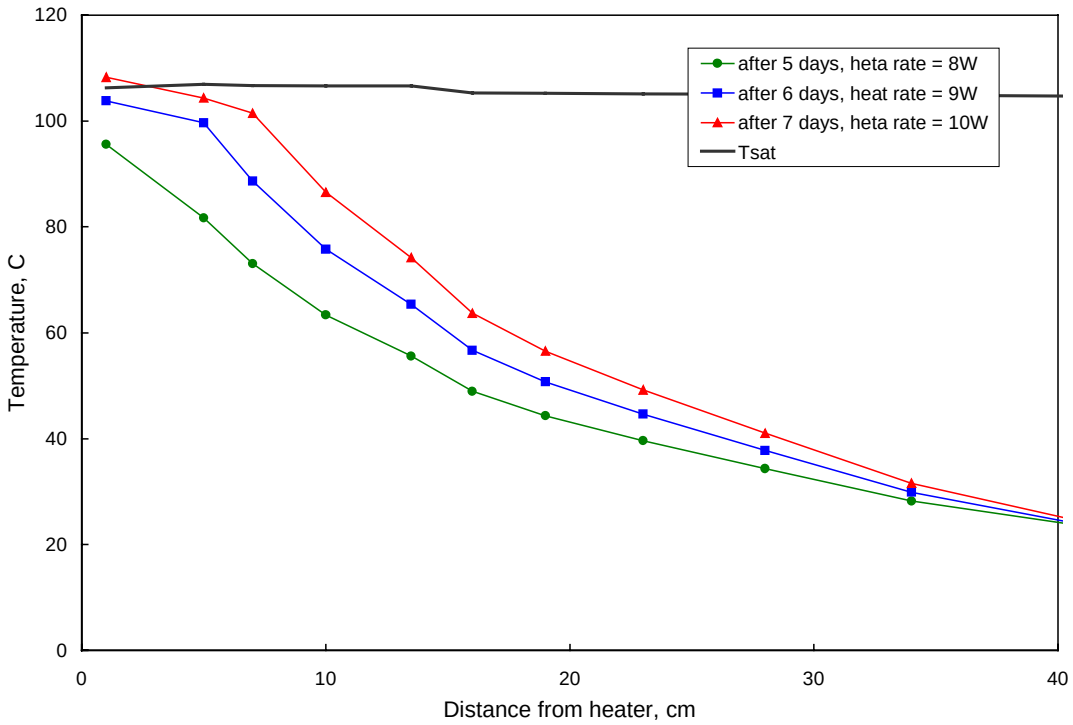

Figure 2-3: Temperature profile of vertical boiling experiment (Satik, Spring 1997).

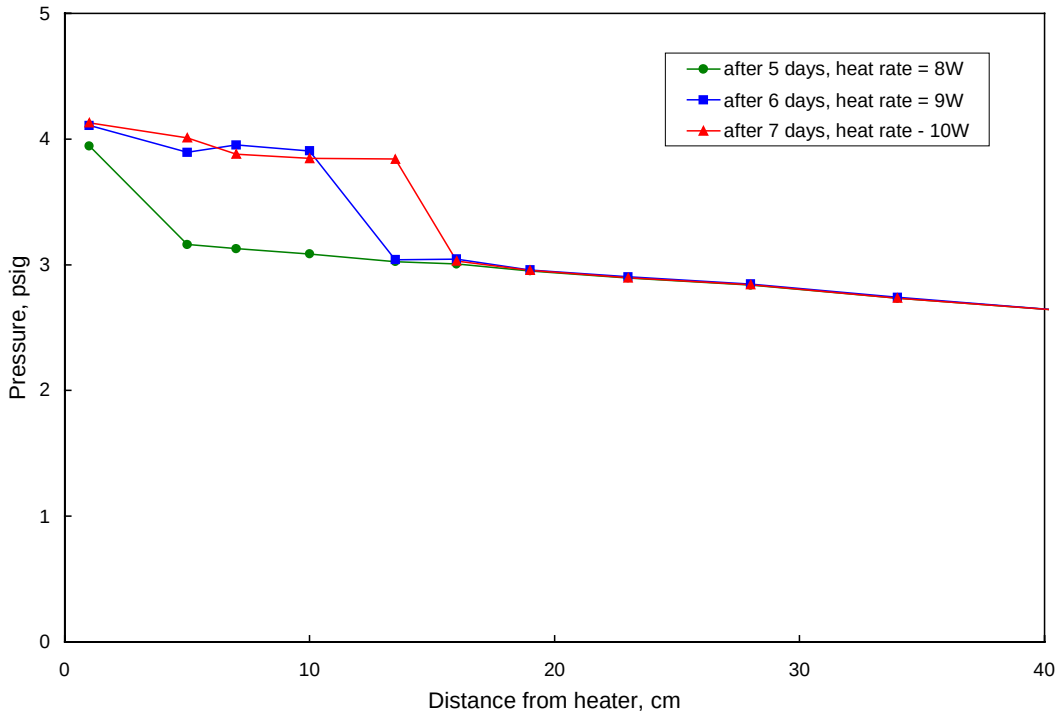

Figure 2-4: Pressure profile of vertical boiling experiment (Satik, Spring 1997).

2.3. Sensitivity Analysis

It was hypothesized that the irreducible water saturation can be correlated with the observed elbow in the steam saturation profile. Analyzing the sensitivity of the boiling process to the irreducible water saturation through numerical modeling was used to test the validity of this hypothesis. The boiling process was simulated using different values of immobile water saturation. The pressure, temperature and saturation profiles were predicted to investigate if the elbow in the saturation profiles could be correlated with the irreducible water saturation.

In 1998, Guerrero et al. developed a two-dimensional radial iTOUGH2 model to infer relative permeability relations from the results of the boiling experiments. The same model was used in the sensitivity analysis but the grids were refined to give a better resolution of the variations in the steam saturation near the heater end of the core. The TOUGH2 and iTOUGH2 input files are included in this report as Appendix A.

Forward calculations in iTOUGH2 were performed to simulate the pressure, temperature, and steam saturation profiles along the core. It was assumed that linear steam-liquid water relative permeability functions (X-curves) and Leverett capillary functions govern the flow of two-phase steam in the sandstone core.

The nonadiabatic boiling process was simulated using constant and variable heating rates. Figure 2-5 shows the simulated steam saturation profiles for the constant heating rate case. The plot corresponds to the profiles after one day of heating the core continuously at a constant rate. As the heating rate was raised, boiling commenced and the steam and two-phase regions formed and expanded.

The boiling process was then simulated using progressively increasing heat rates. Figure 2-6 shows the heat rate as a step function of time. Three different values of immobile water saturation, 0.1, 0.2, and 0.5, were used in the sensitivity analysis. Steam saturation was then plotted at 0.2-cm. intervals and up to a distance 8 cm. away from the heater end. The saturation profiles are shown in Figures 2-7 to 2-9.

The simulation results indicated an apparent correlation between the elbow in the steam saturation profile and the immobile water saturation. In all three cases, the steam region extends to a distance one centimeter from the heater end. An abrupt drop in the steam saturation marks the transition to two-phase conditions, which corresponds to the elbow in the profile. The steam saturation stays close to this value behind the elbow and then goes down further with distance away from the heater end.

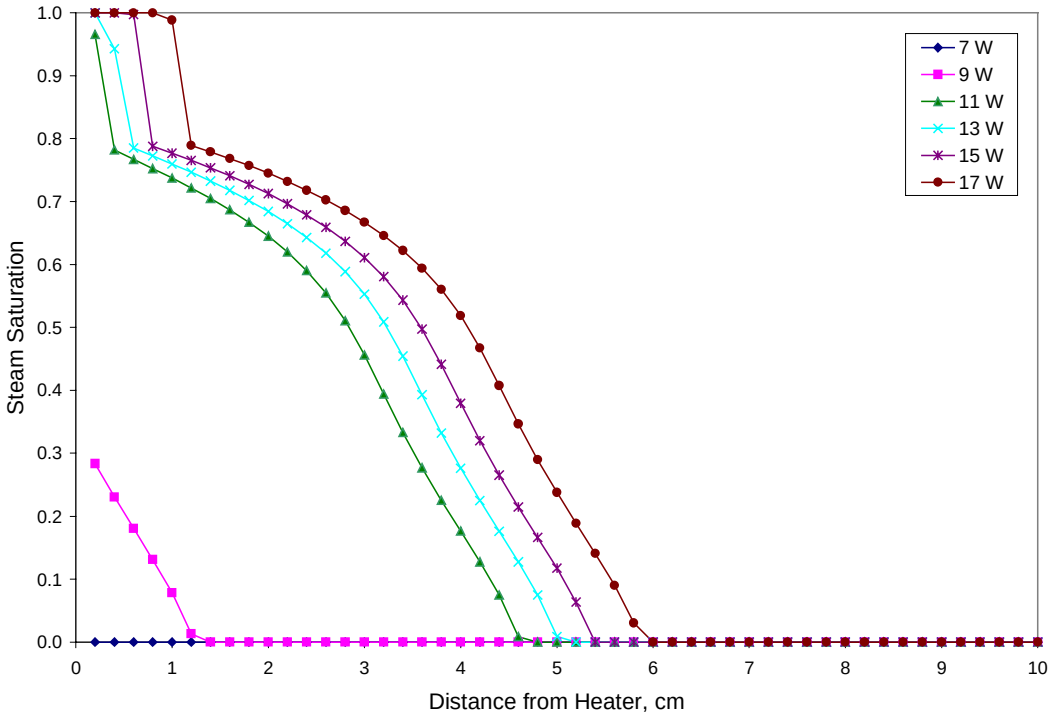

Figure 2-5: Steady state steam saturation profile with distance and constant heating rate: immobile water saturation = 0.2, Berea sandstone rock.

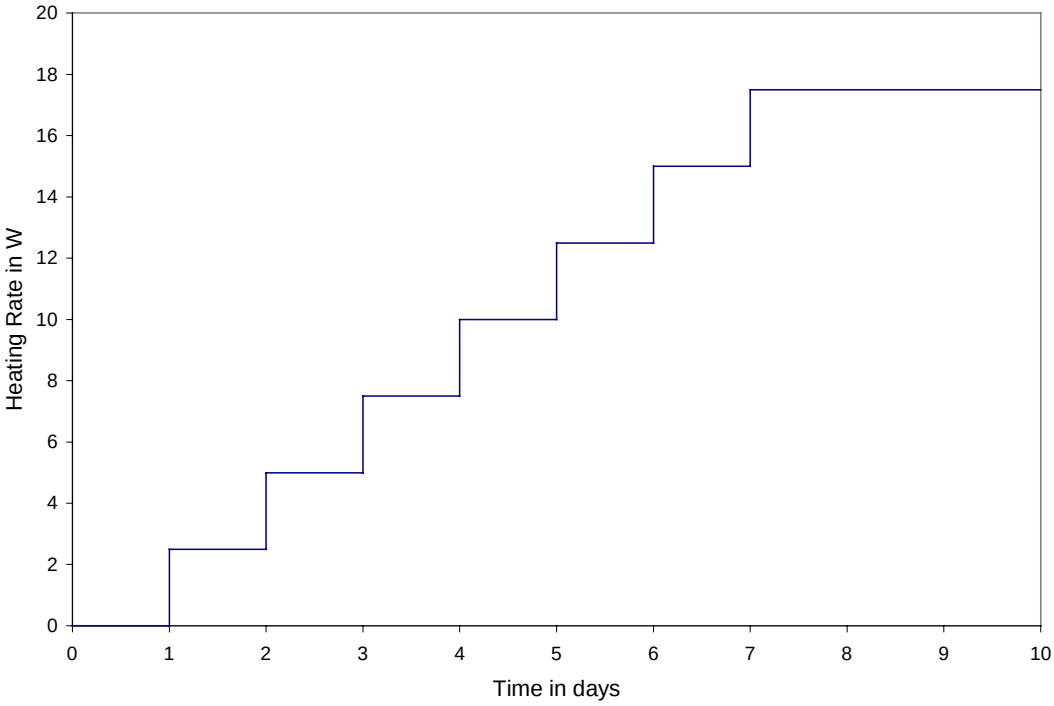

Figure 2-6: Heat rate as a step function of time.

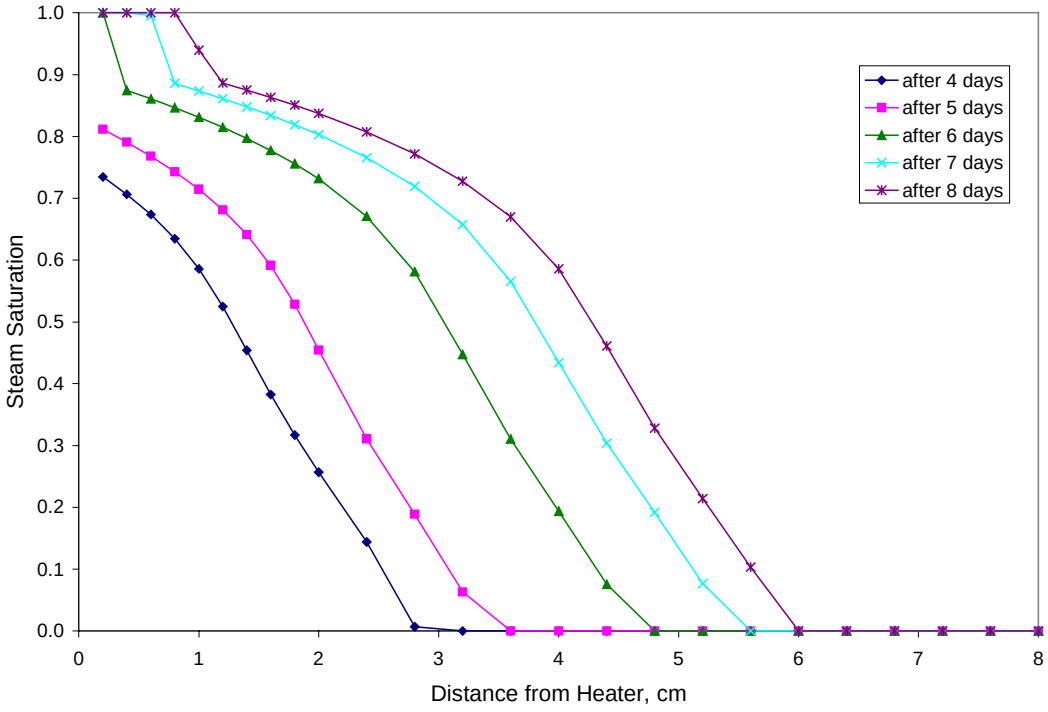

Figure 2-7: Steam saturation profiles with distance and time using variable heating rate: immobile water saturation = 0.1, Berea sandstone rock.

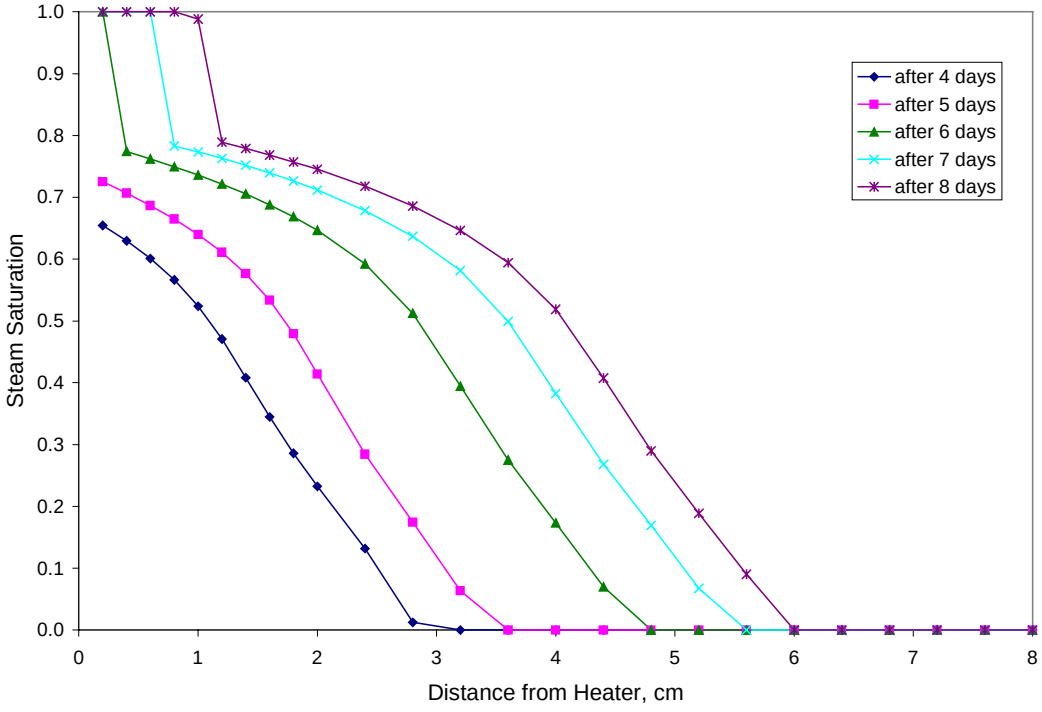

Figure 2-8: Steam saturation profiles with distance and time using variable heating rate: immobile water saturation = 0.2, Berea sandstone rock.

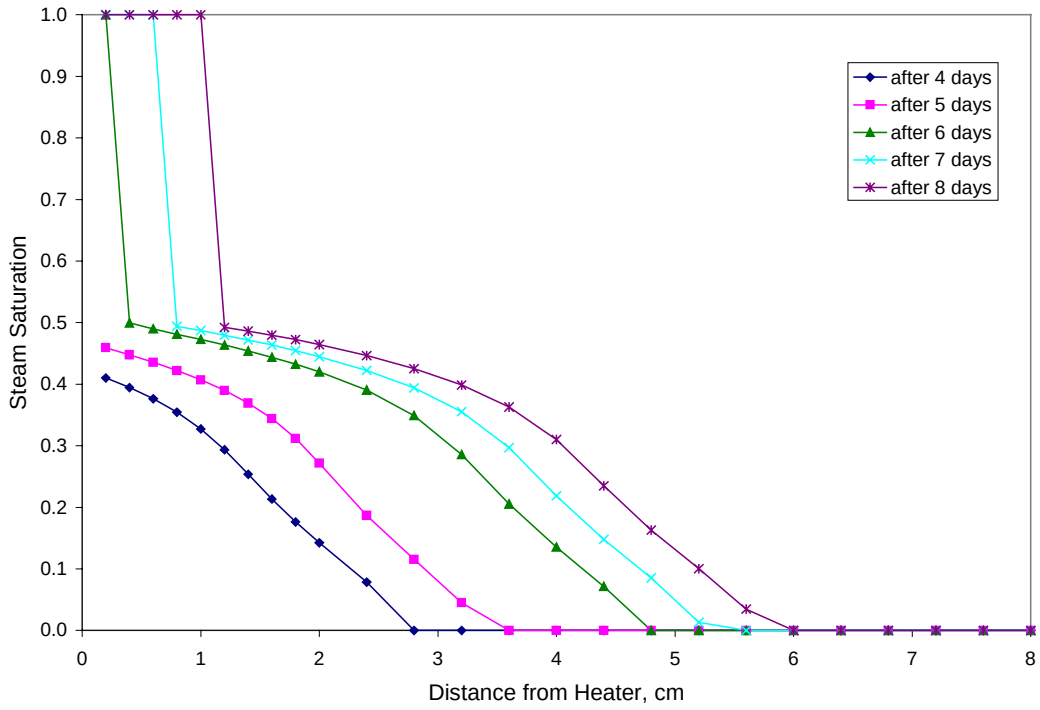

Figure 2-9: Steam saturation profiles with distance and time using variable heating rate: immobile water saturation = 0.5, Berea sandstone rock.

It is important to note that steady-state conditions were reached after about ten days of heating the core. Steady state means that the simulated steam saturation, pressure and temperature profiles remained invariant with time. As a consequence, the simulated steam saturation profiles indicate steam conditions in the region starting from the edge of the core where the heater is attached to a distance one centimeter away. Beyond this region, the simulated steam saturation profiles indicate two-phase and liquid conditions.

2.4. Inferred Immobile Water Saturation in Berea Sandstone

Figures 2-2, and 2-10 to 2-12 show the steam saturation profiles obtained from the boiling experiments that were conducted by Satik in Spring and Summer of 1997. The figures show the steam saturation profile with distance along the core and as a function of the heating rate. It is important to note that steam saturation, pressure and temperature were measured only at 1-cm intervals along the core.

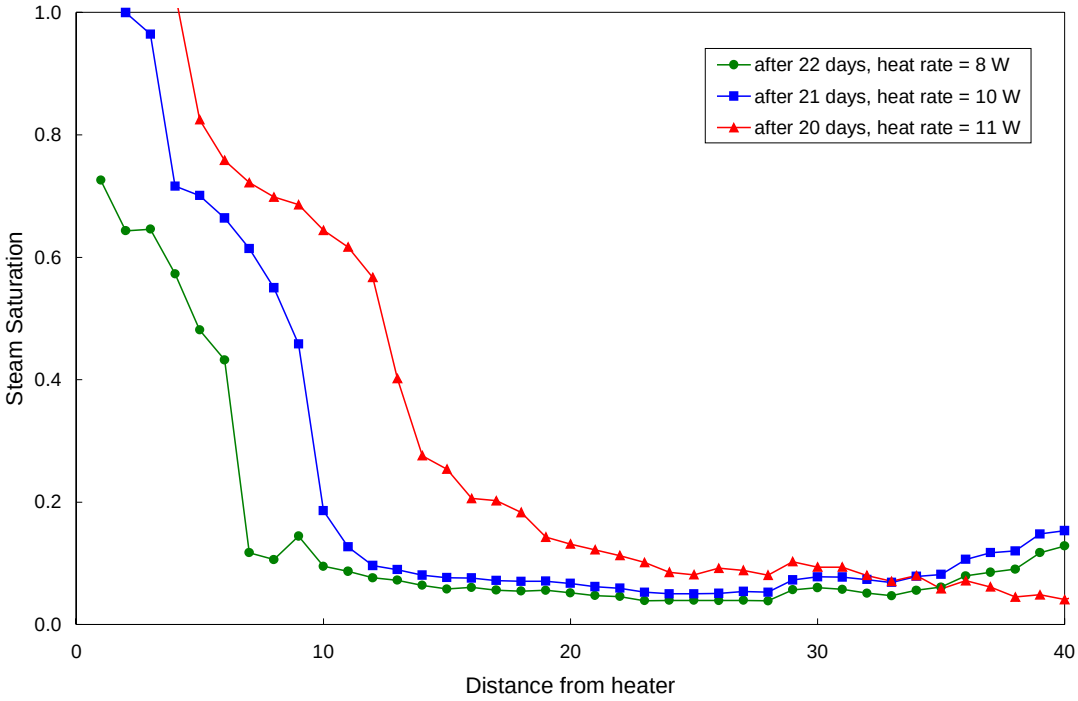

Figure 2-10: Steam saturation profile of vertical boiling experiment (Satik, Spring 1997).

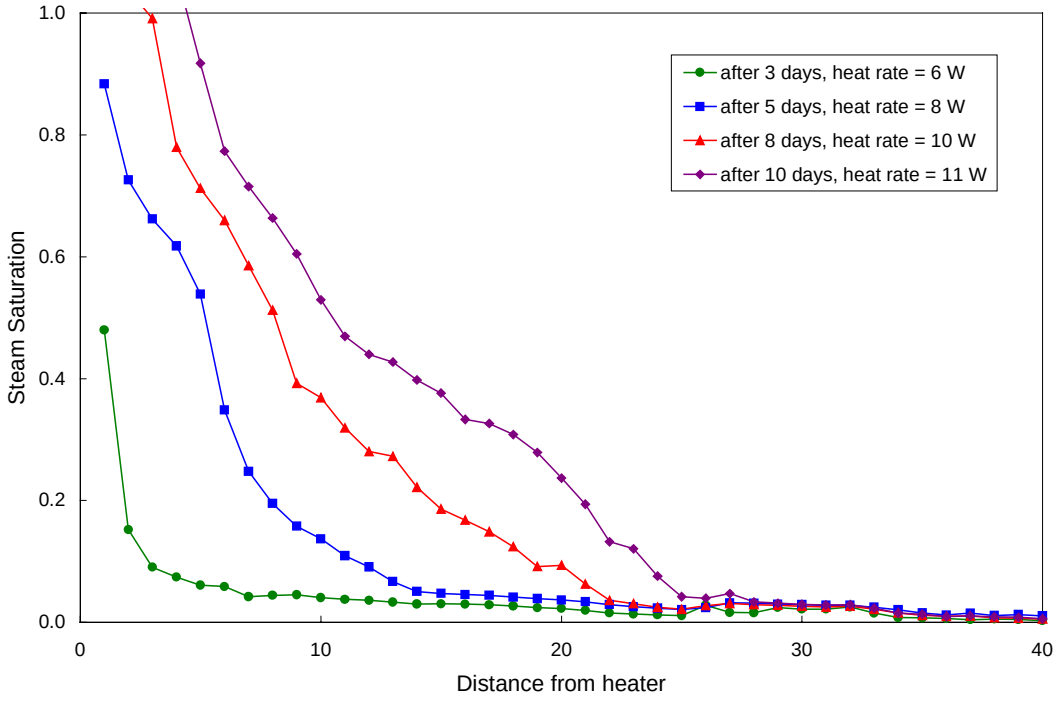

Figure 2-11: Steam saturation profile of horizontal boiling experiment (Satik, Summer 1997).

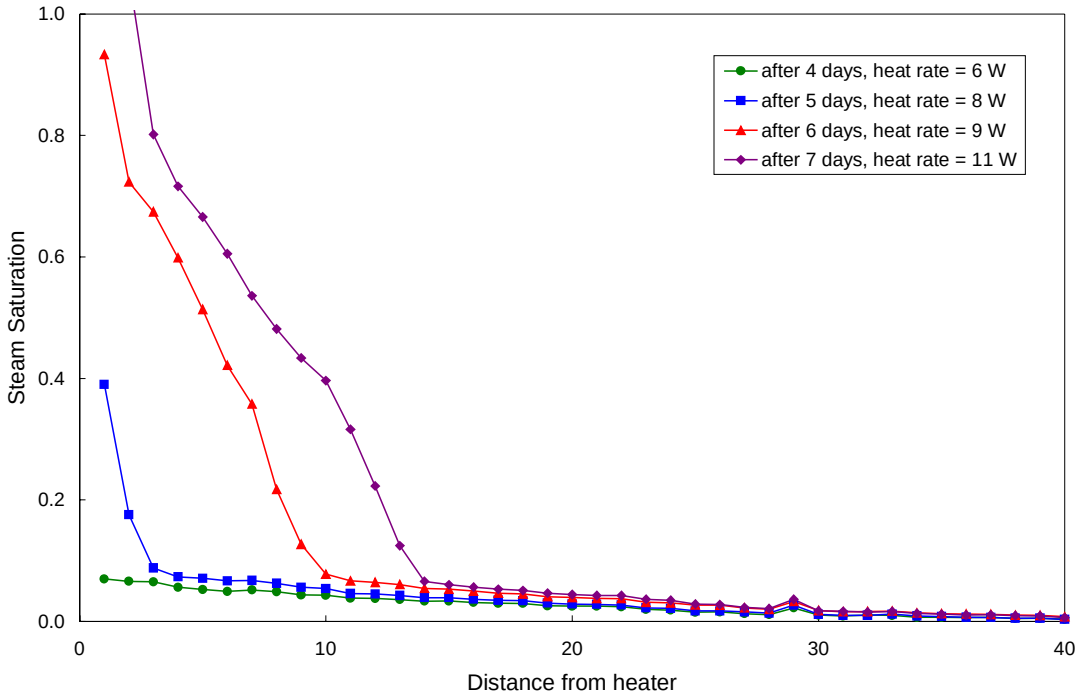

Figure 2-12: Steam saturation profile of top-heating vertical boiling experiment (Satik, Summer 1997).

Based on the location of the elbow in the steam saturation profiles obtained from the actual experimental results, it can be inferred that the irreducible water saturation of Berea sandstone is about 0.25. This value is consistent with the experimental results reported by Mahiya (1999) in relative permeability experiments conducted using similar Berea sandstone cores.

2.5. Modeling Results of Boiling Experiments Using Geysers Geothermal Rocks

Boiling experiments using Geysers geothermal rocks were then simulated to determine the feasibility of this technique in inferring the immobile water saturation of low porosity and low permeability geothermal rocks. The properties of the geothermal rocks used in the simulation runs are tabulated in Table 2-2.

As previously in the Berea sandstone case, the nonadiabatic boiling process was simulated using constant and variable heating rates. An excerpt of the TOUGH2 input file showing the rock properties is included in this report as Appendix B. Figure 2-13 shows the steam saturation profiles with distance and heating rate. The plots correspond to the profiles after one day of heating the core continuously at a constant rate.

Table 2-2: Geysers geothermal rock properties.

Porosity	5%
Permeability	1 x 10^{-13} m^2
Rock density	2600 kg/m^3
Rock specific heat	485 J/kg°C
Rock heat conductivity	2.43 W/m°C

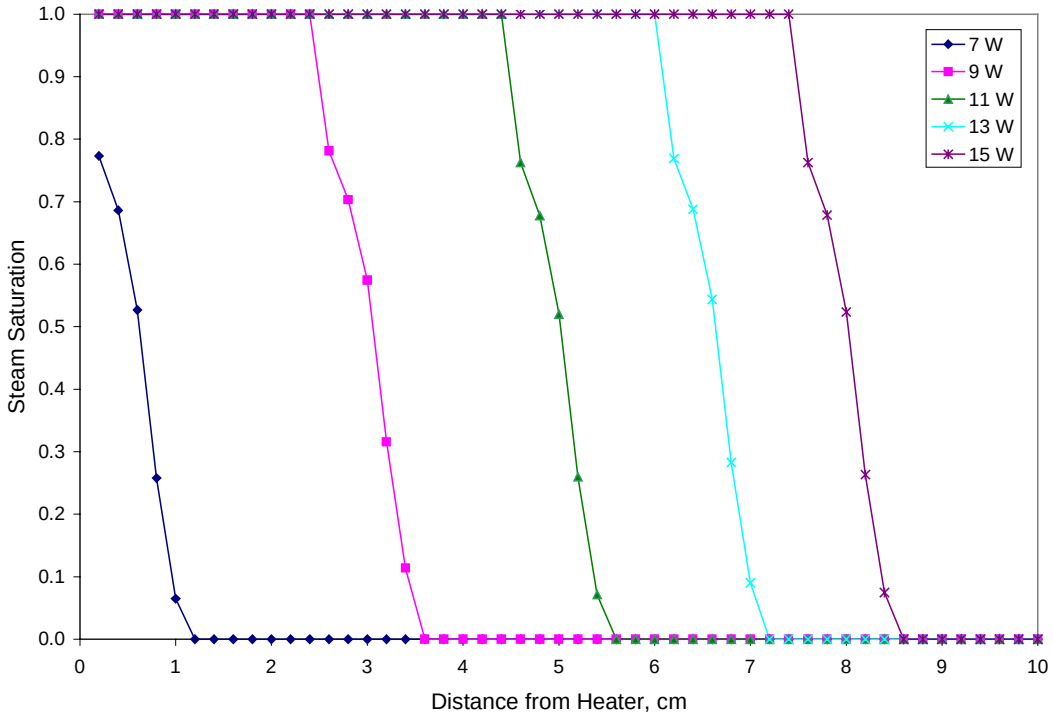

Figure 2-13: Steady state steam saturation profile with distance and constant heating rate: immobile water saturation = 0.2, Geysers geothermal reservoir rock.

It is evident from the simulation results that the steam and two-phase regions expand as the heating rate is increased. However, it is important to note that in the case of the lower-porosity and lower-permeability geothermal rocks, the two-phase region is much shorter and the boiling front is much sharper in comparison to the Berea sandstone case. Consequently, the elbow in the steam saturation profile is less conspicuous in the geothermal rock case.

Figures 2-14 to 2-16 show the simulation results when variable heating rates are used. The same heating rate profile was used in the simulation runs, as shown in Figure 2-6. Likewise, steam and two-phase regions formed and expanded as the boiling process progressed. As expected, the two-phase region covered only a shorter distance and the boiling front was sharper. As a result, it is difficult to identify an elbow in the steam

saturation profile. This very important simulation result must be taken into consideration in planning and designing boiling experiments in tighter and less permeable geothermal reservoir rocks. The difficulty in identifying the elbow in the steam saturation profile may limit the usefulness of this technique in determining the immobile water saturation of geothermal rocks from laboratory data obtained from boiling experiments.

2.6. Conclusion and Recommendations

Based on experimental data and TOUGH2 numerical simulation results of dynamic boiling experiments, there is an apparent correlation between the immobile water saturation and the shape of the steam saturation profile. The inferred immobile water saturation of Berea sandstone rocks is about 0.25, which is consistent with experimental results from past relative permeability experiments reported by Mahiya (1999).

However, this technique may not be useful in inferring the immobile water saturation for low porosity and low permeability geothermal rocks because of the difficulty in locating the elbow in the steam saturation profile.

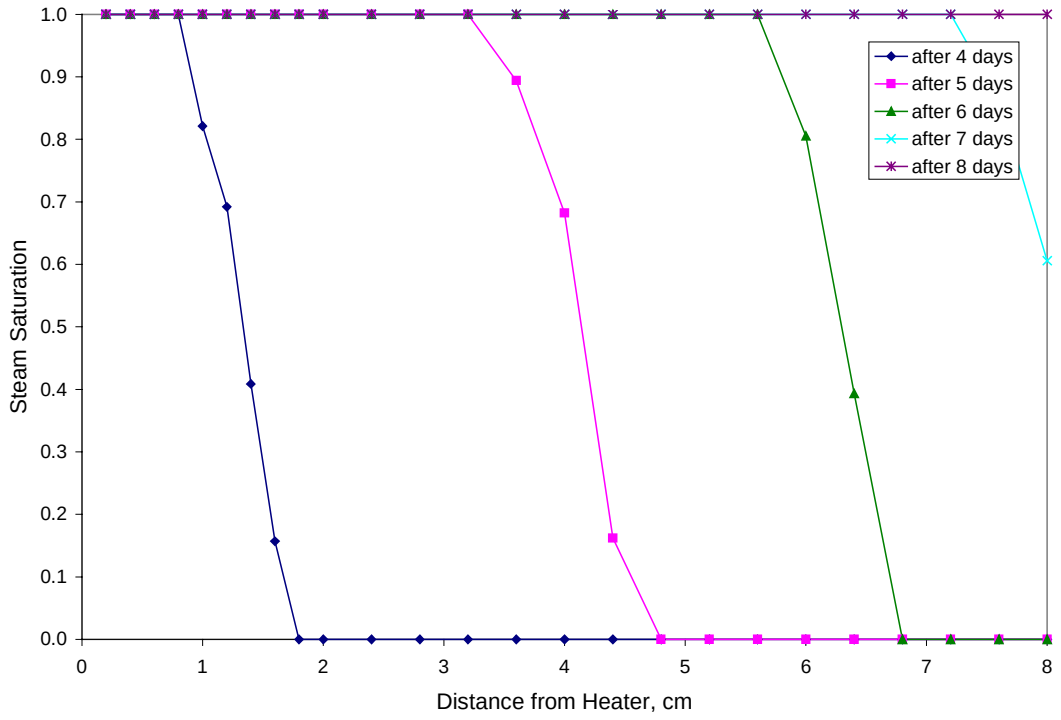

Figure 2-14: Steam saturation profiles with distance and time using variable heating rate: immobile water saturation = 0.1, Geysers geothermal reservoir rock.

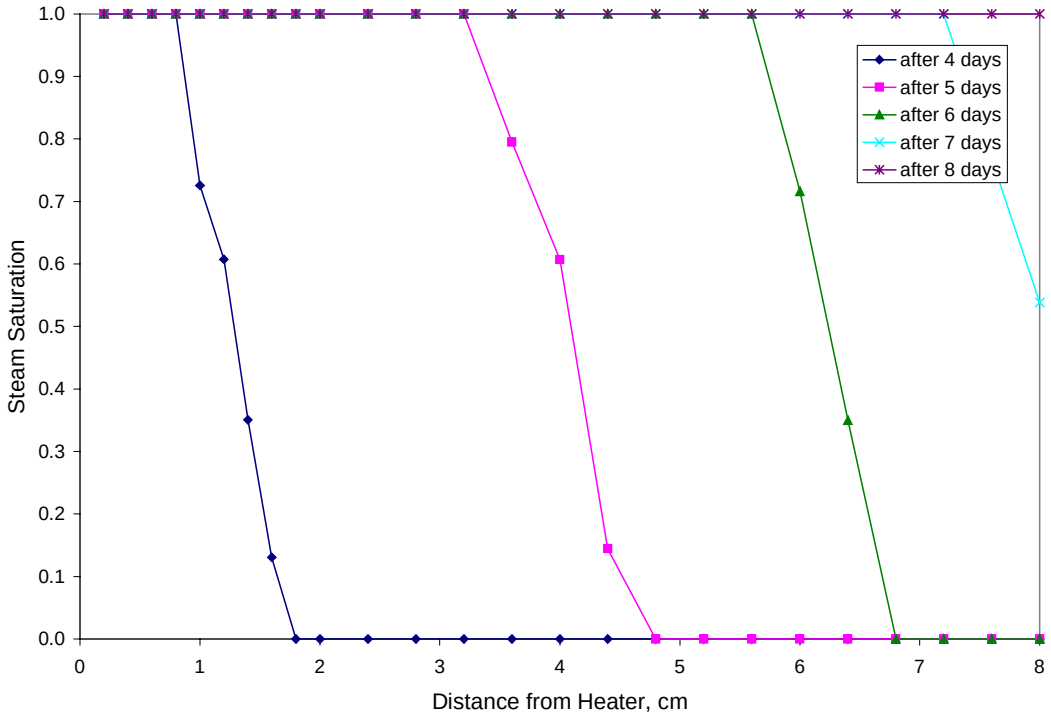

Figure 2-15: Steam saturation profiles with distance and time using variable heating rate: immobile water saturation = 0.2, Geysers geothermal reservoir rock.

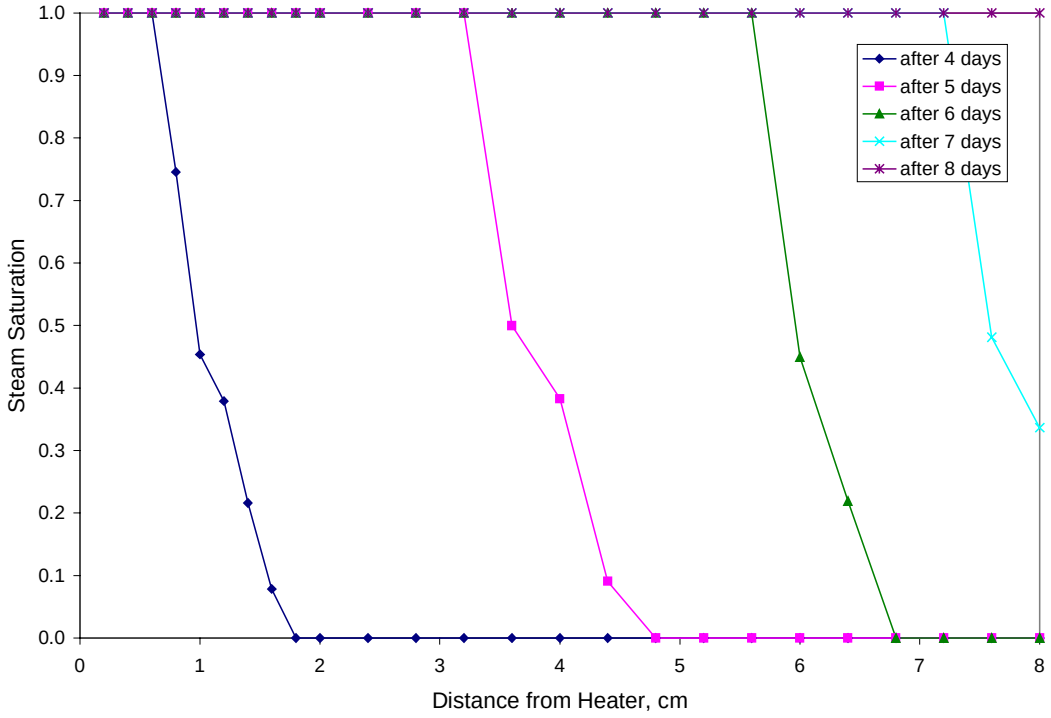

Figure 2-16: Steam saturation profiles with distance and time using variable heating rate: immobile water saturation = 0.5, Geysers geothermal reservoir rock.

Chapter 3

3. Inferring Immobile and In-Situ Water Saturation from Field Measurements

The discharge of saturated or superheated steam during the exploitation of vapor-dominated geothermal reservoirs greatly exceeds the amount that can be stored as vapor. Therefore, vapor-dominated reservoirs must contain substantial amounts of liquid water to sustain production (James, 1968; Nathenson 1975; Grant, 1979). In describing the response of vapor-dominated reservoirs to exploitation, it is valid to assume that the liquid water is completely immobile. Although water may be slightly mobile in the natural state of the reservoir, it soon becomes immobile because the water saturation drops as fluids are produced (Grant, 1979). The liquid water is adsorbed in the pores of the reservoir matrix and is able to vaporize, but is not able to flow as liquid water.

Grant (1979) estimated the in-place water saturation of the Kawah Kamojang geothermal field, Indonesia, based on variations in the gas content of the production fluids. Changing the flow rate at the wellhead produces a response in the reservoir pressure and gas content, which allows for the estimation of the in-place water saturation or the immobile water saturation of the reservoir rock. In contrast, this study aims to infer the in-situ and immobile water saturations from field measurements of changes in the flowing enthalpies of producing wells as well as downhole temperatures.

Zero-dimensional models can be used to describe the pressure, temperature and saturation profiles accompanying production. This study developed models of both vapor and liquid-dominated geothermal reservoirs that can be used to infer the in-situ and immobile water saturations using field measurements of cumulative mass production, discharge enthalpy, and downhole temperature.

3.1. Inferring In-situ Saturations from Variations in Gas Content

Variations in pressure and saturation in the reservoir during exploitation result in the transfer of mass between phases and, consequently, variations in the gas content of the liquid and vapor phases. The changes are determined by the equation for the conservation of gas (Grant, 1977) given by

$$\phi \frac{\partial}{\partial t}\left[s\rho_w n_w + (1-s)\rho_s n_s\right] = k\nabla \cdot \left(\frac{n_s}{\upsilon_s}\nabla p\right) \qquad (3\text{-}1)$$

Using a flow model, Grant (1979) showed that the variations in gas content with flow rate could be described using a parameter, ζ, which depends on gas, steam and reservoir properties. The transient response in the gas content of the steam produced when a well is opened at time $t = 0$ to a flow rate W kg/s is given by

$$\ln\left(\frac{n_s}{n_{s_o}}\right) = -\int_0^{\infty} \frac{\zeta \exp(-\xi)}{\xi + \zeta \exp(-\xi)} d\xi \tag{3-2}$$

$$\zeta = \frac{W}{4\pi kh} \frac{\mu c_t}{\gamma} \tag{3-3}$$

$$\gamma = (1-s)\rho_s + As\rho_w \tag{3-4}$$

$$A = \frac{n_w}{n_s} \tag{3-5}$$

The in-place water saturation can then be inferred from gas data by considering the difference in the response of two gases with production. However, this method is valid only if the total amount of gas is small and each gas obeys Equation 3-2 independently with a different ζ parameter. After further simplification, Grant (1979) showed that the logarithm of the concentration of gas 1 in steam is a linear function of the logarithm of the concentration of gas 2 in steam. The slope of the straight line gives the in-situ water saturation of the undisturbed reservoir.

$$slope\ of\ \ln(n_{s_1})\ vs\ \ln(n_{s_2})\ plot = \frac{(1-s)\rho_s + A_2 s\rho_w}{(1-s)\rho_s + A_1 s\rho_w} \tag{3-6}$$

Figure 3-1 is a log-log plot of CO_2 and H_2S concentrations for production well KMJ11 in the Kawah Kamojang geothermal field. Production data show that Kawah Kamojang is a classic vapor-dominated system (Grant 1979). The slope of the straight line that fits the gas concentration data gives an in-situ water saturation of about 0.35 using Grant's model and approach.

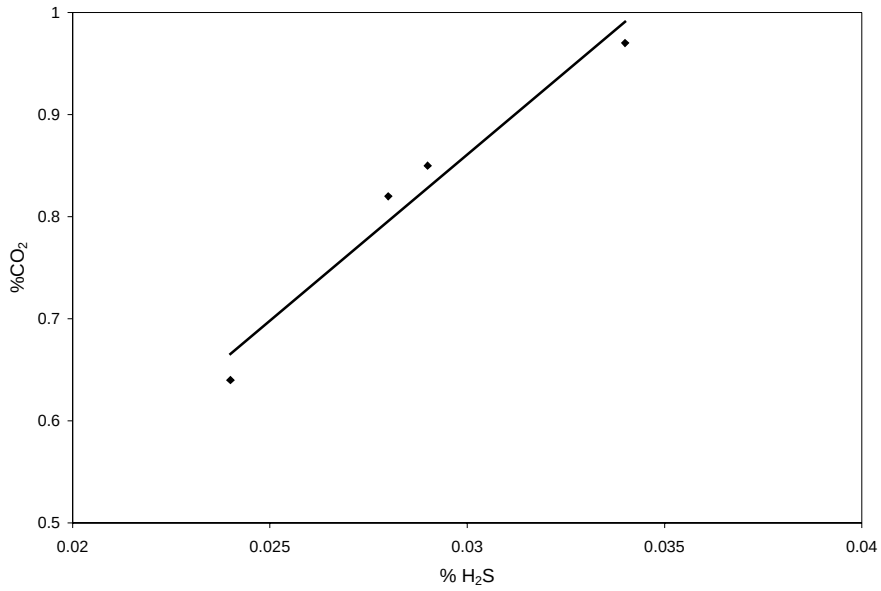

Figure 3-1: Log-log plot of CO2-H2S concentration for KMJ11 (Grant 1979).

3.2. Zero-Dimensional Models

Darcy's law and the differential material and energy conservation equations that describe the response of geothermal reservoirs to exploitation can be combined to form simple zero-dimensional models. For the case of vapor-dominated geothermal systems, the only mobile phase is steam (Figure 3-2). The flow of dry steam can be described by Equations 3-7 to 3-9. It is assumed that the immobile water does not impede the flow of steam and that Darcy's law describes the steam flow.

$$\phi \frac{\partial}{\partial t}\{s\rho_w + (1-s)\rho_s\} = -\nabla \cdot (\vec{u}_s \rho_s) \tag{3-7}$$

$$\frac{\partial}{\partial t}\{(1-\phi)\rho_r c_r T + \phi s \rho_w h_w + \phi(1-s)\rho_s h_s\} = -\nabla \cdot (\vec{u}_s \rho_s h_s) \tag{3-8}$$

$$\vec{u}_s = -\frac{k k_{rs}}{\mu_s} \nabla p \tag{3-9}$$

Under reservoir conditions, the enthalpy of saturated steam is nearly constant with temperature. This approximation results in a simplified relation between pressure and saturation at any point in the reservoir.

$$(1-\phi)\rho_r C_r T + \phi s \rho_w (h_w - h_s) = \text{constant} \tag{3-10}$$

Reduction in the reservoir pressure resulting from production is accompanied by a reduction in reservoir temperature to maintain saturation conditions. Heat must then be mined from the rock to cool it, which is achieved by vaporizing some of the liquid water to steam. Therefore, a decline in the reservoir pressure results in a decline in the reservoir saturation. This mining of heat and consequent decline in saturation continues as long as saturation conditions exist. The saturation falls to zero at dry-out conditions and the in-place water saturation can then be estimated using the initial and dry-out reservoir conditions (Grant 1979).

$$s_o = \frac{(1-\phi)}{\phi} \frac{\rho_r c_r (T_o - T_d)}{\rho_w (h_s - h_w)|_{T_o}} \tag{3-11}$$

This zero-dimensional model allows the calculation of the in-situ water saturation using rock and fluid properties and the initial, T_o, and dry-out, T_d, downhole or reservoir temperatures. In this case, the dry-out temperature is that temperature at which the reservoir has completely dried out and has started to produce superheated steam.

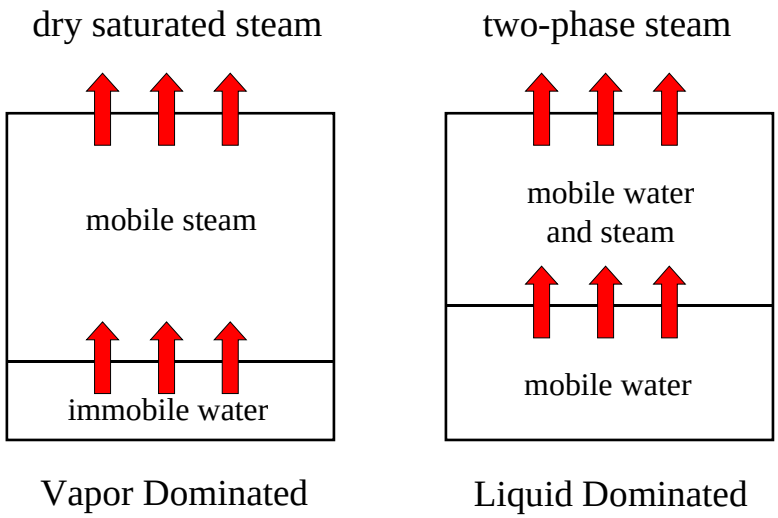

Figure 3-2: Vapor- and liquid-dominated geothermal reservoirs.

On the other hand, for the liquid-dominated reservoir case (Figure 3-2), the differential material and energy balance equations (Equations 3-12 and 3-13) and the simplified equations describing the zero-dimensional model (Equations 3-14 and 3-15) are much more complicated because both water and steam phases are mobile.

$$\phi \frac{\partial}{\partial t} \{ s\rho_w + (1-s)\rho_s \} = -\nabla \cdot (\vec{u}_w \rho_w + \vec{u}_s \rho_s) \tag{3-12}$$

$$\frac{\partial}{\partial t}\{(1-\phi)\rho_r c_r T + \phi s\rho_w h_w + \phi(1-s)\rho_s h_s\} = -\nabla\cdot(\vec{u}_w\rho_w h_w + \vec{u}_s\rho_s h_s) \quad (3\text{-}13)$$

$$\phi V\Delta(s\rho_w) + \phi V\Delta\{(1-s)\rho_s\} + m_w' + m_s' = 0 \quad (3\text{-}14)$$

$$\phi V\Delta(s\rho_w h_w) + \phi V\Delta\{(1-s)\rho_s h_s\} + (1-\phi)V\rho_r C_r\Delta T + m_w' h_w' + m_s' h_s' = 0 \quad (3\text{-}15)$$

The composition and enthalpy of the production fluids are determined by the mobility of steam and liquid water in the porous rock given by the relative permeabilities and viscosities of the two phases as shown in Equations 3-16 and 3-17.

$$m_w' = \frac{\rho_w \frac{k_{rw}}{\mu_w}}{\rho_w \frac{k_{rw}}{\mu_w} + \rho_s \frac{k_{rs}}{\mu_s}}\Delta m \quad (3\text{-}16)$$

$$m_s' = \frac{\rho_s \frac{k_{rs}}{\mu_s}}{\rho_w \frac{k_{rw}}{\mu_w} + \rho_s \frac{k_{rs}}{\mu_s}}\Delta m \quad (3\text{-}17)$$

3.3. TOUGH2 Two-Phase Radial Flow Model

The zero-dimensional models assume that the pressures, temperatures and saturations are uniform throughout the reservoir. These models do not take into account the transient and spatial effects of two-phase steam flow. In order to verify the validity and usefulness of these models in determining the in-situ and immobile saturations, two-phase radial flow was modeled using the numerical simulator TOUGH2. The TOUGH2 simulation results were then compared with those predicted by the zero-dimensional models.

A cylindrical reservoir model was used in the TOUGH2 simulation runs. A single well maintained at constant downhole pressure was placed in the middle of the reservoir. Table 3-1 summarizes the reservoir and wellbore parameters used in the simulation runs.

The reservoir model consisted of 100 grid blocks. The grid size increases logarithmically from the center to the boundary of the reservoir. The effect of the grid block size and number on the simulation results is illustrated in Figure 3-3. Grid refinement minimizes the discretization errors that are particularly large during the early transient production period.

Table 3-1: TOUGH2 reservoir model and wellbore parameters.

Porosity	5%
Permeability	1 x 10^{-13} m^2
Rock density	2600 kg/m^3
Rock specific heat	485 J/kg°C
Reservoir radius	1000 m
Reservoir thickness	10 m
Initial reservoir temperature	280 °C
Constant downhole wellbore pressure	200 psia

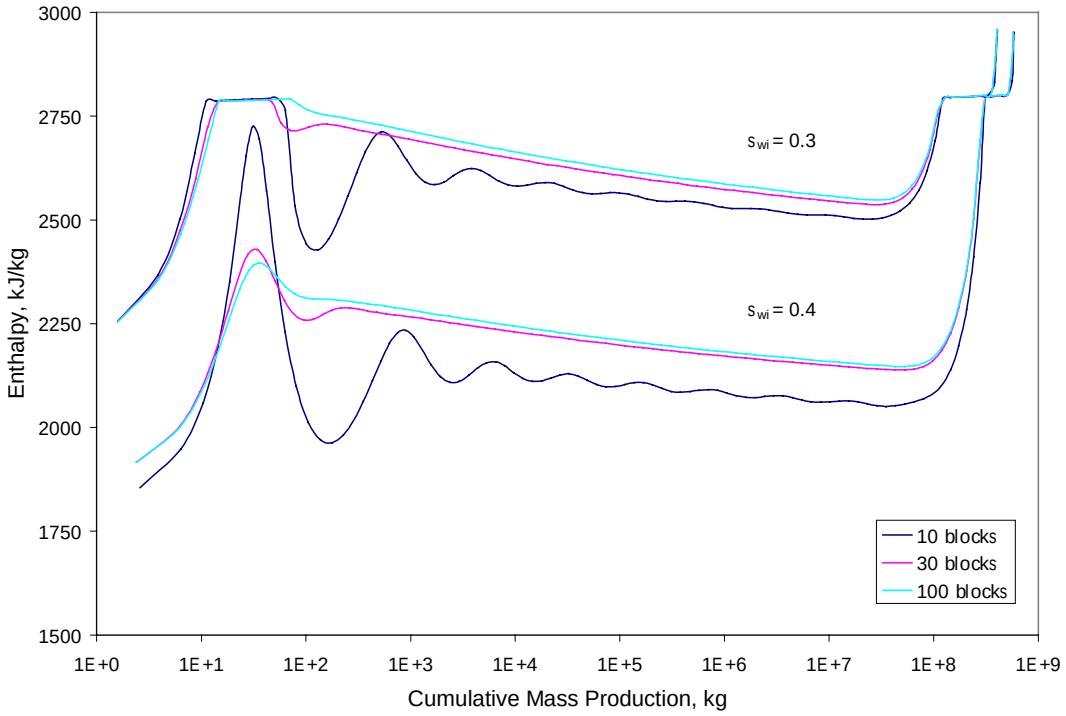

Figure 3-3: Effect of grid refinement on simulation results.

Figures 3-4 to 3-6 are semilog plots of the saturation, temperature and pressure profiles with time and radial distance from the well. Initially, water saturation throughout the reservoir in this particular simulation run is 0.3. As a response to production, reservoir pressure, temperature and saturation drop and boiling near the wellbore commences. The boiling front moves farther into the reservoir away from the well as two-phase steam is produced.

However, water saturation stays above and never goes below the immobile water saturation. The reservoir eventually produces dry saturated steam. During this time, reservoir saturation has dropped below the immobile water saturation. Water remaining

in the reservoir during this period is immobile water, which is able to vaporize but not able to flow.

At some point during production, the reservoir completely dries out and starts to produce superheated steam. Water saturation has dropped to zero throughout the reservoir. The sequence of events in the production history of the reservoir is labeled in Figure 3.4.

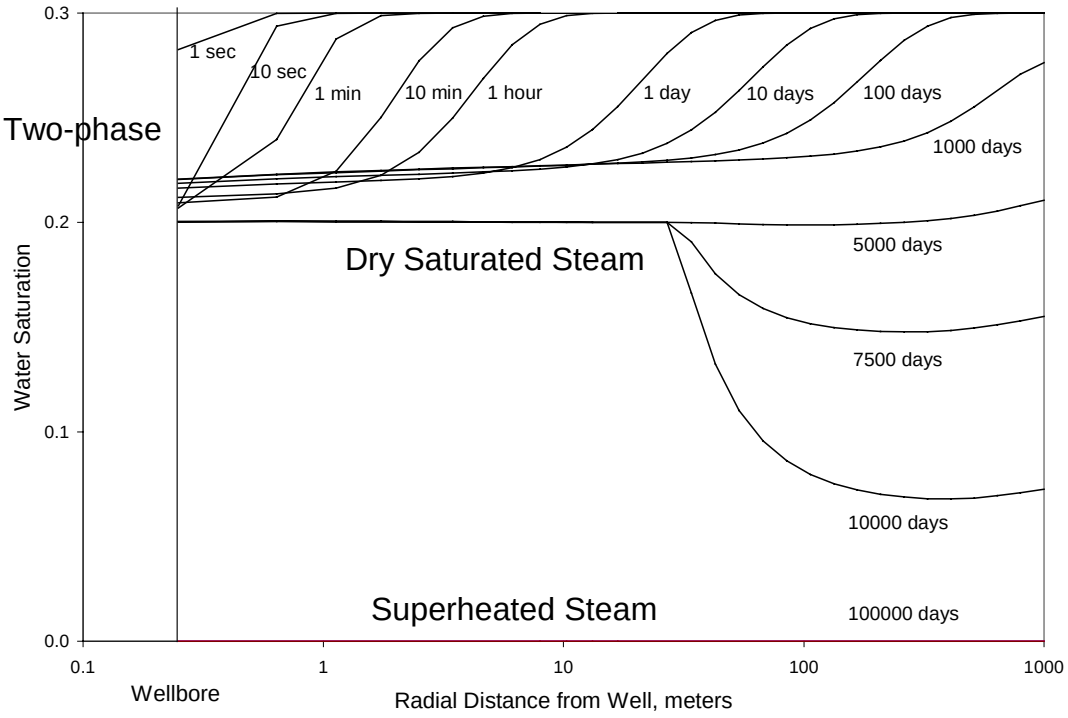

Figure 3-4: Water saturation profile with distance and time: initial water saturation = 0.3, immobile water saturation = 0.2.

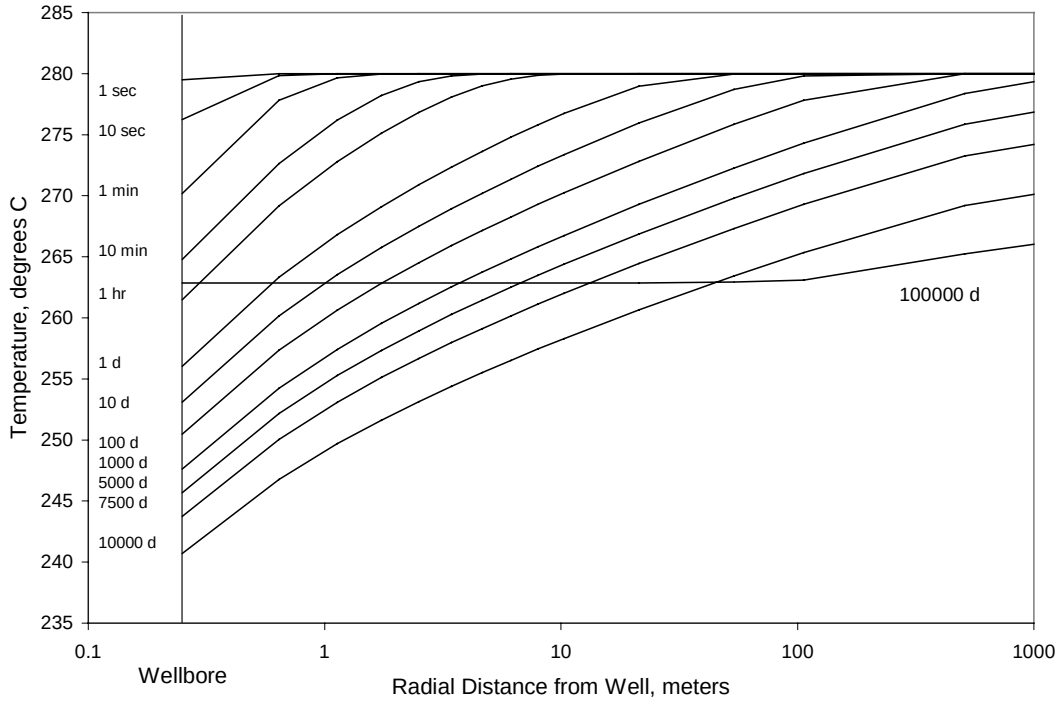

Figure 3-5: Temperature profile with distance and time: initial water saturation = 0.3, immobile water saturation = 0.2.

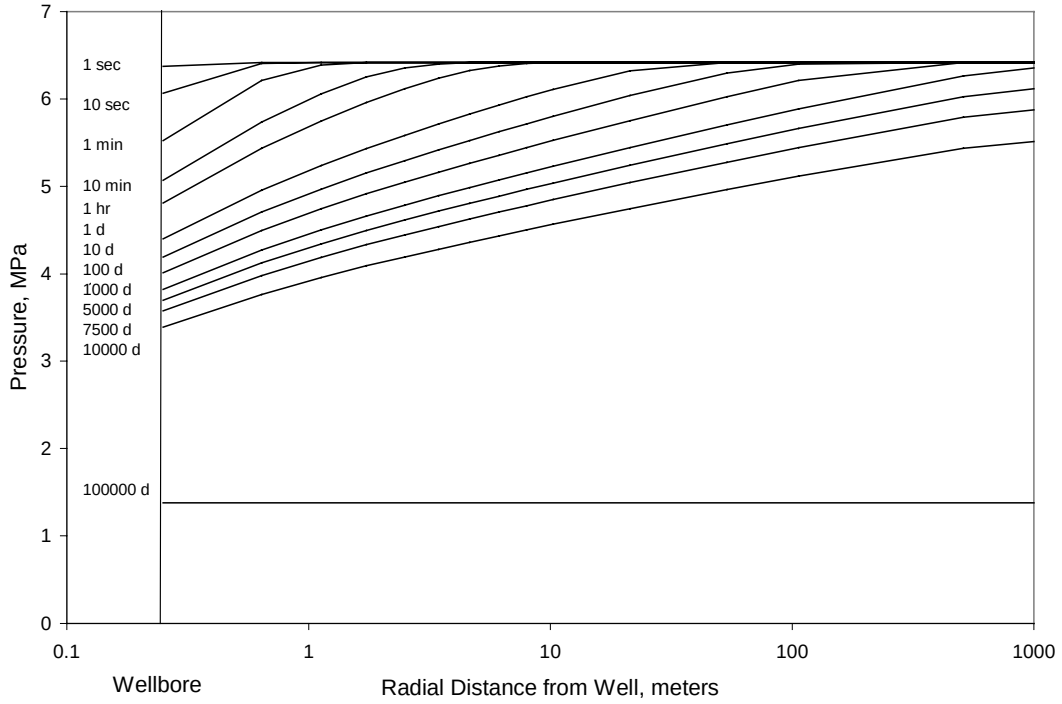

Figure 3-6: Pressure profile with distance and time: initial water saturation = 0.3, immobile water saturation = 0.2.

3.4. Comparison of TOUGH2 Two-Phase Radial Flow Model with Zero-Dimensional Model

3.4.1. Vapor-Dominated Geothermal Reservoirs

Figure 3-7 compares the production enthalpies and reservoir temperatures simulated by TOUGH2 with those predicted by the zero-dimensional model for a vapor-dominated reservoir case with in-situ water saturation equal to 0.2. There appears to be a very good agreement between the simulation and the modeling results.

The modeling results were then used to calculate the in-situ water saturation through Equation 3-11 as shown below.

$$s_o = \frac{(1-\phi)}{\phi}\frac{\rho_r c_r (T_o - T_d)}{\rho_w (h_s - h_w)\big|_{T_o}} = \frac{(1-0.05)}{0.05}\frac{(2600\,{}^{kg}/_{m^3})(0.485\,{}^{kJ}/_{kgC})(280.0^{\circ}C - 270.3^{\circ}C)}{750.5\,{}^{kg}/_{m^3}(2780.4\,{}^{kJ}/_{kg} - 1236.8\,{}^{kJ}/_{kg})} = 0.20$$

The zero-dimensional model gave the correct in-situ water saturation, which in this case, is equal to the immobile water saturation. This result confirms that the zero-dimensional model can be used to infer both the in-place and immobile water saturation of vapor-dominated geothermal reservoirs by knowing the initial and dry-out reservoir temperatures.

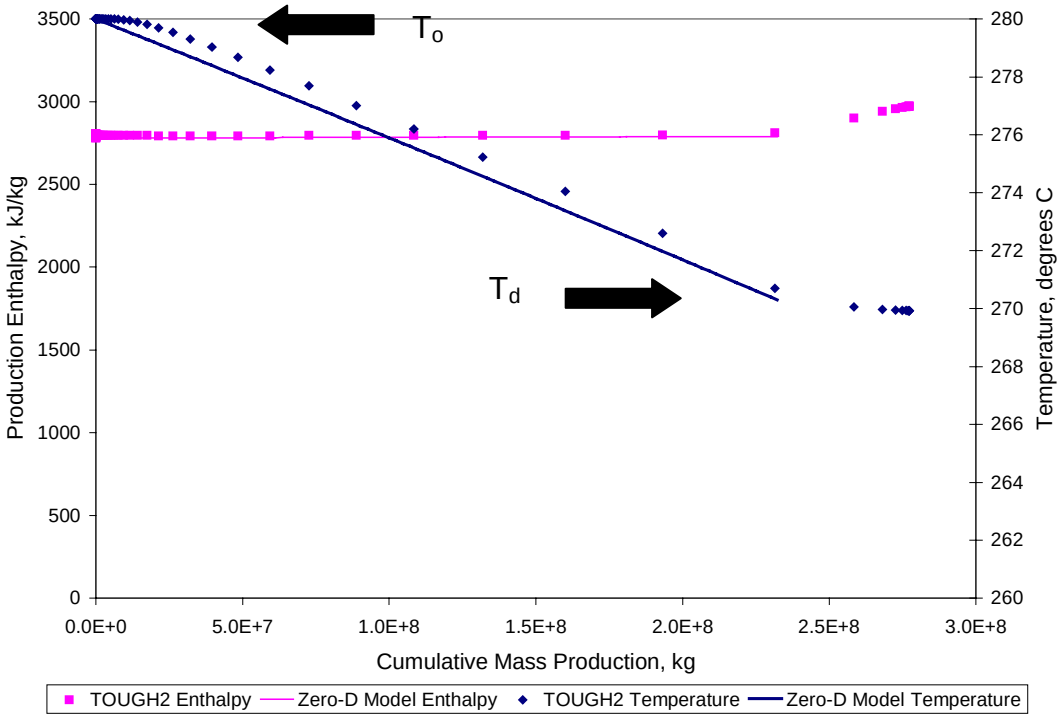

Figure 3-7: Production enthalpy and reservoir temperature profiles: vapor-dominated case, initial water saturation = 0.2, immobile water saturation = 0.2.

Figure 3-8 shows another vapor-dominated case but with a higher in-situ water saturation equal to 0.3. Equation 3-11 gives the correct in-situ water saturation as shown below.

$$s_o = \frac{(1-\phi)}{\phi}\frac{\rho_r c_r (T_o - T_d)}{\rho_w (h_s - h_w)\big|_{T_o}} = \frac{(1-0.05)}{0.05}\frac{\left(2600\,{}^{kg}/_{m^3}\right)\left(0.485\,{}^{kJ}/_{kgC}\right)\left(280.0^{\circ}C - 266.5^{\circ}C\right)}{750.5\,{}^{kg}/_{m^3}\left(2780.4\,{}^{kJ}/_{kg} - 1236.8\,{}^{kJ}/_{kg}\right)} = 0.30$$

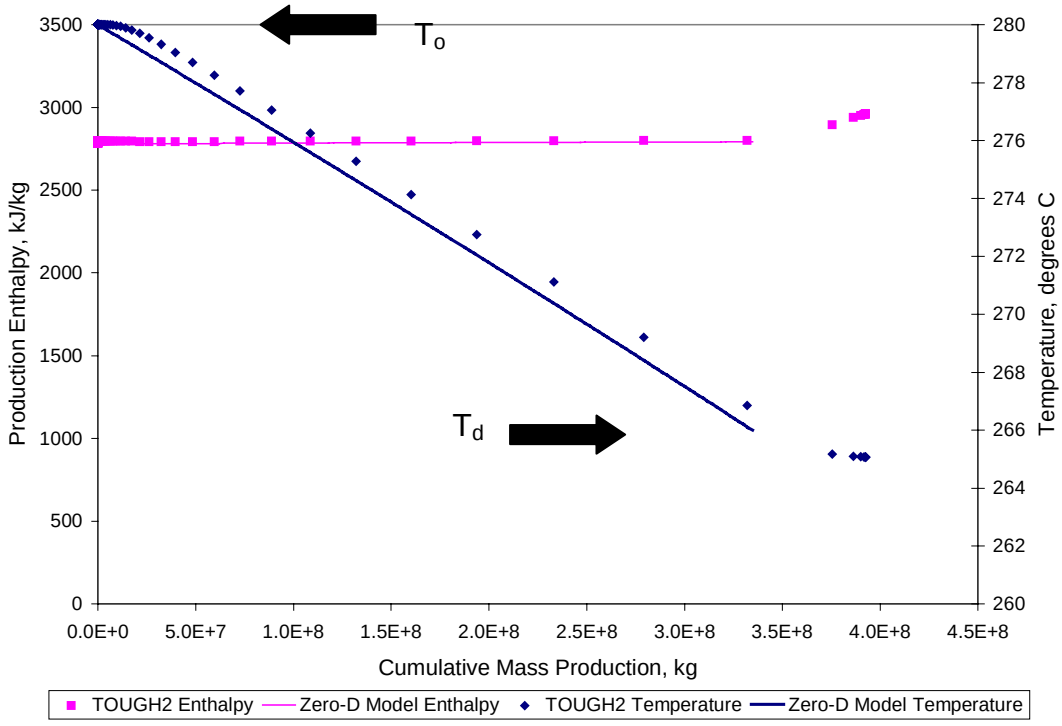

Figure 3-8: Production enthalpy and reservoir temperature profiles: vapor-dominated case, initial water saturation = 0.3, immobile water saturation = 0.3.

In the last two cases, TOUGH2 simulated reservoir temperatures agreed satisfactorily with the modeled temperatures. However, reservoir temperatures are not normally measured in the field. Instead, surface and downhole temperatures are routinely measured in the production wells. Figure 3-9 is a plot comparing TOUGH2 simulated downhole temperatures and modeled reservoir temperatures.

The initial sudden drop in the downhole wellbore temperature as a response to production is clearly evident from Figure 3-9. After this early transient period, downhole temperatures decline at the same rate as the reservoir temperatures. TOUGH2 simulated downhole temperatures were then used to estimate the in-situ water saturation using Equation 3-11. The initial temperature, T_o, was taken to be the stable temperature after the early transient period. The zero-dimensional model still gave a very close approximation of the correct in-situ water saturation as shown in the following calculation.

$$s_o = \frac{(1-\phi)}{\phi}\frac{\rho_r c_r (T_o - T_d)}{\rho_w (h_s - h_w)\big|_{T_o}} = \frac{(1-0.05)}{0.05}\frac{\left(2600\,{}^{kg}/_{m^3}\right)\left(0.485\,{}^{kJ}/_{kgC}\right)\left(251.5^{\circ}C - 238.0^{\circ}C\right)}{750.5\,{}^{kg}/_{m^3}\left(2780.4\,{}^{kJ}/_{kg} - 1236.8\,{}^{kJ}/_{kg}\right)} = 0.28$$

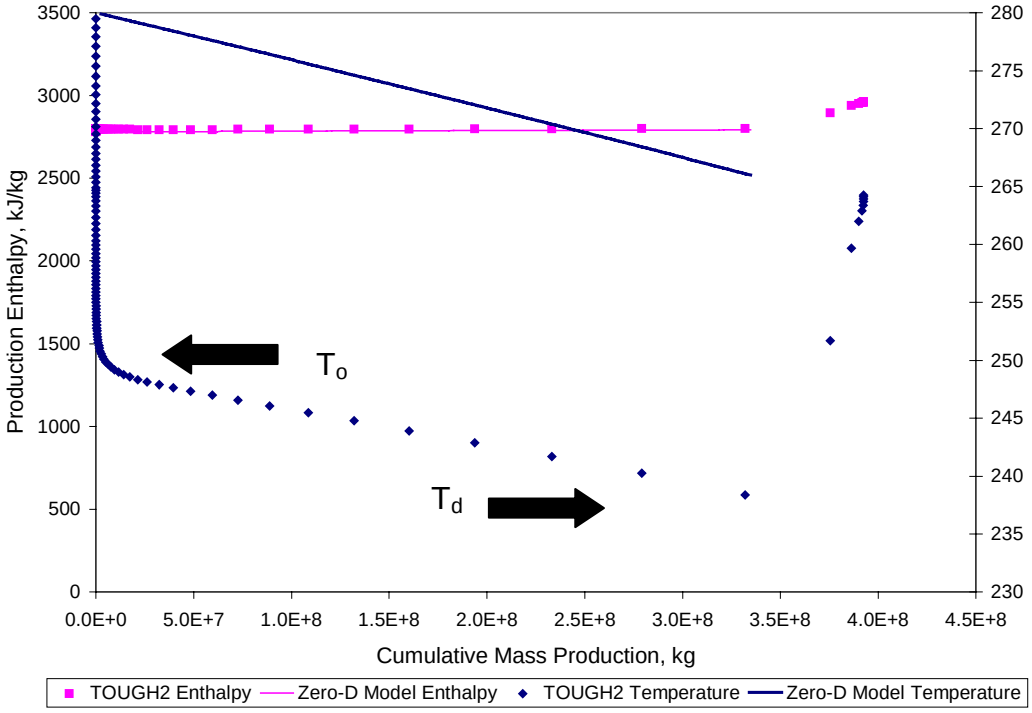

Figure 3-9: Production enthalpy and production temperature profiles: vapor-dominated case, initial water saturation = 0.3, immobile water saturation = 0.3.

Therefore, either downhole wellbore or reservoir temperatures can be used to estimate the in-place water saturation using the zero-dimensional model. However, it is important that the appropriate initial, T_o, and dry-out, T_d, temperatures be used in Equation 3-11.

$$s_o = \frac{(1-\phi)}{\phi}\frac{\rho_r c_r (T_o - T_d)}{\rho_w (h_s - h_w)\big|_{T_o}} \qquad (3\text{-}11)$$

The initial reservoir temperature must be used in evaluating the fluid properties while the stable downhole wellbore temperature must be used in evaluating the temperature difference. The stable downhole wellbore temperature is the temperature measured downhole when flow conditions have already stabilized.

3.4.2. Liquid-Dominated Geothermal Reservoirs

The response of liquid-dominated geothermal reservoirs to exploitation can be described by a sequence of two-phase, dry saturated and superheated steam production. TOUGH2 and the zero-dimensional model predict similar trends in production enthalpy and temperature as illustrated in Figures 3-10 to 3-12. The enthalpy of produced two-phase steam increases and reservoir temperature declines as the reservoir is depleted of its mobile water. The production enthalpy then plateaus as the reservoir continues to dry out and produces dry saturated steam while the temperature continues to fall almost linearly. Finally, the enthalpy increases further as the reservoir completely dries out of immobile water and produces superheated steam.

However, the zero-dimensional model, which does not take into account transient or spatial variations in temperature, pressure and saturation, fails to match the early transient two-phase production period predicted by TOUGH2. The zero-dimensional model predicts a continuous increase in two-phase steam enthalpy with cumulative mass production. On the other hand, TOUGH2 predicts a production period of apparently stable two-phase steam enthalpy immediately after the early transient period. Then the enthalpy increases with production until dry saturated steam is produced.

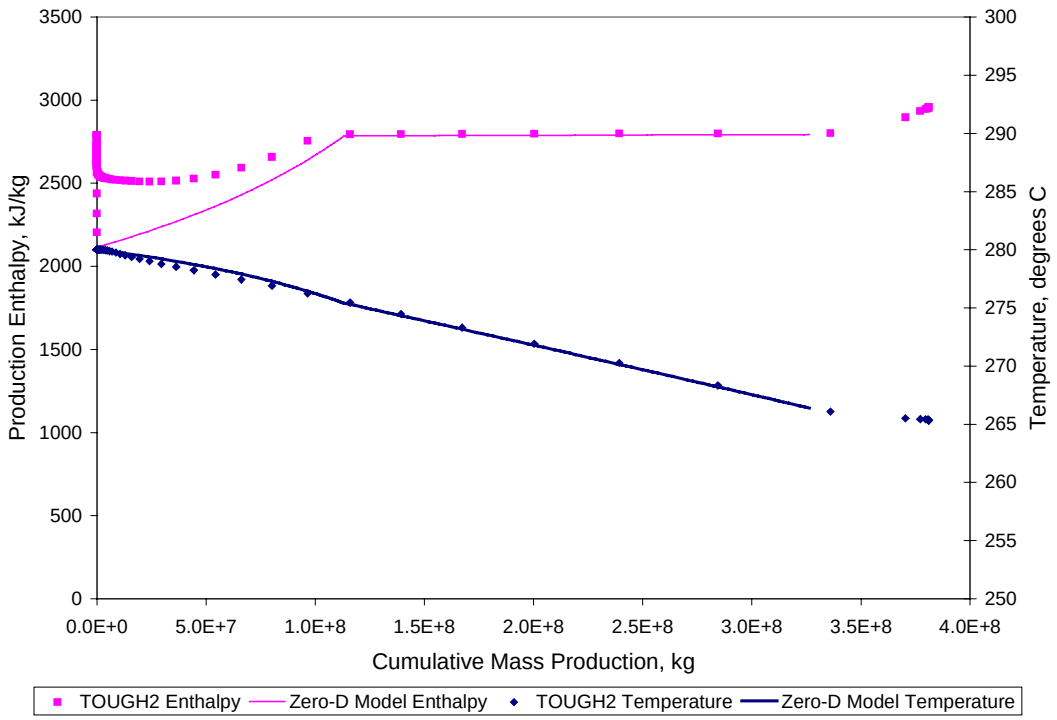

Figure 3-10: Production enthalpy and production temperature profiles: liquid-dominated case, initial water saturation = 0.3, immobile water saturation = 0.2.

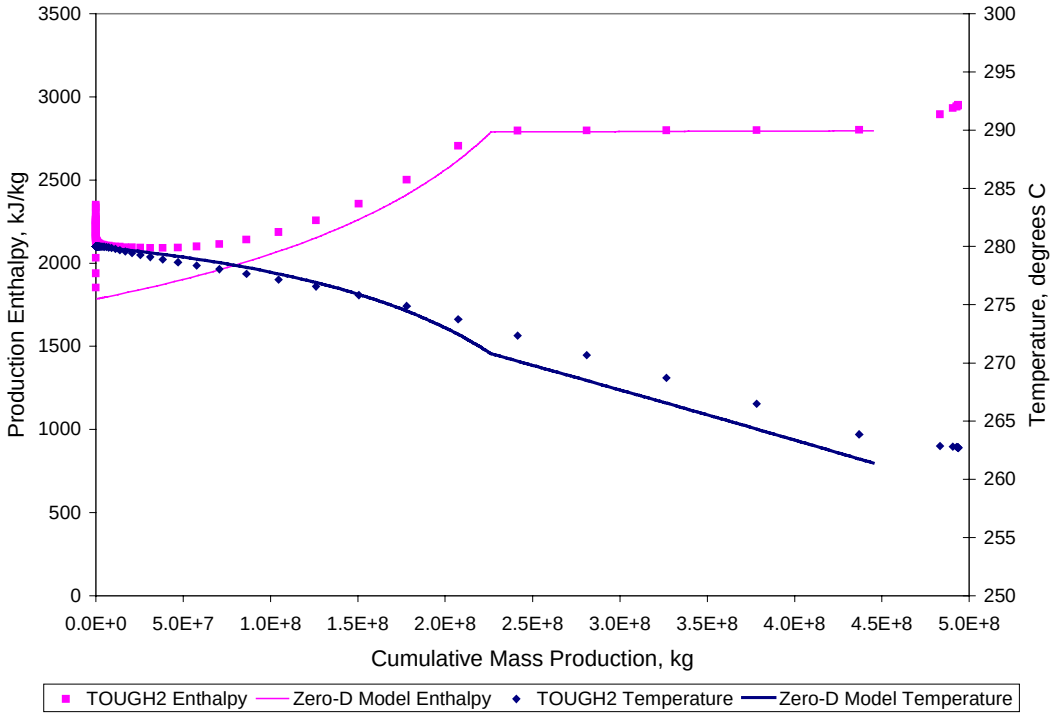

Figure 3-11: Production enthalpy and production temperature profiles: liquid-dominated case, initial water saturation = 0.4, immobile water saturation = 0.2.

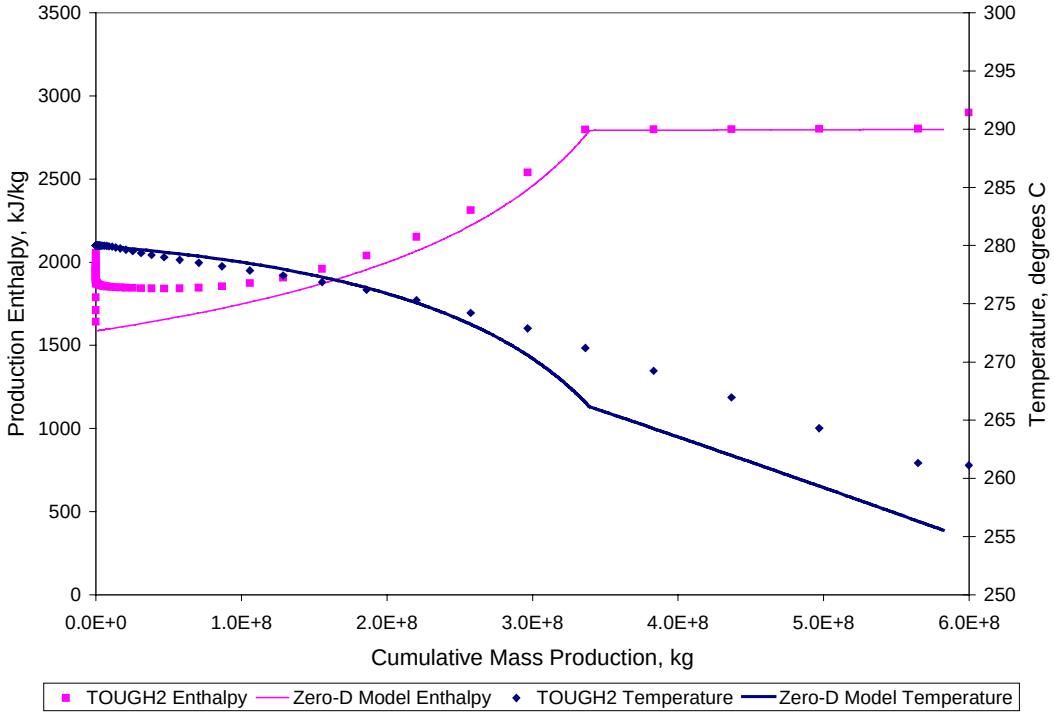

Figure 3-12: Production enthalpy and production temperature profiles: liquid-dominated case, initial water saturation = 0.5, immobile water saturation = 0.2.

Interesting observations can be made from the modeling results. Figures 3-13 and 3-14 are plots of production enthalpy and temperature for different values of in-situ water saturation and a fixed immobile water saturation. On the other hand, Figures 3-15 and 3-16 are plots for different values of immobile water saturation and a fixed in-situ water saturation.

Based on the modeling results, two-phase steam enthalpies are a function of the mobile water content of the reservoir, that is, the difference between the initial and immobile water saturation. Reservoirs with higher mobile water saturations produce two-phase steam with lower enthalpies. This is clearly evident from Figures 3-17 and 3-18, which show production enthalpies for cases of constant mobile water content but varying in-situ and immobile water saturation. Likewise, dry-out temperatures follow the same trend. Reservoirs with higher mobile water content dry-out at lower temperatures. Furthermore, dry saturated steam production commences at a later time in the life of a reservoir containing greater amount of mobile water.

The mobile water content and the immobile water saturation of liquid-dominated geothermal reservoirs can then be inferred from the two-phase steam production enthalpy and the cumulative mass production using the zero-dimensional model. The discharge enthalpy of two-phase steam can be expressed as a weighted average of the individual steam and liquid water enthalpies given by Equation 3-18.

$$h' = \frac{\rho_w \frac{k_{rw}}{\mu_w} h_w + \rho_s \frac{k_{rs}}{\mu_s} h_s}{\rho_w \frac{k_{rw}}{\mu_w} + \rho_s \frac{k_{rs}}{\mu_s}} \tag{3-18}$$

Assuming that linear steam-liquid water relative permeability relations are valid, the above equation can be rearranged to obtain an expression for the mobile water content in the reservoir,

$$\frac{s - s_{wr}}{1 - s_{wr} - s_{sr}} = \frac{\frac{\rho_s}{\mu_s}(h_s - h')}{\frac{\rho_w}{\mu_w}(h' - h_w) + \frac{\rho_s}{\mu_s}(h_s - h')} \tag{3-19}$$

Equation 3-19 can be used to calculate the ratio of the mobile water in the reservoir to the maximum possible mobile water. This ratio gives an indication of how much mobile water is present in the reservoir and how fast the reservoir is drying out. Similar expressions can be obtained by assuming different relative permeability relations. For example, if Corey-type relative permeability relations govern the flow of two-phase steam in the reservoir, the resulting expression for the mobile water content is given by Equation 3-20.

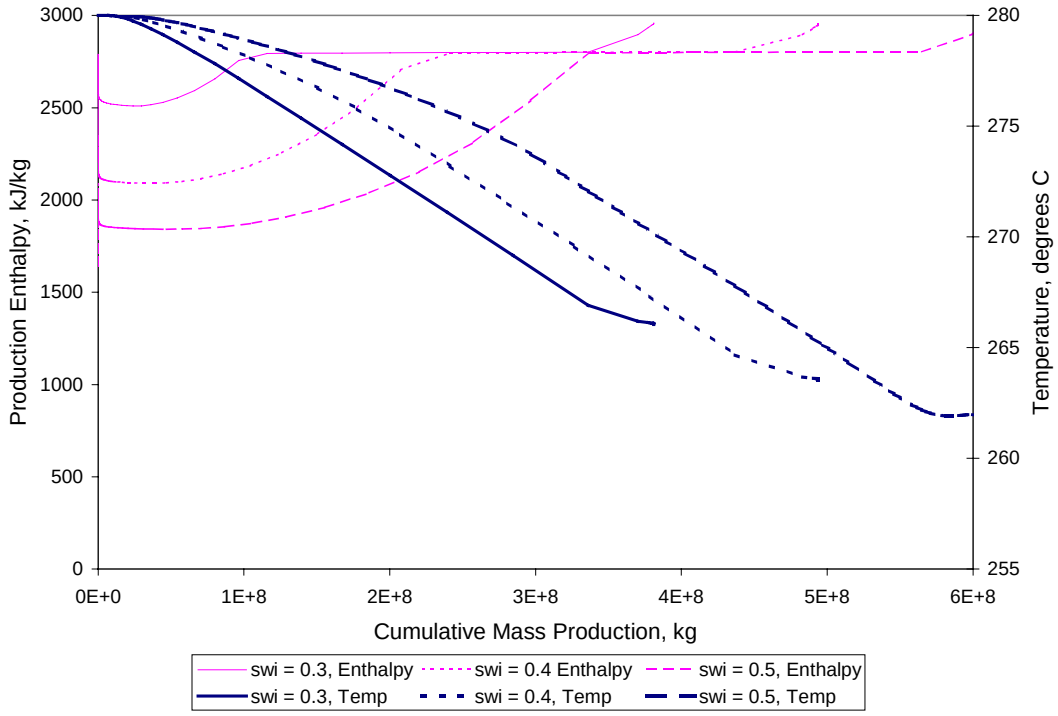

Figure 3-13: TOUGH2 simulated production enthalpy and reservoir temperature profiles: varying initial water saturation, immobile water saturation = 0.2.

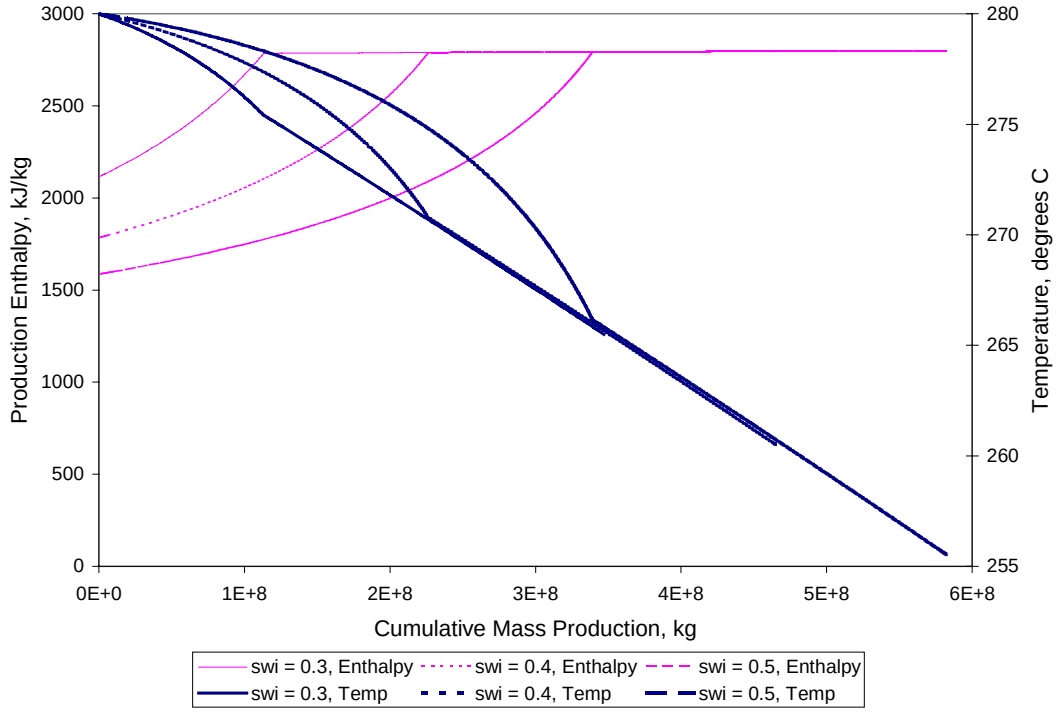

Figure 3-14: Zero-dimensional model production enthalpy and reservoir temperature profiles: varying initial water saturation, immobile water saturation = 0.2.

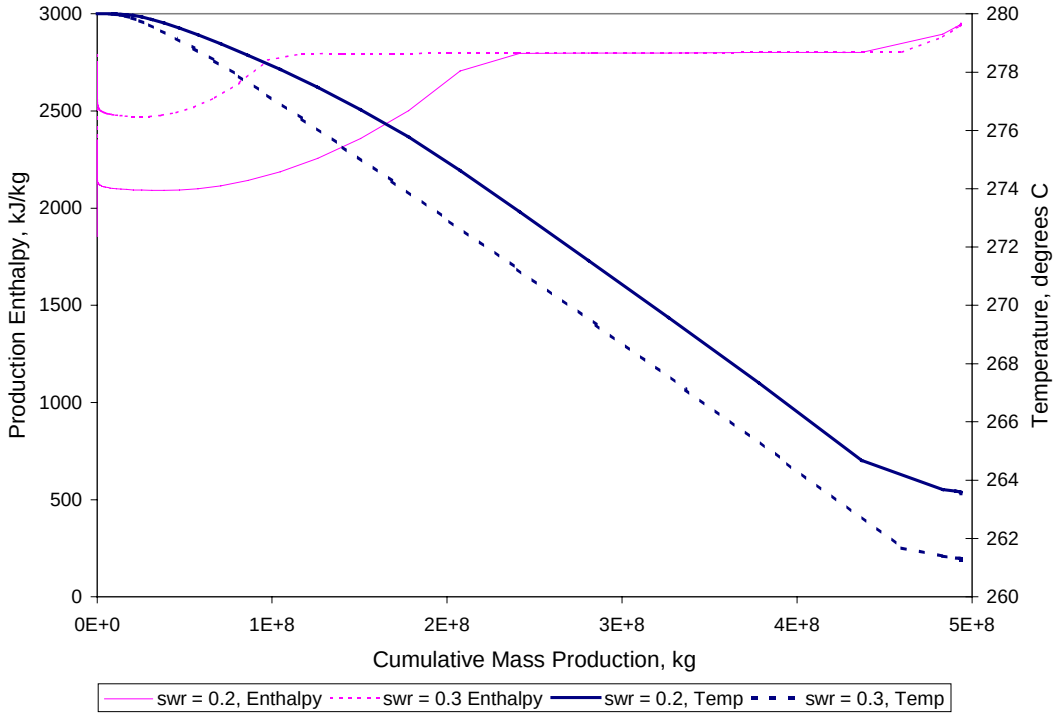

Figure 3-15: TOUGH2 simulated production enthalpy and reservoir temperature profiles: varying immobile water saturation, initial water saturation = 0.4.

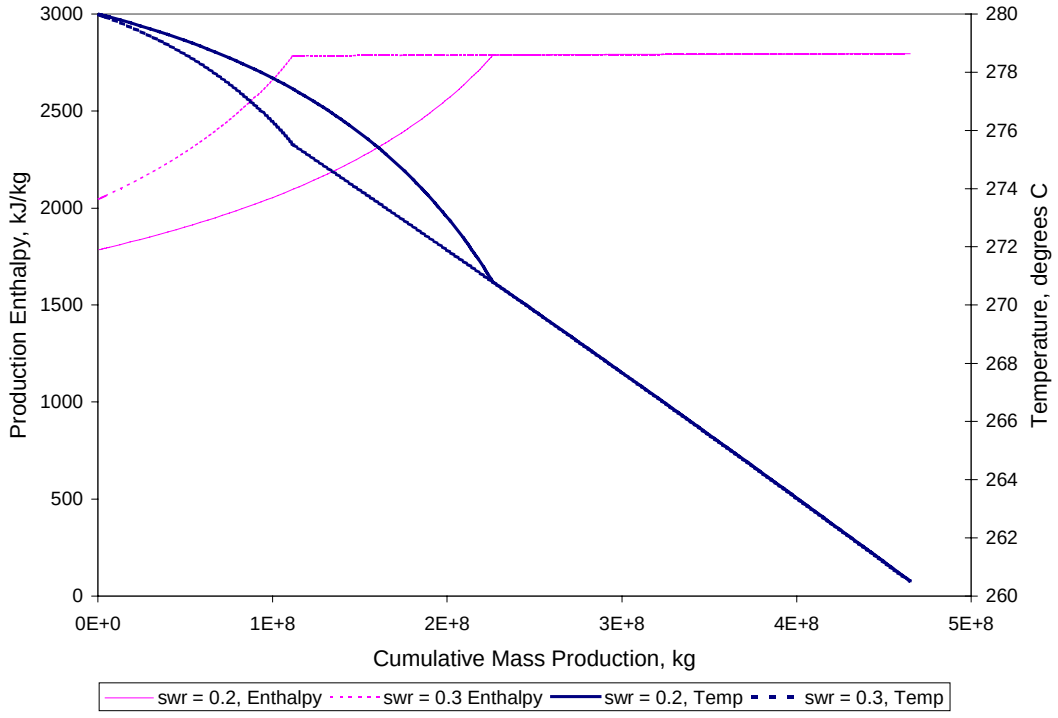

Figure 3-16: Zero-dimensional model production enthalpy and reservoir temperature profiles: varying immobile water saturation, initial water saturation = 0.4.

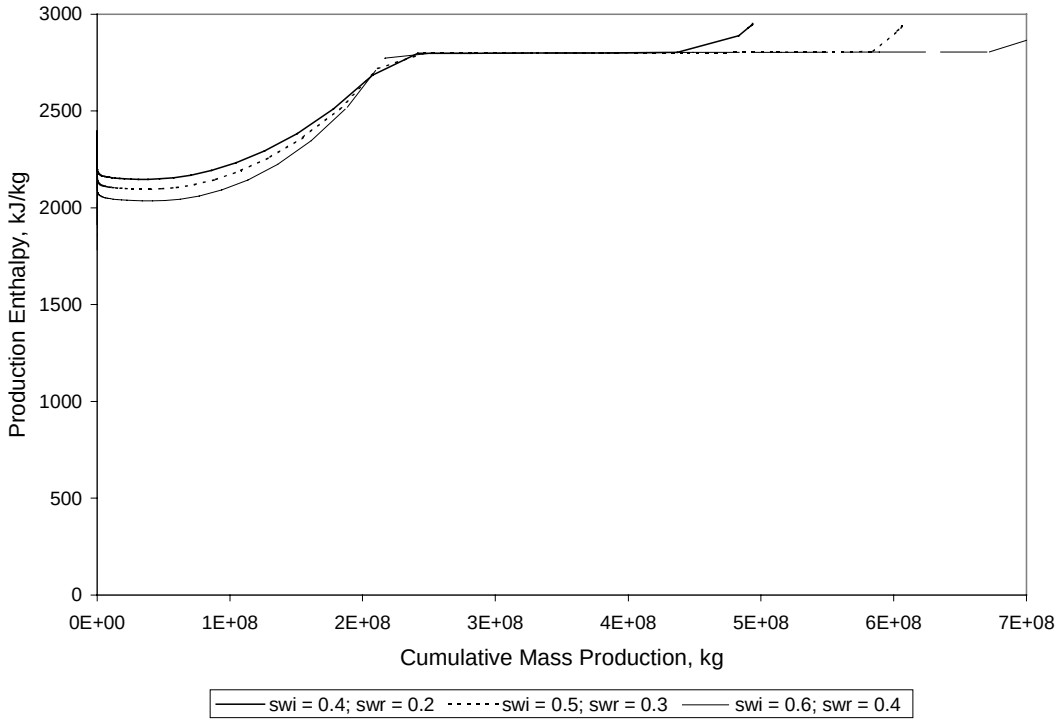

Figure 3-17: TOUGH2 simulated cumulative mass production and enthalpy profiles: mobile water content = 0.2.

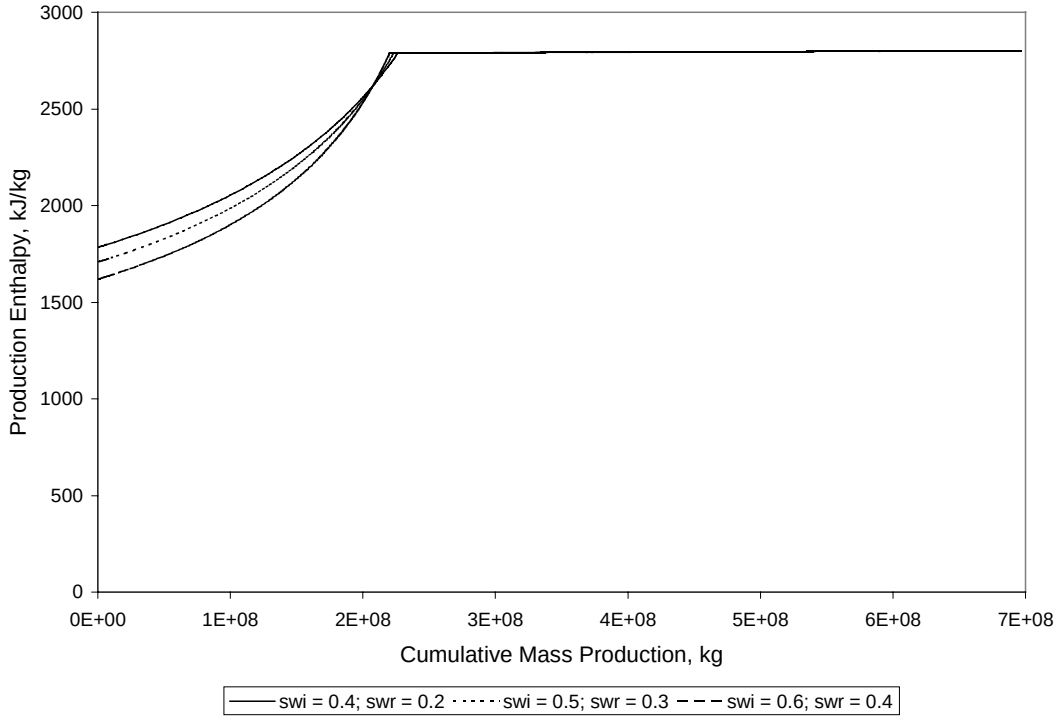

Figure 3-18: Zero-dimensional model cumulative mass production and enthalpy profiles: mobile water content = 0.2.

$$\left(\frac{s-s_{wr}}{1-s_{wr}-s_{sr}}\right)^4 = \frac{\frac{\rho_s}{\mu_s}(h_s - h')}{\frac{\rho_w}{\mu_w}(h'-h_w)+\frac{\rho_s}{\mu_s}(h_s - h')} \qquad (3\text{-}20)$$

The change in the reservoir saturation can be estimated using cumulative mass production data. The material balance equation describing two-phase steam production can be simplified to Equation 3-21 by assuming that the densities of steam and liquid water are approximately invariant with pressure and temperature. This equation gives the change in reservoir saturation as a function of the cumulative mass production, Δm, knowing the reservoir pore volume, ϕV.

$$\Delta s = s_1 - s_2 = \frac{\Delta m}{\phi V(\rho_w - \rho_s)} \qquad (3\text{-}21)$$

The immobile water saturation can then be estimated based on the change in mobile water content from Equation 3-19 and the change in reservoir saturation from Equation 3-21. This technique is demonstrated below using fluid properties, and enthalpy and cumulative mass production values simulated by TOUGH2, which are summarized in Tables 3-2 and 3-3. In both cases, the immobile steam saturation, s_{sr}, was assumed to be equal to 0.1.

Table 3-2: TOUGH2 simulation results and fluid properties: initial water saturation = 0.4, immobile water saturation = 0.2.

T °C	**h' kJ/kg**	**ρ_w kg/m^3**	**ρ_s kg/m^3**	**μ_w cp**	**μ_s cp**	**h_w kJ/kg**	**h_s kJ/kg**
280	1854	750.5	33.2	0.55	0.11	1237	2780
274	2256	750.5	33.2	0.55	0.11	1066	2780

Calculating the mobile water content at the initial state using Equation 3-19:

$$\frac{s_1 - s_{wr}}{1-s_{wr}-s_{sr}} = \frac{\frac{\rho_s}{\mu_s}(h_s - h')}{\frac{\rho_w}{\mu_w}(h'-h_w)+\frac{\rho_s}{\mu_s}(h_s - h')} = 0.2483$$

Calculating the mobile water content at the final state using Equation 3-19:

$$\frac{s_2 - s_{wr}}{1-s_{wr}-s_{sr}} = \frac{\frac{\rho_s}{\mu_s}(h_s - h')}{\frac{\rho_w}{\mu_w}(h'-h_w)+\frac{\rho_s}{\mu_s}(h_s - h')} = 0.0883$$

Calculating the difference in mobile water between the initial and final states:

$$\frac{\Delta s}{1-s_{wr}-s_{sr}} = \frac{s_1 - s_{wr}}{1-s_{wr}-s_{sr}} - \frac{s_2 - s_{wr}}{1-s_{wr}-s_{sr}} = \frac{s_1 - s_2}{1-s_{wr}-s_{sr}} = 0.1600$$

Calculating the change in reservoir saturation using Equation 3-21:

$$\Delta s = s_1 - s_2 = \frac{\Delta m}{\phi V(\rho_w - \rho_s)} = \frac{1.26\times10^8\, kg}{0.05\left(\pi \cdot 1000^2 \cdot 10 m^3\right)\left(750.5\,{}^{kg}\!/_{m^3} - 33.2\,{}^{kg}\!/_{m^3}\right)} = 0.1119$$

Calculating the immobile water saturation based on the change in mobile water content and the change in reservoir saturation:

$$1-s_{wr}-s_{sr} = \frac{\Delta s}{\frac{\Delta s}{1-s_{wr}-s_{sr}}} = \frac{0.1119}{0.1600} = 0.70$$

$$s_{sr} = 0.1, \quad \textit{therefore}, \; s_{wr} = 0.2$$

Table 3-3: TOUGH2 simulation results and fluid properties: initial water saturation = 0.4, immobile water saturation = 0.3.

T °C	**h' kJ/kg**	**ρ_w kg/m^3**	**ρ_s kg/m^3**	**μ_w cp**	**μ_s cp**	**h_w kJ/kg**	**h_s kJ/kg**
280	2144	750.5	33.2	0.55	0.11	1237	2780
274	2645	750.5	33.2	0.55	0.11	1070	2780

Calculating the mobile water content at the initial state using Equation 3-19:

$$\frac{s_1 - s_{wr}}{1-s_{wr}-s_{sr}} = \frac{\frac{\rho_s}{\mu_s}(h_s - h')}{\frac{\rho_w}{\mu_w}(h' - h_w) + \frac{\rho_s}{\mu_s}(h_s - h')} = 0.1334$$

Calculating the mobile water content at the final state using Equation 3-19:

$$\frac{s_2 - s_{wr}}{1 - s_{wr} - s_{sr}} = \frac{\frac{\rho_s}{\mu_s}(h_s - h')}{\frac{\rho_w}{\mu_w}(h' - h_w) + \frac{\rho_s}{\mu_s}(h_s - h')} = 0.0185$$

Calculating the difference in mobile water between the initial and final states:

$$\frac{\Delta s}{1 - s_{wr} - s_{sr}} = \frac{s_1 - s_{wr}}{1 - s_{wr} - s_{sr}} - \frac{s_2 - s_{wr}}{1 - s_{wr} - s_{sr}} = \frac{s_1 - s_2}{1 - s_{wr} - s_{sr}} = 0.1149$$

Calculating the change in reservoir saturation using Equation 3-21:

$$\Delta s = s_1 - s_2 = \frac{\Delta m}{\phi V(\rho_w - \rho_s)} = \frac{8.13 \times 10^7 kg}{0.05(\pi \cdot 1000^2 \cdot 10 m^3)(750.5 \, {}^{kg}/_{m^3} - 33.2 \, {}^{kg}/_{m^3})} = 0.0722$$

Calculating the immobile water saturation based on the change in mobile water content and the change in reservoir saturation:

$$1 - s_{wr} - s_{sr} = \frac{\Delta s}{\frac{\Delta s}{1 - s_{wr} - s_{sr}}} = \frac{0.0722}{0.1149} = 0.63$$

$$s_{sr} = 0.1, \quad \textit{therefore,} \; s_{wr} = 0.27 \approx 0.3$$

Based on the calculation results shown above, the zero-dimensional model proves to be useful in inferring the immobile water saturation from field production data. The model gave fairly good estimates of the immobile water saturation using "field" data from the TOUGH2 simulation results.

Having estimated the immobile water saturation, the in-situ water saturation can be inferred from the initial discharge enthalpy using Equation 3-19.

3.5. Conclusion and Recommendations

The in-situ and immobile water saturations can be inferred from field measurements of cumulative mass production, discharge enthalpy and downhole temperature using simple zero-dimensional models developed based on material and energy conservation equations and Darcy's law. For vapor-dominated reservoirs, the in-situ and immobile water saturation can be estimated knowing rock and fluid properties, and the difference between the stable initial and the dry-out downhole temperatures and using Equation 3-11.

$$s_o = \frac{(1-\phi)}{\phi} \frac{\rho_r c_r (T_o - T_d)}{\rho_w (h_s - h_w)|_{T_o}} \tag{3-11}$$

On the other hand, in liquid-dominated reservoirs the in-situ and immobile water saturation can be inferred from cumulative mass production, discharge enthalpy, and downhole temperature data using Equations 3-19 and 3-21.

$$\frac{s - s_{wr}}{1 - s_{wr} - s_{sr}} = \frac{\frac{\rho_s}{\mu_s}(h_s - h')}{\frac{\rho_w}{\mu_w}(h' - h_w) + \frac{\rho_s}{\mu_s}(h_s - h')} \tag{3-19}$$

$$\Delta s = s_1 - s_2 = \frac{\Delta m}{\phi V (\rho_w - \rho_s)} \tag{3-21}$$

The validity and usefulness of these zero-dimensional models were verified by comparing the modeling results with TOUGH2 two-phase radial flow simulation results. It is recommended that actual field production data be used to further verify the validity and usefulness of these models.

Chapter 4

4. Conclusion

The immobile water saturation can be inferred from laboratory measurements of pressure, temperature and steam saturation in dynamic boiling experiments. There is an apparent correlation between the immobile water saturation and the shape of the steam saturation profile, based on experimental data and TOUGH2 numerical simulation results of dynamic boiling experiments. The inferred immobile water saturation of Berea sandstone rocks is about 0.25 based on experimental results obtained by Satik (1997). This is consistent with experimental results from past relative permeability experiments reported by Mahiya (1999).

However, this technique may not be useful in inferring the immobile water saturation for low porosity and low permeability geothermal rocks because the elbow in the steam saturation profile is less prominent.

The in-situ and immobile water saturations can be inferred from field measurements of cumulative mass production, discharge enthalpy and downhole temperature using simple models developed based on Darcy's law and material and energy conservation equations. For vapor-dominated reservoirs, the in-situ and immobile water saturation can be estimated knowing rock and fluid properties, and the difference between the stable initial, T_o, and the dry-out, T_d, downhole temperatures.

On the other hand, in liquid-dominated reservoirs the in-situ and immobile water saturation can be inferred from cumulative mass production, Δm, enthalpy, h', data. The validity and usefulness of these zero-dimensional models were verified by comparing the modeling results with TOUGH2 two-phase radial flow simulation results. It is recommended that actual field production data be used to further verify the validity and usefulness of these models.

Nomenclature

A	=	partition function
C	=	specific heat capacity
c	=	compressibility
h'	=	enthalpy of production fluids
h	=	enthalpy
k	=	permeability
m'	=	mass of production fluids
n	=	concentration
p	=	pressure
s	=	saturation
T	=	temperature
t	=	time
u	=	velocity
V	=	volume
ϕ	=	porosity
μ	=	dynamic viscosity
ρ	=	density
υ	=	kinematic viscosity
ξ	=	similarity variable
d	=	dry-out conditions
o	=	initial conditions
r	=	rock
r	=	relative
s	=	steam
t	=	total (two-phase)
w	=	water

References

Ambusso W., Satik C., Horne R.: "A Study of Relative Permeability for Steam-Water Flow in Porous Media", Proceedings of 21st Workshop on Geothermal Reservoir Engineering, Stanford University, Stanford, California (1996).

Atkinson P., Celati R., Corsi R., Kucuk F., and Ramey Jr. H.: "Thermodynamic behavior of the Bagnore geothermal field", Geothermics, Volume 7, (1977), 185-208.

Grant M.: "Water Content of the Kawah Kamojang Geothermal Reservoir", Geothermics, Volume 8, (1979), 21-30.

Grant M.: "Broadlands – a gas dominated geothermal field", Geothermics, Volume 6, (1977), 9-29.

Guerrero M.: "Inferring Relative Permeability From Dynamic Boiling Experiments", Masters Report, Stanford University, Stanford, California (1998).

Guerrero M., Satik C., Finsterle S., and Horne R.: "Inferring Relative Permeability From Dynamic Boiling Experiments", Proceedings of 23rd Workshop on Geothermal Reservoir Engineering, Stanford University, Stanford, California (1998).

Horne R.: Notes on Geothermal Reservoir Engineering, Stanford University, Stanford, California (1991).

Mahiya G. and Horne R.: "Measurements of Steam-Water Relative Permeability", Stanford Geothermal Program Quarterly Report April–June 1998, Stanford University, Stanford, California (1998).

Mahiya G.: "Measurements of Steam-Water Relative Permeability", Masters Report, Stanford University, Stanford, California (1999).

Moench, A and Atkinson, P.: "Transient-Pressure Analysis in Geothermal Steam Reservoirs with an Immobile Vaporizing Liquid Phase", Geothermics, Volume 7, (1978), 253-264.

Nathenson, M.: "Some Reservoir Engineering Calculations for the Vapor-dominated System at Larderello, Italy", U.S. Geological Survey Open-file Report 75-142, April 1975.

Satik (1996): "An Experimental Study of Boiling in Porous Media", Fall 1996 Quarterly Report, Stanford Geothermal Program, Stanford University, Stanford, California.

Satik (1997): "An Experimental Study of Boiling in Porous Media", Winter 1997 Quarterly Report, Stanford Geothermal Program, Stanford University, Stanford, California.

Satik (1997): “An Experimental Study of Boiling in Porous Media”, Spring 1997 Quarterly Report, Stanford Geothermal Program, Stanford University, Stanford, California.

Satik (1997): “Experimental Study of Boiling in Porous Media”, Summer 1997 Quarterly Report, Stanford Geothermal Program, Stanford University, Stanford, California.

Satik C. (1997), “Experiments of Boiling in Porous Media”, Proceedings of 22nd Workshop on Geothermal Reservoir Engineering, Stanford University, Stanford, California.

Appendix A

A. TOUGH2 and iTOUGH2 input files for Berea Sandstone Boiling Experiment Simulation

```
*Forward Calculations*
ROCKS----1----*----2----*----3----*----4----*----5----*----6----*----7----*----8
BEREA    2     2163.     0.220   0.0E-20   0.0E-20 7.800E-13     4.989    858.24
0.0000E+000.0000E+09    0.0652       0.0
    1          0.500     0.000     1.000     0.500
    6         1.0E05     0.500
HEATE    0     2200.     0.010   0.0E-15   0.0E-15   0.0E-15     2.885     246.6
HEATB    0      240.     0.010   0.0E-15   0.0E-15   0.0E-15     0.163    1046.6
EPOXY    0     1200.     0.010   0.0E-15   0.0E-15   0.0E-15     0.577    1046.6
INSUL    0      192.     0.010   0.0E-15   0.0E-15   0.0E-15     0.115     104.7
BOUND    2     2163.     0.990   0.0E-15   0.0E-15   0.0E-15     0.642   -1611.0

   10          0.200     0.200     0.000
   10         0.5000  1000.000     0.050    0.0000                 0.0
AMBIE          1.293     0.990   0.0E-20   0.0E-20   1.0E-10     0.055   -1611.0

START----1----*----2----*----3----*----4----*----5----*----6----*----7----*----8
PARAM          12345678901234567890123456789012345
  -31500    15001000001001010004000010000 2.130E-05                 1.0
            6.1020E5  1.00E+03                        9.8100
     1.E-5
            1.0065E5                24.                  0.0

mESHMAKER1----*----2----*----3----*----4----*----5----*----6----*----7----*----8
RZ2D
RADII
    5
         0    0.0254    0.0304    0.0812    5.0812
LAYER----1----*----2----*----3----*----4----*----5----*----6----*----7----*----8
   99
    0.0100    0.0100    0.0100    0.0100    0.0100    0.0100    0.0100    0.0100
    0.0100    0.0100    0.0100    0.0100    0.0100    0.0100    0.0100    0.0100
    0.0100    0.0100    0.0100    0.0100    0.0100    0.0100    0.0100    0.0100
    0.0100    0.0100    0.0100    0.0100    0.0100    0.0100    0.0100    0.0100
    0.0020    0.0020    0.0020    0.0020    0.0020    0.0020    0.0020    0.0020
    0.0020    0.0020    0.0020    0.0020    0.0020    0.0020    0.0020    0.0020
    0.0020    0.0020    0.0020    0.0020    0.0020    0.0020    0.0020    0.0020
    0.0020    0.0020    0.0020    0.0020    0.0020    0.0020    0.0020    0.0020
    0.0020    0.0020    0.0020    0.0020    0.0020    0.0020    0.0020    0.0020
    0.0020    0.0020    0.0020    0.0020    0.0020    0.0020    0.0020    0.0020
    0.0020    0.0020    0.0020    0.0020    0.0020    0.0020    0.0020    0.0020
    0.0020    0.0020    0.0020    0.0020    0.0500    0.0100    0.0100    0.0100
    0.0100    0.0100    5.0000

ELEME ---     4    5    0    0   0.00000     5.081
BOU 1          BOUND .2027E+540.2027E-02          0.1270E-01          -.5000E-02
A2  1          BEREA .2027E-040.0000E+00          0.1270E-01          -.1500E-01
A3  1          BEREA .2027E-040.0000E+00          0.1270E-01          -.2500E-01
A4  1          BEREA .2027E-040.0000E+00          0.1270E-01          -.3500E-01
A5  1          BEREA .2027E-040.0000E+00          0.1270E-01          -.4500E-01
A6  1          BEREA .2027E-040.0000E+00          0.1270E-01          -.5500E-01
A7  1          BEREA .2027E-040.0000E+00          0.1270E-01          -.6500E-01
A8  1          BEREA .2027E-040.0000E+00          0.1270E-01          -.7500E-01
A9  1          BEREA .2027E-040.0000E+00          0.1270E-01          -.8500E-01
AA  1          BEREA .2027E-040.0000E+00          0.1270E-01          -.9500E-01
AB  1          BEREA .2027E-040.0000E+00          0.1270E-01          -.1050E+00
AC  1          BEREA .2027E-040.0000E+00          0.1270E-01          -.1150E+00
AD  1          BEREA .2027E-040.0000E+00          0.1270E-01          -.1250E+00
```

```
AE  1          BEREA .2027E-040.0000E+00          0.1270E-01          -.1350E+00
AF  1          BEREA .2027E-040.0000E+00          0.1270E-01          -.1450E+00
AG  1          BEREA .2027E-040.0000E+00          0.1270E-01          -.1550E+00
AH  1          BEREA .2027E-040.0000E+00          0.1270E-01          -.1650E+00
AI  1          BEREA .2027E-040.0000E+00          0.1270E-01          -.1750E+00
AJ  1          BEREA .2027E-040.0000E+00          0.1270E-01          -.1850E+00
AK  1          BEREA .2027E-040.0000E+00          0.1270E-01          -.1950E+00
AL  1          BEREA .2027E-040.0000E+00          0.1270E-01          -.2050E+00
AM  1          BEREA .2027E-040.0000E+00          0.1270E-01          -.2150E+00
AN  1          BEREA .2027E-040.0000E+00          0.1270E-01          -.2250E+00
AO  1          BEREA .2027E-040.0000E+00          0.1270E-01          -.2350E+00
AP  1          BEREA .2027E-040.0000E+00          0.1270E-01          -.2450E+00
AQ  1          BEREA .2027E-040.0000E+00          0.1270E-01          -.2550E+00
AR  1          BEREA .2027E-040.0000E+00          0.1270E-01          -.2650E+00
AS  1          BEREA .2027E-040.0000E+00          0.1270E-01          -.2750E+00
AT  1          BEREA .2027E-040.0000E+00          0.1270E-01          -.2850E+00
AU  1          BEREA .2027E-040.0000E+00          0.1270E-01          -.2950E+00
AV  1          BEREA .2027E-040.0000E+00          0.1270E-01          -.3050E+00
AW  1          BEREA .2027E-040.0000E+00          0.1270E-01          -.3150E+00
AX  1          BEREA .4054E-050.0000E+00          0.1270E-01          -.3210E+00
AY  1          BEREA .4054E-050.0000E+00          0.1270E-01          -.3230E+00
AZ  1          BEREA .4054E-050.0000E+00          0.1270E-01          -.3250E+00
B1  1          BEREA .4054E-050.0000E+00          0.1270E-01          -.3270E+00
B2  1          BEREA .4054E-050.0000E+00          0.1270E-01          -.3290E+00
B3  1          BEREA .4054E-050.0000E+00          0.1270E-01          -.3310E+00
B4  1          BEREA .4054E-050.0000E+00          0.1270E-01          -.3330E+00
B5  1          BEREA .4054E-050.0000E+00          0.1270E-01          -.3350E+00
B6  1          BEREA .4054E-050.0000E+00          0.1270E-01          -.3370E+00
B7  1          BEREA .4054E-050.0000E+00          0.1270E-01          -.3390E+00
B8  1          BEREA .4054E-050.0000E+00          0.1270E-01          -.3410E+00
B9  1          BEREA .4054E-050.0000E+00          0.1270E-01          -.3430E+00
BA  1          BEREA .4054E-050.0000E+00          0.1270E-01          -.3450E+00
BB  1          BEREA .4054E-050.0000E+00          0.1270E-01          -.3470E+00
BC  1          BEREA .4054E-050.0000E+00          0.1270E-01          -.3490E+00
BD  1          BEREA .4054E-050.0000E+00          0.1270E-01          -.3510E+00
BE  1          BEREA .4054E-050.0000E+00          0.1270E-01          -.3530E+00
BF  1          BEREA .4054E-050.0000E+00          0.1270E-01          -.3550E+00
BG  1          BEREA .4054E-050.0000E+00          0.1270E-01          -.3570E+00
BH  1          BEREA .4054E-050.0000E+00          0.1270E-01          -.3590E+00
BI  1          BEREA .4054E-050.0000E+00          0.1270E-01          -.3610E+00
BJ  1          BEREA .4054E-050.0000E+00          0.1270E-01          -.3630E+00
BK  1          BEREA .4054E-050.0000E+00          0.1270E-01          -.3650E+00
BL  1          BEREA .4054E-050.0000E+00          0.1270E-01          -.3670E+00
BM  1          BEREA .4054E-050.0000E+00          0.1270E-01          -.3690E+00
BN  1          BEREA .4054E-050.0000E+00          0.1270E-01          -.3710E+00
BO  1          BEREA .4054E-050.0000E+00          0.1270E-01          -.3730E+00
BP  1          BEREA .4054E-050.0000E+00          0.1270E-01          -.3750E+00
BQ  1          BEREA .4054E-050.0000E+00          0.1270E-01          -.3770E+00
BR  1          BEREA .4054E-050.0000E+00          0.1270E-01          -.3790E+00
BS  1          BEREA .4054E-050.0000E+00          0.1270E-01          -.3810E+00
BT  1          BEREA .4054E-050.0000E+00          0.1270E-01          -.3830E+00
BU  1          BEREA .4054E-050.0000E+00          0.1270E-01          -.3850E+00
BV  1          BEREA .4054E-050.0000E+00          0.1270E-01          -.3870E+00
BW  1          BEREA .4054E-050.0000E+00          0.1270E-01          -.3890E+00
BX  1          BEREA .4054E-050.0000E+00          0.1270E-01          -.3910E+00
BY  1          BEREA .4054E-050.0000E+00          0.1270E-01          -.3930E+00
BZ  1          BEREA .4054E-050.0000E+00          0.1270E-01          -.3950E+00
C1  1          BEREA .4054E-050.0000E+00          0.1270E-01          -.3970E+00
C2  1          BEREA .4054E-050.0000E+00          0.1270E-01          -.3990E+00
C3  1          BEREA .4054E-050.0000E+00          0.1270E-01          -.4010E+00
C4  1          BEREA .4054E-050.0000E+00          0.1270E-01          -.4030E+00
C5  1          BEREA .4054E-050.0000E+00          0.1270E-01          -.4050E+00
C6  1          BEREA .4054E-050.0000E+00          0.1270E-01          -.4070E+00
C7  1          BEREA .4054E-050.0000E+00          0.1270E-01          -.4090E+00
C8  1          BEREA .4054E-050.0000E+00          0.1270E-01          -.4110E+00
C9  1          BEREA .4054E-050.0000E+00          0.1270E-01          -.4130E+00
CA  1          BEREA .4054E-050.0000E+00          0.1270E-01          -.4150E+00
CB  1          BEREA .4054E-050.0000E+00          0.1270E-01          -.4170E+00
CC  1          BEREA .4054E-050.0000E+00          0.1270E-01          -.4190E+00
CD  1          BEREA .4054E-050.0000E+00          0.1270E-01          -.4210E+00
CE  1          BEREA .4054E-050.0000E+00          0.1270E-01          -.4230E+00
CF  1          BEREA .4054E-050.0000E+00          0.1270E-01          -.4250E+00
CG  1          BEREA .4054E-050.0000E+00          0.1270E-01          -.4270E+00
CH  1          BEREA .4054E-050.0000E+00          0.1270E-01          -.4290E+00
CI  1          BEREA .4054E-050.0000E+00          0.1270E-01          -.4310E+00
CJ  1          BEREA .4054E-050.0000E+00          0.1270E-01          -.4330E+00
```

```
CK  1          BEREA .4054E-050.0000E+00          0.1270E-01          -.4350E+00
CL  1          BEREA .4054E-050.0000E+00          0.1270E-01          -.4370E+00
CM  1          BEREA .4054E-050.0000E+00          0.1270E-01          -.4390E+00
CN1 1          HEATE .2027E-050.0000E+00          0.1270E-01          -.4650E+00
CN2 1          HEATE .2027E-050.0000E+00          0.1270E-01          -.4650E+00
CN3 1          HEATE .2027E-050.0000E+00          0.1270E-01          -.4650E+00
CN4 1          HEATE .2027E-050.0000E+00          0.1270E-01          -.4650E+00
CN5 1          HEATE .2027E-050.0000E+00          0.1270E-01          -.4650E+00
CO  1          HEATB .2027E-040.0000E+00          0.1270E-01          -.4950E+00
CP  1          HEATB .2027E-040.0000E+00          0.1270E-01          -.5050E+00
CQ  1          HEATB .2027E-040.0000E+00          0.1270E-01          -.5150E+00
CR  1          HEATB .2027E-040.0000E+00          0.1270E-01          -.5250E+00
CS  1          HEATB .2027E-040.0000E+00          0.1270E-01          -.5350E+00
AMB 1          AMBIE .1013E+540.2027E-02          0.1270E-01          -.3040E+01
A2  2          EPOXY .8765E-050.0000E+00          0.2790E-01          -.1500E-01
A3  2          EPOXY .8765E-050.0000E+00          0.2790E-01          -.2500E-01
A4  2          EPOXY .8765E-050.0000E+00          0.2790E-01          -.3500E-01
A5  2          EPOXY .8765E-050.0000E+00          0.2790E-01          -.4500E-01
A6  2          EPOXY .8765E-050.0000E+00          0.2790E-01          -.5500E-01
A7  2          EPOXY .8765E-050.0000E+00          0.2790E-01          -.6500E-01
A8  2          EPOXY .8765E-050.0000E+00          0.2790E-01          -.7500E-01
A9  2          EPOXY .8765E-050.0000E+00          0.2790E-01          -.8500E-01
AA  2          EPOXY .8765E-050.0000E+00          0.2790E-01          -.9500E-01
AB  2          EPOXY .8765E-050.0000E+00          0.2790E-01          -.1050E+00
AC  2          EPOXY .8765E-050.0000E+00          0.2790E-01          -.1150E+00
AD  2          EPOXY .8765E-050.0000E+00          0.2790E-01          -.1250E+00
AE  2          EPOXY .8765E-050.0000E+00          0.2790E-01          -.1350E+00
AF  2          EPOXY .8765E-050.0000E+00          0.2790E-01          -.1450E+00
AG  2          EPOXY .8765E-050.0000E+00          0.2790E-01          -.1550E+00
AH  2          EPOXY .8765E-050.0000E+00          0.2790E-01          -.1650E+00
AI  2          EPOXY .8765E-050.0000E+00          0.2790E-01          -.1750E+00
AJ  2          EPOXY .8765E-050.0000E+00          0.2790E-01          -.1850E+00
AK  2          EPOXY .8765E-050.0000E+00          0.2790E-01          -.1950E+00
AL  2          EPOXY .8765E-050.0000E+00          0.2790E-01          -.2050E+00
AM  2          EPOXY .8765E-050.0000E+00          0.2790E-01          -.2150E+00
AN  2          EPOXY .8765E-050.0000E+00          0.2790E-01          -.2250E+00
AO  2          EPOXY .8765E-050.0000E+00          0.2790E-01          -.2350E+00
AP  2          EPOXY .8765E-050.0000E+00          0.2790E-01          -.2450E+00
AQ  2          EPOXY .8765E-050.0000E+00          0.2790E-01          -.2550E+00
AR  2          EPOXY .8765E-050.0000E+00          0.2790E-01          -.2650E+00
AS  2          EPOXY .8765E-050.0000E+00          0.2790E-01          -.2750E+00
AT  2          EPOXY .8765E-050.0000E+00          0.2790E-01          -.2850E+00
AU  2          EPOXY .8765E-050.0000E+00          0.2790E-01          -.2950E+00
AV  2          EPOXY .8765E-050.0000E+00          0.2790E-01          -.3050E+00
AW  2          EPOXY .8765E-050.0000E+00          0.2790E-01          -.3150E+00
AX  2          EPOXY .1753E-050.0000E+00          0.2790E-01          -.3210E+00
AY  2          EPOXY .1753E-050.0000E+00          0.2790E-01          -.3230E+00
AZ  2          EPOXY .1753E-050.0000E+00          0.2790E-01          -.3250E+00
B1  2          EPOXY .1753E-050.0000E+00          0.2790E-01          -.3270E+00
B2  2          EPOXY .1753E-050.0000E+00          0.2790E-01          -.3290E+00
B3  2          EPOXY .1753E-050.0000E+00          0.2790E-01          -.3310E+00
B4  2          EPOXY .1753E-050.0000E+00          0.2790E-01          -.3330E+00
B5  2          EPOXY .1753E-050.0000E+00          0.2790E-01          -.3350E+00
B6  2          EPOXY .1753E-050.0000E+00          0.2790E-01          -.3370E+00
B7  2          EPOXY .1753E-050.0000E+00          0.2790E-01          -.3390E+00
B8  2          EPOXY .1753E-050.0000E+00          0.2790E-01          -.3410E+00
B9  2          EPOXY .1753E-050.0000E+00          0.2790E-01          -.3430E+00
BA  2          EPOXY .1753E-050.0000E+00          0.2790E-01          -.3450E+00
BB  2          EPOXY .1753E-050.0000E+00          0.2790E-01          -.3470E+00
BC  2          EPOXY .1753E-050.0000E+00          0.2790E-01          -.3490E+00
BD  2          EPOXY .1753E-050.0000E+00          0.2790E-01          -.3510E+00
BE  2          EPOXY .1753E-050.0000E+00          0.2790E-01          -.3530E+00
BF  2          EPOXY .1753E-050.0000E+00          0.2790E-01          -.3550E+00
BG  2          EPOXY .1753E-050.0000E+00          0.2790E-01          -.3570E+00
BH  2          EPOXY .1753E-050.0000E+00          0.2790E-01          -.3590E+00
BI  2          EPOXY .1753E-050.0000E+00          0.2790E-01          -.3610E+00
BJ  2          EPOXY .1753E-050.0000E+00          0.2790E-01          -.3630E+00
BK  2          EPOXY .1753E-050.0000E+00          0.2790E-01          -.3650E+00
BL  2          EPOXY .1753E-050.0000E+00          0.2790E-01          -.3670E+00
BM  2          EPOXY .1753E-050.0000E+00          0.2790E-01          -.3690E+00
BN  2          EPOXY .1753E-050.0000E+00          0.2790E-01          -.3710E+00
BO  2          EPOXY .1753E-050.0000E+00          0.2790E-01          -.3730E+00
BP  2          EPOXY .1753E-050.0000E+00          0.2790E-01          -.3750E+00
BQ  2          EPOXY .1753E-050.0000E+00          0.2790E-01          -.3770E+00
BR  2          EPOXY .1753E-050.0000E+00          0.2790E-01          -.3790E+00
BS  2          EPOXY .1753E-050.0000E+00          0.2790E-01          -.3810E+00
```

```
BT  2          EPOXY .1753E-050.0000E+00          0.2790E-01          -.3830E+00
BU  2          EPOXY .1753E-050.0000E+00          0.2790E-01          -.3850E+00
BV  2          EPOXY .1753E-050.0000E+00          0.2790E-01          -.3870E+00
BW  2          EPOXY .1753E-050.0000E+00          0.2790E-01          -.3890E+00
BX  2          EPOXY .1753E-050.0000E+00          0.2790E-01          -.3910E+00
BY  2          EPOXY .1753E-050.0000E+00          0.2790E-01          -.3930E+00
BZ  2          EPOXY .1753E-050.0000E+00          0.2790E-01          -.3950E+00
C1  2          EPOXY .1753E-050.0000E+00          0.2790E-01          -.3970E+00
C2  2          EPOXY .1753E-050.0000E+00          0.2790E-01          -.3990E+00
C3  2          EPOXY .1753E-050.0000E+00          0.2790E-01          -.4010E+00
C4  2          EPOXY .1753E-050.0000E+00          0.2790E-01          -.4030E+00
C5  2          EPOXY .1753E-050.0000E+00          0.2790E-01          -.4050E+00
C6  2          EPOXY .1753E-050.0000E+00          0.2790E-01          -.4070E+00
C7  2          EPOXY .1753E-050.0000E+00          0.2790E-01          -.4090E+00
C8  2          EPOXY .1753E-050.0000E+00          0.2790E-01          -.4110E+00
C9  2          EPOXY .1753E-050.0000E+00          0.2790E-01          -.4130E+00
CA  2          EPOXY .1753E-050.0000E+00          0.2790E-01          -.4150E+00
CB  2          EPOXY .1753E-050.0000E+00          0.2790E-01          -.4170E+00
CC  2          EPOXY .1753E-050.0000E+00          0.2790E-01          -.4190E+00
CD  2          EPOXY .1753E-050.0000E+00          0.2790E-01          -.4210E+00
CE  2          EPOXY .1753E-050.0000E+00          0.2790E-01          -.4230E+00
CF  2          EPOXY .1753E-050.0000E+00          0.2790E-01          -.4250E+00
CG  2          EPOXY .1753E-050.0000E+00          0.2790E-01          -.4270E+00
CH  2          EPOXY .1753E-050.0000E+00          0.2790E-01          -.4290E+00
CI  2          EPOXY .1753E-050.0000E+00          0.2790E-01          -.4310E+00
CJ  2          EPOXY .1753E-050.0000E+00          0.2790E-01          -.4330E+00
CK  2          EPOXY .1753E-050.0000E+00          0.2790E-01          -.4350E+00
CL  2          EPOXY .1753E-050.0000E+00          0.2790E-01          -.4370E+00
CM  2          EPOXY .1753E-050.0000E+00          0.2790E-01          -.4390E+00
CN  2          EPOXY .4383E-040.0000E+00          0.2790E-01          -.4650E+00
CO  2          HEATB .8765E-050.0000E+00          0.2790E-01          -.4950E+00
CP  2          HEATB .8765E-050.0000E+00          0.2790E-01          -.5050E+00
CQ  2          HEATB .8765E-050.0000E+00          0.2790E-01          -.5150E+00
CR  2          HEATB .8765E-050.0000E+00          0.2790E-01          -.5250E+00
CS  2          HEATB .8765E-050.0000E+00          0.2790E-01          -.5350E+00
A2  3          INSUL .1781E-030.0000E+00          0.5580E-01          -.1500E-01
A3  3          INSUL .1781E-030.0000E+00          0.5580E-01          -.2500E-01
A4  3          INSUL .1781E-030.0000E+00          0.5580E-01          -.3500E-01
A5  3          INSUL .1781E-030.0000E+00          0.5580E-01          -.4500E-01
A6  3          INSUL .1781E-030.0000E+00          0.5580E-01          -.5500E-01
A7  3          INSUL .1781E-030.0000E+00          0.5580E-01          -.6500E-01
A8  3          INSUL .1781E-030.0000E+00          0.5580E-01          -.7500E-01
A9  3          INSUL .1781E-030.0000E+00          0.5580E-01          -.8500E-01
AA  3          INSUL .1781E-030.0000E+00          0.5580E-01          -.9500E-01
AB  3          INSUL .1781E-030.0000E+00          0.5580E-01          -.1050E+00
AC  3          INSUL .1781E-030.0000E+00          0.5580E-01          -.1150E+00
AD  3          INSUL .1781E-030.0000E+00          0.5580E-01          -.1250E+00
AE  3          INSUL .1781E-030.0000E+00          0.5580E-01          -.1350E+00
AF  3          INSUL .1781E-030.0000E+00          0.5580E-01          -.1450E+00
AG  3          INSUL .1781E-030.0000E+00          0.5580E-01          -.1550E+00
AH  3          INSUL .1781E-030.0000E+00          0.5580E-01          -.1650E+00
AI  3          INSUL .1781E-030.0000E+00          0.5580E-01          -.1750E+00
AJ  3          INSUL .1781E-030.0000E+00          0.5580E-01          -.1850E+00
AK  3          INSUL .1781E-030.0000E+00          0.5580E-01          -.1950E+00
AL  3          INSUL .1781E-030.0000E+00          0.5580E-01          -.2050E+00
AM  3          INSUL .1781E-030.0000E+00          0.5580E-01          -.2150E+00
AN  3          INSUL .1781E-030.0000E+00          0.5580E-01          -.2250E+00
AO  3          INSUL .1781E-030.0000E+00          0.5580E-01          -.2350E+00
AP  3          INSUL .1781E-030.0000E+00          0.5580E-01          -.2450E+00
AQ  3          INSUL .1781E-030.0000E+00          0.5580E-01          -.2550E+00
AR  3          INSUL .1781E-030.0000E+00          0.5580E-01          -.2650E+00
AS  3          INSUL .1781E-030.0000E+00          0.5580E-01          -.2750E+00
AT  3          INSUL .1781E-030.0000E+00          0.5580E-01          -.2850E+00
AU  3          INSUL .1781E-030.0000E+00          0.5580E-01          -.2950E+00
AV  3          INSUL .1781E-030.0000E+00          0.5580E-01          -.3050E+00
AW  3          INSUL .1781E-030.0000E+00          0.5580E-01          -.3150E+00
AX  3          INSUL .3562E-040.0000E+00          0.5580E-01          -.3210E+00
AY  3          INSUL .3562E-040.0000E+00          0.5580E-01          -.3230E+00
AZ  3          INSUL .3562E-040.0000E+00          0.5580E-01          -.3250E+00
B1  3          INSUL .3562E-040.0000E+00          0.5580E-01          -.3270E+00
B2  3          INSUL .3562E-040.0000E+00          0.5580E-01          -.3290E+00
B3  3          INSUL .3562E-040.0000E+00          0.5580E-01          -.3310E+00
B4  3          INSUL .3562E-040.0000E+00          0.5580E-01          -.3330E+00
B5  3          INSUL .3562E-040.0000E+00          0.5580E-01          -.3350E+00
B6  3          INSUL .3562E-040.0000E+00          0.5580E-01          -.3370E+00
B7  3          INSUL .3562E-040.0000E+00          0.5580E-01          -.3390E+00
```

```
B8  3          INSUL .3562E-040.0000E+00          0.5580E-01          -.3410E+00
B9  3          INSUL .3562E-040.0000E+00          0.5580E-01          -.3430E+00
BA  3          INSUL .3562E-040.0000E+00          0.5580E-01          -.3450E+00
BB  3          INSUL .3562E-040.0000E+00          0.5580E-01          -.3470E+00
BC  3          INSUL .3562E-040.0000E+00          0.5580E-01          -.3490E+00
BD  3          INSUL .3562E-040.0000E+00          0.5580E-01          -.3510E+00
BE  3          INSUL .3562E-040.0000E+00          0.5580E-01          -.3530E+00
BF  3          INSUL .3562E-040.0000E+00          0.5580E-01          -.3550E+00
BG  3          INSUL .3562E-040.0000E+00          0.5580E-01          -.3570E+00
BH  3          INSUL .3562E-040.0000E+00          0.5580E-01          -.3590E+00
BI  3          INSUL .3562E-040.0000E+00          0.5580E-01          -.3610E+00
BJ  3          INSUL .3562E-040.0000E+00          0.5580E-01          -.3630E+00
BK  3          INSUL .3562E-040.0000E+00          0.5580E-01          -.3650E+00
BL  3          INSUL .3562E-040.0000E+00          0.5580E-01          -.3670E+00
BM  3          INSUL .3562E-040.0000E+00          0.5580E-01          -.3690E+00
BN  3          INSUL .3562E-040.0000E+00          0.5580E-01          -.3710E+00
BO  3          INSUL .3562E-040.0000E+00          0.5580E-01          -.3730E+00
BP  3          INSUL .3562E-040.0000E+00          0.5580E-01          -.3750E+00
BQ  3          INSUL .3562E-040.0000E+00          0.5580E-01          -.3770E+00
BR  3          INSUL .3562E-040.0000E+00          0.5580E-01          -.3790E+00
BS  3          INSUL .3562E-040.0000E+00          0.5580E-01          -.3810E+00
BT  3          INSUL .3562E-040.0000E+00          0.5580E-01          -.3830E+00
BU  3          INSUL .3562E-040.0000E+00          0.5580E-01          -.3850E+00
BV  3          INSUL .3562E-040.0000E+00          0.5580E-01          -.3870E+00
BW  3          INSUL .3562E-040.0000E+00          0.5580E-01          -.3890E+00
BX  3          INSUL .3562E-040.0000E+00          0.5580E-01          -.3910E+00
BY  3          INSUL .3562E-040.0000E+00          0.5580E-01          -.3930E+00
BZ  3          INSUL .3562E-040.0000E+00          0.5580E-01          -.3950E+00
C1  3          INSUL .3562E-040.0000E+00          0.5580E-01          -.3970E+00
C2  3          INSUL .3562E-040.0000E+00          0.5580E-01          -.3990E+00
C3  3          INSUL .3562E-040.0000E+00          0.5580E-01          -.4010E+00
C4  3          INSUL .3562E-040.0000E+00          0.5580E-01          -.4030E+00
C5  3          INSUL .3562E-040.0000E+00          0.5580E-01          -.4050E+00
C6  3          INSUL .3562E-040.0000E+00          0.5580E-01          -.4070E+00
C7  3          INSUL .3562E-040.0000E+00          0.5580E-01          -.4090E+00
C8  3          INSUL .3562E-040.0000E+00          0.5580E-01          -.4110E+00
C9  3          INSUL .3562E-040.0000E+00          0.5580E-01          -.4130E+00
CA  3          INSUL .3562E-040.0000E+00          0.5580E-01          -.4150E+00
CB  3          INSUL .3562E-040.0000E+00          0.5580E-01          -.4170E+00
CC  3          INSUL .3562E-040.0000E+00          0.5580E-01          -.4190E+00
CD  3          INSUL .3562E-040.0000E+00          0.5580E-01          -.4210E+00
CE  3          INSUL .3562E-040.0000E+00          0.5580E-01          -.4230E+00
CF  3          INSUL .3562E-040.0000E+00          0.5580E-01          -.4250E+00
CG  3          INSUL .3562E-040.0000E+00          0.5580E-01          -.4270E+00
CH  3          INSUL .3562E-040.0000E+00          0.5580E-01          -.4290E+00
CI  3          INSUL .3562E-040.0000E+00          0.5580E-01          -.4310E+00
CJ  3          INSUL .3562E-040.0000E+00          0.5580E-01          -.4330E+00
CK  3          INSUL .3562E-040.0000E+00          0.5580E-01          -.4350E+00
CL  3          INSUL .3562E-040.0000E+00          0.5580E-01          -.4370E+00
CM  3          INSUL .3562E-040.0000E+00          0.5580E-01          -.4390E+00
CN  3          INSUL .8905E-030.0000E+00          0.5580E-01          -.4650E+00
CO  3          HEATB .1781E-030.0000E+00          0.5580E-01          -.4950E+00
CP  3          HEATB .1781E-030.0000E+00          0.5580E-01          -.5050E+00
CQ  3          HEATB .1781E-030.0000E+00          0.5580E-01          -.5150E+00
CR  3          HEATB .1781E-030.0000E+00          0.5580E-01          -.5250E+00
CS  3          HEATB .1781E-030.0000E+00          0.5580E-01          -.5350E+00

CONNE
A2  1A2  2                  10.1270E-010.2500E-020.1596E-02
A3  1A3  2                  10.1270E-010.2500E-020.1596E-02
A4  1A4  2                  10.1270E-010.2500E-020.1596E-02
A5  1A5  2                  10.1270E-010.2500E-020.1596E-02
A6  1A6  2                  10.1270E-010.2500E-020.1596E-02
A7  1A7  2                  10.1270E-010.2500E-020.1596E-02
A8  1A8  2                  10.1270E-010.2500E-020.1596E-02
A9  1A9  2                  10.1270E-010.2500E-020.1596E-02
AA  1AA  2                  10.1270E-010.2500E-020.1596E-02
AB  1AB  2                  10.1270E-010.2500E-020.1596E-02
AC  1AC  2                  10.1270E-010.2500E-020.1596E-02
AD  1AD  2                  10.1270E-010.2500E-020.1596E-02
AE  1AE  2                  10.1270E-010.2500E-020.1596E-02
AF  1AF  2                  10.1270E-010.2500E-020.1596E-02
AG  1AG  2                  10.1270E-010.2500E-020.1596E-02
AH  1AH  2                  10.1270E-010.2500E-020.1596E-02
AI  1AI  2                  10.1270E-010.2500E-020.1596E-02
AJ  1AJ  2                  10.1270E-010.2500E-020.1596E-02
```

```
AK  1AK  2                 10.1270E-010.2500E-020.1596E-02
AL  1AL  2                 10.1270E-010.2500E-020.1596E-02
AM  1AM  2                 10.1270E-010.2500E-020.1596E-02
AN  1AN  2                 10.1270E-010.2500E-020.1596E-02
AO  1AO  2                 10.1270E-010.2500E-020.1596E-02
AP  1AP  2                 10.1270E-010.2500E-020.1596E-02
AQ  1AQ  2                 10.1270E-010.2500E-020.1596E-02
AR  1AR  2                 10.1270E-010.2500E-020.1596E-02
AS  1AS  2                 10.1270E-010.2500E-020.1596E-02
AT  1AT  2                 10.1270E-010.2500E-020.1596E-02
AU  1AU  2                 10.1270E-010.2500E-020.1596E-02
AV  1AV  2                 10.1270E-010.2500E-020.1596E-02
AW  1AW  2                 10.1270E-010.2500E-020.1596E-02
AX  1AX  2                 10.1270E-010.2500E-020.3192E-03
AY  1AY  2                 10.1270E-010.2500E-020.3192E-03
AZ  1AZ  2                 10.1270E-010.2500E-020.3192E-03
B1  1B1  2                 10.1270E-010.2500E-020.3192E-03
B2  1B2  2                 10.1270E-010.2500E-020.3192E-03
B3  1B3  2                 10.1270E-010.2500E-020.3192E-03
B4  1B4  2                 10.1270E-010.2500E-020.3192E-03
B5  1B5  2                 10.1270E-010.2500E-020.3192E-03
B6  1B6  2                 10.1270E-010.2500E-020.3192E-03
B7  1B7  2                 10.1270E-010.2500E-020.3192E-03
B8  1B8  2                 10.1270E-010.2500E-020.3192E-03
B9  1B9  2                 10.1270E-010.2500E-020.3192E-03
BA  1BA  2                 10.1270E-010.2500E-020.3192E-03
BB  1BB  2                 10.1270E-010.2500E-020.3192E-03
BC  1BC  2                 10.1270E-010.2500E-020.3192E-03
BD  1BD  2                 10.1270E-010.2500E-020.3192E-03
BE  1BE  2                 10.1270E-010.2500E-020.3192E-03
BF  1BF  2                 10.1270E-010.2500E-020.3192E-03
BG  1BG  2                 10.1270E-010.2500E-020.3192E-03
BH  1BH  2                 10.1270E-010.2500E-020.3192E-03
BI  1BI  2                 10.1270E-010.2500E-020.3192E-03
BJ  1BJ  2                 10.1270E-010.2500E-020.3192E-03
BK  1BK  2                 10.1270E-010.2500E-020.3192E-03
BL  1BL  2                 10.1270E-010.2500E-020.3192E-03
BM  1BM  2                 10.1270E-010.2500E-020.3192E-03
BN  1BN  2                 10.1270E-010.2500E-020.3192E-03
BO  1BO  2                 10.1270E-010.2500E-020.3192E-03
BP  1BP  2                 10.1270E-010.2500E-020.3192E-03
BQ  1BQ  2                 10.1270E-010.2500E-020.3192E-03
BR  1BR  2                 10.1270E-010.2500E-020.3192E-03
BS  1BS  2                 10.1270E-010.2500E-020.3192E-03
BT  1BT  2                 10.1270E-010.2500E-020.3192E-03
BU  1BU  2                 10.1270E-010.2500E-020.3192E-03
BV  1BV  2                 10.1270E-010.2500E-020.3192E-03
BW  1BW  2                 10.1270E-010.2500E-020.3192E-03
BX  1BX  2                 10.1270E-010.2500E-020.3192E-03
BY  1BY  2                 10.1270E-010.2500E-020.3192E-03
BZ  1BZ  2                 10.1270E-010.2500E-020.3192E-03
C1  1C1  2                 10.1270E-010.2500E-020.3192E-03
C2  1C2  2                 10.1270E-010.2500E-020.3192E-03
C3  1C3  2                 10.1270E-010.2500E-020.3192E-03
C4  1C4  2                 10.1270E-010.2500E-020.3192E-03
C5  1C5  2                 10.1270E-010.2500E-020.3192E-03
C6  1C6  2                 10.1270E-010.2500E-020.3192E-03
C7  1C7  2                 10.1270E-010.2500E-020.3192E-03
C8  1C8  2                 10.1270E-010.2500E-020.3192E-03
C9  1C9  2                 10.1270E-010.2500E-020.3192E-03
CA  1CA  2                 10.1270E-010.2500E-020.3192E-03
CB  1CB  2                 10.1270E-010.2500E-020.3192E-03
CC  1CC  2                 10.1270E-010.2500E-020.3192E-03
CD  1CD  2                 10.1270E-010.2500E-020.3192E-03
CE  1CE  2                 10.1270E-010.2500E-020.3192E-03
CF  1CF  2                 10.1270E-010.2500E-020.3192E-03
CG  1CG  2                 10.1270E-010.2500E-020.3192E-03
CH  1CH  2                 10.1270E-010.2500E-020.3192E-03
CI  1CI  2                 10.1270E-010.2500E-020.3192E-03
CJ  1CJ  2                 10.1270E-010.2500E-020.3192E-03
CK  1CK  2                 10.1270E-010.2500E-020.3192E-03
CL  1CL  2                 10.1270E-010.2500E-020.3192E-03
CM  1CM  2                 10.1270E-010.2500E-020.3192E-03
CN1 1CN  2                 10.1270E-010.2500E-020.1596E-03
CN2 1CN  2                 10.1270E-010.2500E-020.1596E-03
CN3 1CN  2                 10.1270E-010.2500E-020.1596E-03
```

```
CN4 1CN  2                10.1270E-010.2500E-020.1596E-03
CN5 1CN  2                10.1270E-010.2500E-020.1596E-03
CO  1CO  2                10.1270E-010.2500E-020.1596E-02
CP  1CP  2                10.1270E-010.2500E-020.1596E-02
CQ  1CQ  2                10.1270E-010.2500E-020.1596E-02
CR  1CR  2                10.1270E-010.2500E-020.1596E-02
CS  1CS  2                10.1270E-010.2500E-020.1596E-02
A2  2A2  3                10.2500E-020.2540E-010.1910E-02
A3  2A3  3                10.2500E-020.2540E-010.1910E-02
A4  2A4  3                10.2500E-020.2540E-010.1910E-02
A5  2A5  3                10.2500E-020.2540E-010.1910E-02
A6  2A6  3                10.2500E-020.2540E-010.1910E-02
A7  2A7  3                10.2500E-020.2540E-010.1910E-02
A8  2A8  3                10.2500E-020.2540E-010.1910E-02
A9  2A9  3                10.2500E-020.2540E-010.1910E-02
AA  2AA  3                10.2500E-020.2540E-010.1910E-02
AB  2AB  3                10.2500E-020.2540E-010.1910E-02
AC  2AC  3                10.2500E-020.2540E-010.1910E-02
AD  2AD  3                10.2500E-020.2540E-010.1910E-02
AE  2AE  3                10.2500E-020.2540E-010.1910E-02
AF  2AF  3                10.2500E-020.2540E-010.1910E-02
AG  2AG  3                10.2500E-020.2540E-010.1910E-02
AH  2AH  3                10.2500E-020.2540E-010.1910E-02
AI  2AI  3                10.2500E-020.2540E-010.1910E-02
AJ  2AJ  3                10.2500E-020.2540E-010.1910E-02
AK  2AK  3                10.2500E-020.2540E-010.1910E-02
AL  2AL  3                10.2500E-020.2540E-010.1910E-02
AM  2AM  3                10.2500E-020.2540E-010.1910E-02
AN  2AN  3                10.2500E-020.2540E-010.1910E-02
AO  2AO  3                10.2500E-020.2540E-010.1910E-02
AP  2AP  3                10.2500E-020.2540E-010.1910E-02
AQ  2AQ  3                10.2500E-020.2540E-010.1910E-02
AR  2AR  3                10.2500E-020.2540E-010.1910E-02
AS  2AS  3                10.2500E-020.2540E-010.1910E-02
AT  2AT  3                10.2500E-020.2540E-010.1910E-02
AU  2AU  3                10.2500E-020.2540E-010.1910E-02
AV  2AV  3                10.2500E-020.2540E-010.1910E-02
AW  2AW  3                10.2500E-020.2540E-010.1910E-02
AX  2AX  3                10.2500E-020.2540E-010.3820E-03
AY  2AY  3                10.2500E-020.2540E-010.3820E-03
AZ  2AZ  3                10.2500E-020.2540E-010.3820E-03
B1  2B1  3                10.2500E-020.2540E-010.3820E-03
B2  2B2  3                10.2500E-020.2540E-010.3820E-03
B3  2B3  3                10.2500E-020.2540E-010.3820E-03
B4  2B4  3                10.2500E-020.2540E-010.3820E-03
B5  2B5  3                10.2500E-020.2540E-010.3820E-03
B6  2B6  3                10.2500E-020.2540E-010.3820E-03
B7  2B7  3                10.2500E-020.2540E-010.3820E-03
B8  2B8  3                10.2500E-020.2540E-010.3820E-03
B9  2B9  3                10.2500E-020.2540E-010.3820E-03
BA  2BA  3                10.2500E-020.2540E-010.3820E-03
BB  2BB  3                10.2500E-020.2540E-010.3820E-03
BC  2BC  3                10.2500E-020.2540E-010.3820E-03
BD  2BD  3                10.2500E-020.2540E-010.3820E-03
BE  2BE  3                10.2500E-020.2540E-010.3820E-03
BF  2BF  3                10.2500E-020.2540E-010.3820E-03
BG  2BG  3                10.2500E-020.2540E-010.3820E-03
BH  2BH  3                10.2500E-020.2540E-010.3820E-03
BI  2BI  3                10.2500E-020.2540E-010.3820E-03
BJ  2BJ  3                10.2500E-020.2540E-010.3820E-03
BK  2BK  3                10.2500E-020.2540E-010.3820E-03
BL  2BL  3                10.2500E-020.2540E-010.3820E-03
BM  2BM  3                10.2500E-020.2540E-010.3820E-03
BN  2BN  3                10.2500E-020.2540E-010.3820E-03
BO  2BO  3                10.2500E-020.2540E-010.3820E-03
BP  2BP  3                10.2500E-020.2540E-010.3820E-03
BQ  2BQ  3                10.2500E-020.2540E-010.3820E-03
BR  2BR  3                10.2500E-020.2540E-010.3820E-03
BS  2BS  3                10.2500E-020.2540E-010.3820E-03
BT  2BT  3                10.2500E-020.2540E-010.3820E-03
BU  2BU  3                10.2500E-020.2540E-010.3820E-03
BV  2BV  3                10.2500E-020.2540E-010.3820E-03
BW  2BW  3                10.2500E-020.2540E-010.3820E-03
BX  2BX  3                10.2500E-020.2540E-010.3820E-03
BY  2BY  3                10.2500E-020.2540E-010.3820E-03
BZ  2BZ  3                10.2500E-020.2540E-010.3820E-03
```

```
C1  2C1  3                  10.2500E-020.2540E-010.3820E-03
C2  2C2  3                  10.2500E-020.2540E-010.3820E-03
C3  2C3  3                  10.2500E-020.2540E-010.3820E-03
C4  2C4  3                  10.2500E-020.2540E-010.3820E-03
C5  2C5  3                  10.2500E-020.2540E-010.3820E-03
C6  2C6  3                  10.2500E-020.2540E-010.3820E-03
C7  2C7  3                  10.2500E-020.2540E-010.3820E-03
C8  2C8  3                  10.2500E-020.2540E-010.3820E-03
C9  2C9  3                  10.2500E-020.2540E-010.3820E-03
CA  2CA  3                  10.2500E-020.2540E-010.3820E-03
CB  2CB  3                  10.2500E-020.2540E-010.3820E-03
CC  2CC  3                  10.2500E-020.2540E-010.3820E-03
CD  2CD  3                  10.2500E-020.2540E-010.3820E-03
CE  2CE  3                  10.2500E-020.2540E-010.3820E-03
CF  2CF  3                  10.2500E-020.2540E-010.3820E-03
CG  2CG  3                  10.2500E-020.2540E-010.3820E-03
CH  2CH  3                  10.2500E-020.2540E-010.3820E-03
CI  2CI  3                  10.2500E-020.2540E-010.3820E-03
CJ  2CJ  3                  10.2500E-020.2540E-010.3820E-03
CK  2CK  3                  10.2500E-020.2540E-010.3820E-03
CL  2CL  3                  10.2500E-020.2540E-010.3820E-03
CM  2CM  3                  10.2500E-020.2540E-010.3820E-03
CN  2CN  3                  10.2500E-020.2540E-010.9550E-03
CO  2CO  3                  10.2500E-020.2540E-010.1910E-02
CP  2CP  3                  10.2500E-020.2540E-010.1910E-02
CQ  2CQ  3                  10.2500E-020.2540E-010.1910E-02
CR  2CR  3                  10.2500E-020.2540E-010.1910E-02
CS  2CS  3                  10.2500E-020.2540E-010.1910E-02
A2  3AMB 1                  10.2540E-011.0000E-110.5102E-02
A3  3AMB 1                  10.2540E-011.0000E-110.5102E-02
A4  3AMB 1                  10.2540E-011.0000E-110.5102E-02
A5  3AMB 1                  10.2540E-011.0000E-110.5102E-02
A6  3AMB 1                  10.2540E-011.0000E-110.5102E-02
A7  3AMB 1                  10.2540E-011.0000E-110.5102E-02
A8  3AMB 1                  10.2540E-011.0000E-110.5102E-02
A9  3AMB 1                  10.2540E-011.0000E-110.5102E-02
AA  3AMB 1                  10.2540E-011.0000E-110.5102E-02
AB  3AMB 1                  10.2540E-011.0000E-110.5102E-02
AC  3AMB 1                  10.2540E-011.0000E-110.5102E-02
AD  3AMB 1                  10.2540E-011.0000E-110.5102E-02
AE  3AMB 1                  10.2540E-011.0000E-110.5102E-02
AF  3AMB 1                  10.2540E-011.0000E-110.5102E-02
AG  3AMB 1                  10.2540E-011.0000E-110.5102E-02
AH  3AMB 1                  10.2540E-011.0000E-110.5102E-02
AI  3AMB 1                  10.2540E-011.0000E-110.5102E-02
AJ  3AMB 1                  10.2540E-011.0000E-110.5102E-02
AK  3AMB 1                  10.2540E-011.0000E-110.5102E-02
AL  3AMB 1                  10.2540E-011.0000E-110.5102E-02
AM  3AMB 1                  10.2540E-011.0000E-110.5102E-02
AN  3AMB 1                  10.2540E-011.0000E-110.5102E-02
AO  3AMB 1                  10.2540E-011.0000E-110.5102E-02
AP  3AMB 1                  10.2540E-011.0000E-110.5102E-02
AQ  3AMB 1                  10.2540E-011.0000E-110.5102E-02
AR  3AMB 1                  10.2540E-011.0000E-110.5102E-02
AS  3AMB 1                  10.2540E-011.0000E-110.5102E-02
AT  3AMB 1                  10.2540E-011.0000E-110.5102E-02
AU  3AMB 1                  10.2540E-011.0000E-110.5102E-02
AV  3AMB 1                  10.2540E-011.0000E-110.5102E-02
AW  3AMB 1                  10.2540E-011.0000E-110.5102E-02
AX  3AMB 1                  10.2540E-011.0000E-110.1020E-02
AY  3AMB 1                  10.2540E-011.0000E-110.1020E-02
AZ  3AMB 1                  10.2540E-011.0000E-110.1020E-02
B1  3AMB 1                  10.2540E-011.0000E-110.1020E-02
B2  3AMB 1                  10.2540E-011.0000E-110.1020E-02
B3  3AMB 1                  10.2540E-011.0000E-110.1020E-02
B4  3AMB 1                  10.2540E-011.0000E-110.1020E-02
B5  3AMB 1                  10.2540E-011.0000E-110.1020E-02
B6  3AMB 1                  10.2540E-011.0000E-110.1020E-02
B7  3AMB 1                  10.2540E-011.0000E-110.1020E-02
B8  3AMB 1                  10.2540E-011.0000E-110.1020E-02
B9  3AMB 1                  10.2540E-011.0000E-110.1020E-02
BA  3AMB 1                  10.2540E-011.0000E-110.1020E-02
BB  3AMB 1                  10.2540E-011.0000E-110.1020E-02
BC  3AMB 1                  10.2540E-011.0000E-110.1020E-02
BD  3AMB 1                  10.2540E-011.0000E-110.1020E-02
BE  3AMB 1                  10.2540E-011.0000E-110.1020E-02
```

```
BF  3AMB 1                  10.2540E-011.0000E-110.1020E-02
BG  3AMB 1                  10.2540E-011.0000E-110.1020E-02
BH  3AMB 1                  10.2540E-011.0000E-110.1020E-02
BI  3AMB 1                  10.2540E-011.0000E-110.1020E-02
BJ  3AMB 1                  10.2540E-011.0000E-110.1020E-02
BK  3AMB 1                  10.2540E-011.0000E-110.1020E-02
BL  3AMB 1                  10.2540E-011.0000E-110.1020E-02
BM  3AMB 1                  10.2540E-011.0000E-110.1020E-02
BN  3AMB 1                  10.2540E-011.0000E-110.1020E-02
BO  3AMB 1                  10.2540E-011.0000E-110.1020E-02
BP  3AMB 1                  10.2540E-011.0000E-110.1020E-02
BQ  3AMB 1                  10.2540E-011.0000E-110.1020E-02
BR  3AMB 1                  10.2540E-011.0000E-110.1020E-02
BS  3AMB 1                  10.2540E-011.0000E-110.1020E-02
BT  3AMB 1                  10.2540E-011.0000E-110.1020E-02
BU  3AMB 1                  10.2540E-011.0000E-110.1020E-02
BV  3AMB 1                  10.2540E-011.0000E-110.1020E-02
BW  3AMB 1                  10.2540E-011.0000E-110.1020E-02
BX  3AMB 1                  10.2540E-011.0000E-110.1020E-02
BY  3AMB 1                  10.2540E-011.0000E-110.1020E-02
BZ  3AMB 1                  10.2540E-011.0000E-110.1020E-02
C1  3AMB 1                  10.2540E-011.0000E-110.1020E-02
C2  3AMB 1                  10.2540E-011.0000E-110.1020E-02
C3  3AMB 1                  10.2540E-011.0000E-110.1020E-02
C4  3AMB 1                  10.2540E-011.0000E-110.1020E-02
C5  3AMB 1                  10.2540E-011.0000E-110.1020E-02
C6  3AMB 1                  10.2540E-011.0000E-110.1020E-02
C7  3AMB 1                  10.2540E-011.0000E-110.1020E-02
C8  3AMB 1                  10.2540E-011.0000E-110.1020E-02
C9  3AMB 1                  10.2540E-011.0000E-110.1020E-02
CA  3AMB 1                  10.2540E-011.0000E-110.1020E-02
CB  3AMB 1                  10.2540E-011.0000E-110.1020E-02
CC  3AMB 1                  10.2540E-011.0000E-110.1020E-02
CD  3AMB 1                  10.2540E-011.0000E-110.1020E-02
CE  3AMB 1                  10.2540E-011.0000E-110.1020E-02
CF  3AMB 1                  10.2540E-011.0000E-110.1020E-02
CG  3AMB 1                  10.2540E-011.0000E-110.1020E-02
CH  3AMB 1                  10.2540E-011.0000E-110.1020E-02
CI  3AMB 1                  10.2540E-011.0000E-110.1020E-02
CJ  3AMB 1                  10.2540E-011.0000E-110.1020E-02
CK  3AMB 1                  10.2540E-011.0000E-110.1020E-02
CL  3AMB 1                  10.2540E-011.0000E-110.1020E-02
CM  3AMB 1                  10.2540E-011.0000E-110.1020E-02
CN  3AMB 1                  10.2540E-011.0000E-110.2551E-02
CO  3AMB 1                  10.2540E-011.0000E-110.5102E-02
CP  3AMB 1                  10.2540E-011.0000E-110.5102E-02
CQ  3AMB 1                  10.2540E-011.0000E-110.5102E-02
CR  3AMB 1                  10.2540E-011.0000E-110.5102E-02
CS  3AMB 1                  10.2540E-011.0000E-110.5102E-02
BOU 1A2  1                  31.0000E-020.5000E-020.2027E-021.
A2  1A3  1                  30.5000E-020.5000E-020.2027E-021.
A3  1A4  1                  30.5000E-020.5000E-020.2027E-021.
A4  1A5  1                  30.5000E-020.5000E-020.2027E-021.
A5  1A6  1                  30.5000E-020.5000E-020.2027E-021.
A6  1A7  1                  30.5000E-020.5000E-020.2027E-021.
A7  1A8  1                  30.5000E-020.5000E-020.2027E-021.
A8  1A9  1                  30.5000E-020.5000E-020.2027E-021.
A9  1AA  1                  30.5000E-020.5000E-020.2027E-021.
AA  1AB  1                  30.5000E-020.5000E-020.2027E-021.
AB  1AC  1                  30.5000E-020.5000E-020.2027E-021.
AC  1AD  1                  30.5000E-020.5000E-020.2027E-021.
AD  1AE  1                  30.5000E-020.5000E-020.2027E-021.
AE  1AF  1                  30.5000E-020.5000E-020.2027E-021.
AF  1AG  1                  30.5000E-020.5000E-020.2027E-021.
AG  1AH  1                  30.5000E-020.5000E-020.2027E-021.
AH  1AI  1                  30.5000E-020.5000E-020.2027E-021.
AI  1AJ  1                  30.5000E-020.5000E-020.2027E-021.
AJ  1AK  1                  30.5000E-020.5000E-020.2027E-021.
AK  1AL  1                  30.5000E-020.5000E-020.2027E-021.
AL  1AM  1                  30.5000E-020.5000E-020.2027E-021.
AM  1AN  1                  30.5000E-020.5000E-020.2027E-021.
AN  1AO  1                  30.5000E-020.5000E-020.2027E-021.
AO  1AP  1                  30.5000E-020.5000E-020.2027E-021.
AP  1AQ  1                  30.5000E-020.5000E-020.2027E-021.
AQ  1AR  1                  30.5000E-020.5000E-020.2027E-021.
AR  1AS  1                  30.5000E-020.5000E-020.2027E-021.
```

```
AS  1AT  1                  30.5000E-020.5000E-020.2027E-021.
AT  1AU  1                  30.5000E-020.5000E-020.2027E-021.
AU  1AV  1                  30.5000E-020.5000E-020.2027E-021.
AV  1AW  1                  30.5000E-020.5000E-020.2027E-021.
AW  1AX  1                  30.5000E-020.1000E-020.2027E-021.
AX  1AY  1                  30.1000E-020.1000E-020.2027E-021.
AY  1AZ  1                  30.1000E-020.1000E-020.2027E-021.
AZ  1B1  1                  30.1000E-020.1000E-020.2027E-021.
B1  1B2  1                  30.1000E-020.1000E-020.2027E-021.
B2  1B3  1                  30.1000E-020.1000E-020.2027E-021.
B3  1B4  1                  30.1000E-020.1000E-020.2027E-021.
B4  1B5  1                  30.1000E-020.1000E-020.2027E-021.
B5  1B6  1                  30.1000E-020.1000E-020.2027E-021.
B6  1B7  1                  30.1000E-020.1000E-020.2027E-021.
B7  1B8  1                  30.1000E-020.1000E-020.2027E-021.
B8  1B9  1                  30.1000E-020.1000E-020.2027E-021.
B9  1BA  1                  30.1000E-020.1000E-020.2027E-021.
BA  1BB  1                  30.1000E-020.1000E-020.2027E-021.
BB  1BC  1                  30.1000E-020.1000E-020.2027E-021.
BC  1BD  1                  30.1000E-020.1000E-020.2027E-021.
BD  1BE  1                  30.1000E-020.1000E-020.2027E-021.
BE  1BF  1                  30.1000E-020.1000E-020.2027E-021.
BF  1BG  1                  30.1000E-020.1000E-020.2027E-021.
BG  1BH  1                  30.1000E-020.1000E-020.2027E-021.
BH  1BI  1                  30.1000E-020.1000E-020.2027E-021.
BI  1BJ  1                  30.1000E-020.1000E-020.2027E-021.
BJ  1BK  1                  30.1000E-020.1000E-020.2027E-021.
BK  1BL  1                  30.1000E-020.1000E-020.2027E-021.
BL  1BM  1                  30.1000E-020.1000E-020.2027E-021.
BM  1BN  1                  30.1000E-020.1000E-020.2027E-021.
BN  1BO  1                  30.1000E-020.1000E-020.2027E-021.
BO  1BP  1                  30.1000E-020.1000E-020.2027E-021.
BP  1BQ  1                  30.1000E-020.1000E-020.2027E-021.
BQ  1BR  1                  30.1000E-020.1000E-020.2027E-021.
BR  1BS  1                  30.1000E-020.1000E-020.2027E-021.
BS  1BT  1                  30.1000E-020.1000E-020.2027E-021.
BT  1BU  1                  30.1000E-020.1000E-020.2027E-021.
BU  1BV  1                  30.1000E-020.1000E-020.2027E-021.
BV  1BW  1                  30.1000E-020.1000E-020.2027E-021.
BW  1BX  1                  30.1000E-020.1000E-020.2027E-021.
BX  1BY  1                  30.1000E-020.1000E-020.2027E-021.
BY  1BZ  1                  30.1000E-020.1000E-020.2027E-021.
BZ  1C1  1                  30.1000E-020.1000E-020.2027E-021.
C1  1C2  1                  30.1000E-020.1000E-020.2027E-021.
C2  1C3  1                  30.1000E-020.1000E-020.2027E-021.
C3  1C4  1                  30.1000E-020.1000E-020.2027E-021.
C4  1C5  1                  30.1000E-020.1000E-020.2027E-021.
C5  1C6  1                  30.1000E-020.1000E-020.2027E-021.
C6  1C7  1                  30.1000E-020.1000E-020.2027E-021.
C7  1C8  1                  30.1000E-020.1000E-020.2027E-021.
C8  1C9  1                  30.1000E-020.1000E-020.2027E-021.
C9  1CA  1                  30.1000E-020.1000E-020.2027E-021.
CA  1CB  1                  30.1000E-020.1000E-020.2027E-021.
CB  1CC  1                  30.1000E-020.1000E-020.2027E-021.
CC  1CD  1                  30.1000E-020.1000E-020.2027E-021.
CD  1CE  1                  30.1000E-020.1000E-020.2027E-021.
CE  1CF  1                  30.1000E-020.1000E-020.2027E-021.
CF  1CG  1                  30.1000E-020.1000E-020.2027E-021.
CG  1CH  1                  30.1000E-020.1000E-020.2027E-021.
CH  1CI  1                  30.1000E-020.1000E-020.2027E-021.
CI  1CJ  1                  30.1000E-020.1000E-020.2027E-021.
CJ  1CK  1                  30.1000E-020.1000E-020.2027E-021.
CK  1CL  1                  30.1000E-020.1000E-020.2027E-021.
CL  1CM  1                  30.1000E-020.1000E-020.2027E-021.
CM  1CN1 1                  30.1000E-020.5000E-030.2027E-021.
CN1 1CN2 1                  30.5000E-030.5000E-030.2027E-021.
CN2 1CN3 1                  30.5000E-030.5000E-030.2027E-021.
CN3 1CN4 1                  30.5000E-030.5000E-030.2027E-021.
CN4 1CN5 1                  30.5000E-030.5000E-030.2027E-021.
CN5 1CO  1                  30.5000E-030.5000E-020.2027E-021.
CO  1CP  1                  30.5000E-020.5000E-020.2027E-021.
CP  1CQ  1                  30.5000E-020.5000E-020.2027E-021.
CQ  1CR  1                  30.5000E-020.5000E-020.2027E-021.
CR  1CS  1                  30.5000E-020.5000E-020.2027E-021.
CS  1AMB 1                  30.5000E-020.1000E-100.2027E-021.
BOU 1A2  2                  30.1000E-000.5000E-020.8765E-031.
```

```
A2  2A3  2                  30.5000E-020.5000E-020.8765E-031.
A3  2A4  2                  30.5000E-020.5000E-020.8765E-031.
A4  2A5  2                  30.5000E-020.5000E-020.8765E-031.
A5  2A6  2                  30.5000E-020.5000E-020.8765E-031.
A6  2A7  2                  30.5000E-020.5000E-020.8765E-031.
A7  2A8  2                  30.5000E-020.5000E-020.8765E-031.
A8  2A9  2                  30.5000E-020.5000E-020.8765E-031.
A9  2AA  2                  30.5000E-020.5000E-020.8765E-031.
AA  2AB  2                  30.5000E-020.5000E-020.8765E-031.
AB  2AC  2                  30.5000E-020.5000E-020.8765E-031.
AC  2AD  2                  30.5000E-020.5000E-020.8765E-031.
AD  2AE  2                  30.5000E-020.5000E-020.8765E-031.
AE  2AF  2                  30.5000E-020.5000E-020.8765E-031.
AF  2AG  2                  30.5000E-020.5000E-020.8765E-031.
AG  2AH  2                  30.5000E-020.5000E-020.8765E-031.
AH  2AI  2                  30.5000E-020.5000E-020.8765E-031.
AI  2AJ  2                  30.5000E-020.5000E-020.8765E-031.
AJ  2AK  2                  30.5000E-020.5000E-020.8765E-031.
AK  2AL  2                  30.5000E-020.5000E-020.8765E-031.
AL  2AM  2                  30.5000E-020.5000E-020.8765E-031.
AM  2AN  2                  30.5000E-020.5000E-020.8765E-031.
AN  2AO  2                  30.5000E-020.5000E-020.8765E-031.
AO  2AP  2                  30.5000E-020.5000E-020.8765E-031.
AP  2AQ  2                  30.5000E-020.5000E-020.8765E-031.
AQ  2AR  2                  30.5000E-020.5000E-020.8765E-031.
AR  2AS  2                  30.5000E-020.5000E-020.8765E-031.
AS  2AT  2                  30.5000E-020.5000E-020.8765E-031.
AT  2AU  2                  30.5000E-020.5000E-020.8765E-031.
AU  2AV  2                  30.5000E-020.5000E-020.8765E-031.
AV  2AW  2                  30.5000E-020.5000E-020.8765E-031.
AW  2AX  2                  30.5000E-020.1000E-020.8765E-031.
AX  2AY  2                  30.1000E-020.1000E-020.8765E-031.
AY  2AZ  2                  30.1000E-020.1000E-020.8765E-031.
AZ  2B1  2                  30.1000E-020.1000E-020.8765E-031.
B1  2B2  2                  30.1000E-020.1000E-020.8765E-031.
B2  2B3  2                  30.1000E-020.1000E-020.8765E-031.
B3  2B4  2                  30.1000E-020.1000E-020.8765E-031.
B4  2B5  2                  30.1000E-020.1000E-020.8765E-031.
B5  2B6  2                  30.1000E-020.1000E-020.8765E-031.
B6  2B7  2                  30.1000E-020.1000E-020.8765E-031.
B7  2B8  2                  30.1000E-020.1000E-020.8765E-031.
B8  2B9  2                  30.1000E-020.1000E-020.8765E-031.
B9  2BA  2                  30.1000E-020.1000E-020.8765E-031.
BA  2BB  2                  30.1000E-020.1000E-020.8765E-031.
BB  2BC  2                  30.1000E-020.1000E-020.8765E-031.
BC  2BD  2                  30.1000E-020.1000E-020.8765E-031.
BD  2BE  2                  30.1000E-020.1000E-020.8765E-031.
BE  2BF  2                  30.1000E-020.1000E-020.8765E-031.
BF  2BG  2                  30.1000E-020.1000E-020.8765E-031.
BG  2BH  2                  30.1000E-020.1000E-020.8765E-031.
BH  2BI  2                  30.1000E-020.1000E-020.8765E-031.
BI  2BJ  2                  30.1000E-020.1000E-020.8765E-031.
BJ  2BK  2                  30.1000E-020.1000E-020.8765E-031.
BK  2BL  2                  30.1000E-020.1000E-020.8765E-031.
BL  2BM  2                  30.1000E-020.1000E-020.8765E-031.
BM  2BN  2                  30.1000E-020.1000E-020.8765E-031.
BN  2BO  2                  30.1000E-020.1000E-020.8765E-031.
BO  2BP  2                  30.1000E-020.1000E-020.8765E-031.
BP  2BQ  2                  30.1000E-020.1000E-020.8765E-031.
BQ  2BR  2                  30.1000E-020.1000E-020.8765E-031.
BR  2BS  2                  30.1000E-020.1000E-020.8765E-031.
BS  2BT  2                  30.1000E-020.1000E-020.8765E-031.
BT  2BU  2                  30.1000E-020.1000E-020.8765E-031.
BU  2BV  2                  30.1000E-020.1000E-020.8765E-031.
BV  2BW  2                  30.1000E-020.1000E-020.8765E-031.
BW  2BX  2                  30.1000E-020.1000E-020.8765E-031.
BX  2BY  2                  30.1000E-020.1000E-020.8765E-031.
BY  2BZ  2                  30.1000E-020.1000E-020.8765E-031.
BZ  2C1  2                  30.1000E-020.1000E-020.8765E-031.
C1  2C2  2                  30.1000E-020.1000E-020.8765E-031.
C2  2C3  2                  30.1000E-020.1000E-020.8765E-031.
C3  2C4  2                  30.1000E-020.1000E-020.8765E-031.
C4  2C5  2                  30.1000E-020.1000E-020.8765E-031.
C5  2C6  2                  30.1000E-020.1000E-020.8765E-031.
C6  2C7  2                  30.1000E-020.1000E-020.8765E-031.
C7  2C8  2                  30.1000E-020.1000E-020.8765E-031.
```

```
C8  2C9  2                30.1000E-020.1000E-020.8765E-031.
C9  2CA  2                30.1000E-020.1000E-020.8765E-031.
CA  2CB  2                30.1000E-020.1000E-020.8765E-031.
CB  2CC  2                30.1000E-020.1000E-020.8765E-031.
CC  2CD  2                30.1000E-020.1000E-020.8765E-031.
CD  2CE  2                30.1000E-020.1000E-020.8765E-031.
CE  2CF  2                30.1000E-020.1000E-020.8765E-031.
CF  2CG  2                30.1000E-020.1000E-020.8765E-031.
CG  2CH  2                30.1000E-020.1000E-020.8765E-031.
CH  2CI  2                30.1000E-020.1000E-020.8765E-031.
CI  2CJ  2                30.1000E-020.1000E-020.8765E-031.
CJ  2CK  2                30.1000E-020.1000E-020.8765E-031.
CK  2CL  2                30.1000E-020.1000E-020.8765E-031.
CL  2CM  2                30.1000E-020.1000E-020.8765E-031.
CM  2CN  2                30.1000E-020.2500E-020.8765E-031.
CN  2CO  2                30.2500E-020.5000E-020.8765E-031.
CO  2CP  2                30.5000E-020.5000E-020.8765E-031.
CP  2CQ  2                30.5000E-020.5000E-020.8765E-031.
CQ  2CR  2                30.5000E-020.5000E-020.8765E-031.
CR  2CS  2                30.5000E-020.5000E-020.8765E-031.
CS  2AMB 1                30.5000E-020.1000E-100.8765E-031.
BOU 1A2  3                30.1000E-000.5000E-020.1781E-011.
A2  3A3  3                30.5000E-020.5000E-020.1781E-011.
A3  3A4  3                30.5000E-020.5000E-020.1781E-011.
A4  3A5  3                30.5000E-020.5000E-020.1781E-011.
A5  3A6  3                30.5000E-020.5000E-020.1781E-011.
A6  3A7  3                30.5000E-020.5000E-020.1781E-011.
A7  3A8  3                30.5000E-020.5000E-020.1781E-011.
A8  3A9  3                30.5000E-020.5000E-020.1781E-011.
A9  3AA  3                30.5000E-020.5000E-020.1781E-011.
AA  3AB  3                30.5000E-020.5000E-020.1781E-011.
AB  3AC  3                30.5000E-020.5000E-020.1781E-011.
AC  3AD  3                30.5000E-020.5000E-020.1781E-011.
AD  3AE  3                30.5000E-020.5000E-020.1781E-011.
AE  3AF  3                30.5000E-020.5000E-020.1781E-011.
AF  3AG  3                30.5000E-020.5000E-020.1781E-011.
AG  3AH  3                30.5000E-020.5000E-020.1781E-011.
AH  3AI  3                30.5000E-020.5000E-020.1781E-011.
AI  3AJ  3                30.5000E-020.5000E-020.1781E-011.
AJ  3AK  3                30.5000E-020.5000E-020.1781E-011.
AK  3AL  3                30.5000E-020.5000E-020.1781E-011.
AL  3AM  3                30.5000E-020.5000E-020.1781E-011.
AM  3AN  3                30.5000E-020.5000E-020.1781E-011.
AN  3AO  3                30.5000E-020.5000E-020.1781E-011.
AO  3AP  3                30.5000E-020.5000E-020.1781E-011.
AP  3AQ  3                30.5000E-020.5000E-020.1781E-011.
AQ  3AR  3                30.5000E-020.5000E-020.1781E-011.
AR  3AS  3                30.5000E-020.5000E-020.1781E-011.
AS  3AT  3                30.5000E-020.5000E-020.1781E-011.
AT  3AU  3                30.5000E-020.5000E-020.1781E-011.
AU  3AV  3                30.5000E-020.5000E-020.1781E-011.
AV  3AW  3                30.5000E-020.5000E-020.1781E-011.
AW  3AX  3                30.5000E-020.1000E-020.1781E-011.
AX  3AY  3                30.1000E-020.1000E-020.1781E-011.
AY  3AZ  3                30.1000E-020.1000E-020.1781E-011.
AZ  3B1  3                30.1000E-020.1000E-020.1781E-011.
B1  3B2  3                30.1000E-020.1000E-020.1781E-011.
B2  3B3  3                30.1000E-020.1000E-020.1781E-011.
B3  3B4  3                30.1000E-020.1000E-020.1781E-011.
B4  3B5  3                30.1000E-020.1000E-020.1781E-011.
B5  3B6  3                30.1000E-020.1000E-020.1781E-011.
B6  3B7  3                30.1000E-020.1000E-020.1781E-011.
B7  3B8  3                30.1000E-020.1000E-020.1781E-011.
B8  3B9  3                30.1000E-020.1000E-020.1781E-011.
B9  3BA  3                30.1000E-020.1000E-020.1781E-011.
BA  3BB  3                30.1000E-020.1000E-020.1781E-011.
BB  3BC  3                30.1000E-020.1000E-020.1781E-011.
BC  3BD  3                30.1000E-020.1000E-020.1781E-011.
BD  3BE  3                30.1000E-020.1000E-020.1781E-011.
BE  3BF  3                30.1000E-020.1000E-020.1781E-011.
BF  3BG  3                30.1000E-020.1000E-020.1781E-011.
BG  3BH  3                30.1000E-020.1000E-020.1781E-011.
BH  3BI  3                30.1000E-020.1000E-020.1781E-011.
BI  3BJ  3                30.1000E-020.1000E-020.1781E-011.
BJ  3BK  3                30.1000E-020.1000E-020.1781E-011.
BK  3BL  3                30.1000E-020.1000E-020.1781E-011.
```

```
BL  3BM  3                  30.1000E-020.1000E-020.1781E-011.
BM  3BN  3                  30.1000E-020.1000E-020.1781E-011.
BN  3BO  3                  30.1000E-020.1000E-020.1781E-011.
BO  3BP  3                  30.1000E-020.1000E-020.1781E-011.
BP  3BQ  3                  30.1000E-020.1000E-020.1781E-011.
BQ  3BR  3                  30.1000E-020.1000E-020.1781E-011.
BR  3BS  3                  30.1000E-020.1000E-020.1781E-011.
BS  3BT  3                  30.1000E-020.1000E-020.1781E-011.
BT  3BU  3                  30.1000E-020.1000E-020.1781E-011.
BU  3BV  3                  30.1000E-020.1000E-020.1781E-011.
BV  3BW  3                  30.1000E-020.1000E-020.1781E-011.
BW  3BX  3                  30.1000E-020.1000E-020.1781E-011.
BX  3BY  3                  30.1000E-020.1000E-020.1781E-011.
BY  3BZ  3                  30.1000E-020.1000E-020.1781E-011.
BZ  3C1  3                  30.1000E-020.1000E-020.1781E-011.
C1  3C2  3                  30.1000E-020.1000E-020.1781E-011.
C2  3C3  3                  30.1000E-020.1000E-020.1781E-011.
C3  3C4  3                  30.1000E-020.1000E-020.1781E-011.
C4  3C5  3                  30.1000E-020.1000E-020.1781E-011.
C5  3C6  3                  30.1000E-020.1000E-020.1781E-011.
C6  3C7  3                  30.1000E-020.1000E-020.1781E-011.
C7  3C8  3                  30.1000E-020.1000E-020.1781E-011.
C8  3C9  3                  30.1000E-020.1000E-020.1781E-011.
C9  3CA  3                  30.1000E-020.1000E-020.1781E-011.
CA  3CB  3                  30.1000E-020.1000E-020.1781E-011.
CB  3CC  3                  30.1000E-020.1000E-020.1781E-011.
CC  3CD  3                  30.1000E-020.1000E-020.1781E-011.
CD  3CE  3                  30.1000E-020.1000E-020.1781E-011.
CE  3CF  3                  30.1000E-020.1000E-020.1781E-011.
CF  3CG  3                  30.1000E-020.1000E-020.1781E-011.
CG  3CH  3                  30.1000E-020.1000E-020.1781E-011.
CH  3CI  3                  30.1000E-020.1000E-020.1781E-011.
CI  3CJ  3                  30.1000E-020.1000E-020.1781E-011.
CJ  3CK  3                  30.1000E-020.1000E-020.1781E-011.
CK  3CL  3                  30.1000E-020.1000E-020.1781E-011.
CL  3CM  3                  30.1000E-020.1000E-020.1781E-011.
CM  3CN  3                  30.1000E-020.2500E-020.1781E-011.
CN  3CO  3                  30.2500E-020.5000E-020.1781E-011.
CO  3CP  3                  30.5000E-020.5000E-020.1781E-011.
CP  3CQ  3                  30.5000E-020.5000E-020.1781E-011.
CQ  3CR  3                  30.5000E-020.5000E-020.1781E-011.
CR  3CS  3                  30.5000E-020.5000E-020.1781E-011.
CS  3AMB 1                  30.5000E-020.1000E-100.1781E-011.

TIMES----1----*----2----*----3----*----4----*----5----*----6----*----7----*----8
    1
  8.64E+04

INDOM----1----*----2----*----3----*----4----*----5----*----6----*----7----*----8
BOUND
           1.1861E5               24.
AMBIE
           1.0065E5               24.

GENER----1----*----2----*----3----*----4----*----5----*----6----*----7----*----8
CN1 1HTR 1                      HEAT        2.0
CN2 1HTR 2                      HEAT        2.0
CN3 1HTR 3                      HEAT        1.0
CN4 1HTR 4                      HEAT        1.0
CN5 1HTR 5                      HEAT        1.0

ENDCY----1----*----2----*----3----*----4----*----5----*----6----*----7----*----8




# Linear RP / Leverett CP ITOUGH2 input file
> PARAMETERS
  >> ABSOLUTE permeability
     >>> MATERIAL: BEREA
         >>>> LOGARITHM
         >>>> INDEX: 3
         >>>> DEVIATION: 0.2
         <<<<
     <<<
```

```
  >> RELATIVE permeability function
    >>> MATERIAL: BEREA
         >>>> PARAMETER No.: 1
         >>>> ANNOTATION   : Slr (RP)
         >>>> standard DEVIATION : 0.05
         >>>> max STEP : 0.05
         >>>> PERTURB : -0.001
         >>>> estimate VALUE
         >>>> RANGE  : 0.00 0.50
         <<<<
    >>> MATERIAL: BEREA
         >>>> PARAMETER No.: 2
         >>>> ANNOTATION   : Sgr
         >>>> standard DEVIATION : 0.05
         >>>> max STEP : 0.05
         >>>> PERTURB : -0.001
         >>>> estimate VALUE
         >>>> RANGE  : 0.00 0.50
         <<<<
    >>> MATERIAL: BEREA
         >>>> PARAMETER No.: 3
         >>>> ANNOTATION   : Sls
         >>>> standard DEVIATION : 0.05
         >>>> max STEP : 0.05
         >>>> PERTURB : -0.001
         >>>> estimate VALUE
         >>>> RANGE  : 0.51 1.00
         <<<<
    >>> MATERIAL: BEREA
         >>>> PARAMETER No.: 4
         >>>> ANNOTATION   : Sgs
         >>>> standard DEVIATION : 0.05
         >>>> max STEP : 0.02
         >>>> estimate VALUE
         >>>> RANGE  : 0.51 1.00
         >>>> PERTURB : -0.001
         <<<<
     <<<

  >> parameters of the CAPILLARY pressure function
     >>> MATERIAL: BEREA
         >>>> PARAMETER No.:  1
         >>>> ANNOTATION  :  Po
         >>>> standard DEVIATION : 0.50
         >>>> max STEP: 0.2
         >>>> estimate LOGARITHM
         <<<<
     >>> MATERIAL: BEREA
         >>>> PARAMETER No.: 2
         >>>> ANNOTATION   : Slr
         >>>> standard DEVIATION : 0.05
         >>>> max STEP : 0.05
         >>>> PERTURB : -0.001
         >>>> estimate VALUE
         >>>> RANGE  : 0.00 1.00
         <<<<
     <<<
  >> RATE
     >>> SOURCE: HTR_1 +4
         >>>> ANNOTATION   : H7
         >>>> PARAMETER No.: 7
         >>>> DEVIATION    : 0.1
         >>>> VALUE
         >>>> STEP         : 0.1
         <<<<
     >>> SOURCE: HTR_1 +4
         >>>> ANNOTATION   : H8
         >>>> PARAMETER No.: 8
         >>>> DEVIATION    : 0.1
         >>>> VALUE
         >>>> STEP         : 0.1
         <<<<
     <<<
  <<

> OBSERVATIONS
```

```
>> TIMES: 100 LOGARITHMICALLY spaced in [DAYS] between
   0.25  1000

>> TEMPERATURE
   >>> ELEMENT: CM__1
       >>>> ANNOTATION: T1
       >>>> COLUMNS: 1 2
       >>>> PICK : 10
       >>>> NO DATA
       >>>> DEVIATION: 1.0 deg C
       <<<<

   >>> ELEMENT: CL__1
       >>>> ANNOTATION: T2
       >>>> COLUMNS: 1 3
       >>>> PICK : 10
       >>>> NO DATA
       >>>> DEVIATION: 1.0 deg C
       <<<<

   >>> ELEMENT: CK__1
       >>>> ANNOTATION: T3
       >>>> COLUMNS: 1 4
       >>>> PICK : 10
       >>>> NO DATA
       >>>> DEVIATION: 1.0 deg C
       <<<<

   >>> ELEMENT: CJ__1
       >>>> ANNOTATION: T4
       >>>> COLUMNS: 1 5
       >>>> PICK : 10
       >>>> NO DATA
       >>>> DEVIATION: 1.0 deg C
       <<<<

   >>> ELEMENT: CI__1
       >>>> ANNOTATION: T5
       >>>> COLUMNS: 1 6
       >>>> PICK : 10
       >>>> NO DATA
       >>>> DEVIATION: 1.0 deg C
       <<<<

   >>> ELEMENT: CH__1
       >>>> ANNOTATION: T6
       >>>> COLUMNS: 1 7
       >>>> PICK : 10
       >>>> NO DATA
       >>>> DEVIATION: 1.0 deg C
       <<<<

   >>> ELEMENT: CG__1
       >>>> ANNOTATION: T7
       >>>> COLUMNS: 1 8
       >>>> PICK : 10
       >>>> NO DATA
       >>>> DEVIATION: 1.0 deg C
       <<<<

   >>> ELEMENT: CF__1
       >>>> ANNOTATION: T8
       >>>> COLUMNS: 1 9
       >>>> PICK : 10
       >>>> NO DATA
       >>>> DEVIATION: 1.0 deg C
       <<<<

   >>> ELEMENT: CE__1
       >>>> ANNOTATION: T9
       >>>> COLUMNS: 1 10
       >>>> PICK : 10
       >>>> NO DATA
       >>>> DEVIATION: 1.0 deg C
       <<<<
```

```
>>> ELEMENT: CD__1
    >>>> ANNOTATION: T10
    >>>> COLUMNS: 1 11
    >>>> PICK : 10
    >>>> NO DATA
    >>>> DEVIATION: 1.0 deg C
    <<<<

>>> ELEMENT: CB__1
    >>>> ANNOTATION: T11
    >>>> COLUMNS: 1 12
    >>>> PICK : 10
    >>>> NO DATA
    >>>> DEVIATION: 1.0 deg C
    <<<<

>>> ELEMENT: C9__1
    >>>> ANNOTATION: T12
    >>>> COLUMNS: 1 13
    >>>> PICK : 10
    >>>> NO DATA
    >>>> DEVIATION: 1.0 deg C
    <<<<

>>> ELEMENT: C7__1
    >>>> ANNOTATION: T13
    >>>> COLUMNS: 1 14
    >>>> PICK : 10
    >>>> NO DATA
    >>>> DEVIATION: 1.0 deg C
    <<<<

>>> ELEMENT: C5__1
    >>>> ANNOTATION: T14
    >>>> COLUMNS: 1 15
    >>>> PICK : 10
    >>>> NO DATA
    >>>> DEVIATION: 1.0 deg C
    <<<<

>>> ELEMENT: C3__1
    >>>> ANNOTATION: T15
    >>>> COLUMNS: 1 16
    >>>> PICK : 10
    >>>> NO DATA
    >>>> DEVIATION: 1.0 deg C
    <<<<

>>> ELEMENT: C1__1
    >>>> ANNOTATION: T16
    >>>> COLUMNS: 1 17
    >>>> PICK : 10
    >>>> NO DATA
    >>>> DEVIATION: 1.0 deg C
    <<<<

>>> ELEMENT: BY__1
    >>>> ANNOTATION: T17
    >>>> COLUMNS: 1 18
    >>>> PICK : 10
    >>>> NO DATA
    >>>> DEVIATION: 1.0 deg C
    <<<<

>>> ELEMENT: BW__1
    >>>> ANNOTATION: T18
    >>>> COLUMNS: 1 19
    >>>> PICK : 10
    >>>> NO DATA
    >>>> DEVIATION: 1.0 deg C
    <<<<

>>> ELEMENT: BU__1
    >>>> ANNOTATION: T19
    >>>> COLUMNS: 1 20
    >>>> PICK : 10
```

```
        >>>> NO DATA
        >>>> DEVIATION: 1.0 deg C
        <<<<

    >>> ELEMENT: BS__1
        >>>> ANNOTATION: T20
        >>>> COLUMNS: 1 21
        >>>> PICK : 10
        >>>> NO DATA
        >>>> DEVIATION: 1.0 deg C
        <<<<
    <<<

>> PRESSURE
    >>> ELEMENT: CM__1
        >>>> ANNOTATION: P1
        >>>> SHIFT: 1.0065E5
        >>>> COLUMNS: 1 2
        >>>> PICK : 10
        >>>> NO DATA
        >>>> DEVIATION:  1000.0 Pa
        <<<<

    >>> ELEMENT: CL__1
        >>>> ANNOTATION: P2
        >>>> SHIFT: 1.0065E5
        >>>> COLUMNS: 1 3
        >>>> PICK : 10
        >>>> NO DATA
        >>>> DEVIATION:  1000.0 Pa
        <<<<

    >>> ELEMENT: CK__1
        >>>> ANNOTATION: P3
        >>>> SHIFT: 1.0065E5
        >>>> COLUMNS: 1 4
        >>>> PICK : 10
        >>>> NO DATA
        >>>> DEVIATION:  1000.0 Pa
        <<<<

    >>> ELEMENT: CJ__1
        >>>> ANNOTATION: P4
        >>>> SHIFT: 1.0065E5
        >>>> COLUMNS: 1 5
        >>>> PICK : 10
        >>>> NO DATA
        >>>> DEVIATION:  1000.0 Pa
        <<<<

    >>> ELEMENT: CI__1
        >>>> ANNOTATION: P5
        >>>> SHIFT: 1.0065E5
        >>>> COLUMNS: 1 6
        >>>> PICK : 10
        >>>> NO DATA
        >>>> DEVIATION:  1000.0 Pa
        <<<<

    >>> ELEMENT: CH__1
        >>>> ANNOTATION: P6
        >>>> SHIFT: 1.0065E5
        >>>> COLUMNS: 1 7
        >>>> PICK : 10
        >>>> NO DATA
        >>>> DEVIATION:  1000.0 Pa
        <<<<

    >>> ELEMENT: CG__1
        >>>> ANNOTATION: P7
        >>>> SHIFT: 1.0065E5
        >>>> COLUMNS: 1 8
        >>>> PICK : 10
        >>>> NO DATA
        >>>> DEVIATION:  1000.0 Pa
        <<<<
```

```
    >>> ELEMENT: CF__1
        >>>> ANNOTATION: P8
        >>>> SHIFT: 1.0065E5
        >>>> COLUMNS: 1 9
        >>>> PICK : 10
        >>>> NO DATA
        >>>> DEVIATION:  1000.0 Pa
        <<<<

    >>> ELEMENT: CE__1
        >>>> ANNOTATION: P9
        >>>> SHIFT: 1.0065E5
        >>>> COLUMNS: 1 10
        >>>> PICK : 10
        >>>> NO DATA
        >>>> DEVIATION:  1000.0 Pa
        <<<<

    >>> ELEMENT: CD__1
        >>>> ANNOTATION: P10
        >>>> SHIFT: 1.0065E5
        >>>> COLUMNS: 1 11
        >>>> PICK : 10
        >>>> NO DATA
        >>>> DEVIATION:  1000.0 Pa
        <<<<
    <<<

>> VAPOR SATURATION
    >>> ELEMENT: CM__1
        >>>> ANNOTATION: Sst1
        >>>> COLUMNS: 1 2
        >>>> NO DATA
        >>>> DEVIATION: 0.02
        <<<<

    >>> ELEMENT: CL__1
        >>>> ANNOTATION: Sst2
        >>>> COLUMNS: 1 3
        >>>> NO DATA
        >>>> DEVIATION: 0.01
        <<<<

    >>> ELEMENT: CK__1
        >>>> ANNOTATION: Sst3
        >>>> COLUMNS: 1 4
        >>>> NO DATA
        >>>> DEVIATION: 0.01
        <<<<

    >>> ELEMENT: CJ__1
        >>>> ANNOTATION: Sst4
        >>>> COLUMNS: 1 5
        >>>> NO DATA
        >>>> DEVIATION: 0.01
        <<<<

    >>> ELEMENT: CI__1
        >>>> ANNOTATION: Sst5
        >>>> COLUMNS: 1 6
        >>>> NO DATA
        >>>> DEVIATION: 0.01
        <<<<

    >>> ELEMENT: CH__1
        >>>> ANNOTATION: Sst6
        >>>> COLUMNS: 1 7
        >>>> NO DATA
        >>>> DEVIATION: 0.01
        <<<<

    >>> ELEMENT: CG__1
        >>>> ANNOTATION: Sst7
        >>>> COLUMNS: 1 8
        >>>> NO DATA
```

```
    >>>> DEVIATION: 0.01
    <<<<

>>> ELEMENT: CF__1
    >>>> ANNOTATION: Sst8
    >>>> COLUMNS: 1 9
    >>>> NO DATA
    >>>> DEVIATION: 0.01
    <<<<

>>> ELEMENT: CE__1
    >>>> ANNOTATION: Sst9
    >>>> COLUMNS: 1 10
    >>>> NO DATA
    >>>> DEVIATION: 0.01
    <<<<

>>> ELEMENT: CD__1
    >>>> ANNOTATION: Sst10
    >>>> COLUMNS: 1 11
    >>>> NO DATA
    >>>> DEVIATION: 0.01
    <<<<

>>> ELEMENT: CB__1
    >>>> ANNOTATION: Sst11
    >>>> COLUMNS: 1 12
    >>>> NO DATA
    >>>> DEVIATION: 0.02
    <<<<

>>> ELEMENT: C9__1
    >>>> ANNOTATION: Sst12
    >>>> COLUMNS: 1 13
    >>>> NO DATA
    >>>> DEVIATION: 0.01
    <<<<

>>> ELEMENT: C7__1
    >>>> ANNOTATION: Sst13
    >>>> COLUMNS: 1 14
    >>>> NO DATA
    >>>> DEVIATION: 0.01
    <<<<

>>> ELEMENT: C5__1
    >>>> ANNOTATION: Sst14
    >>>> COLUMNS: 1 15
    >>>> NO DATA
    >>>> DEVIATION: 0.01
    <<<<

>>> ELEMENT: C3__1
    >>>> ANNOTATION: Sst15
    >>>> COLUMNS: 1 16
    >>>> NO DATA
    >>>> DEVIATION: 0.01
    <<<<

>>> ELEMENT: C1__1
    >>>> ANNOTATION: Sst16
    >>>> COLUMNS: 1 17
    >>>> NO DATA
    >>>> DEVIATION: 0.01
    <<<<

>>> ELEMENT: BY__1
    >>>> ANNOTATION: Sst17
    >>>> COLUMNS: 1 18
    >>>> NO DATA
    >>>> DEVIATION: 0.01
    <<<<

>>> ELEMENT: BW__1
    >>>> ANNOTATION: Sst18
    >>>> COLUMNS: 1 19
```

```
          >>>> NO DATA
          >>>> DEVIATION: 0.01
          <<<<

     >>> ELEMENT: BU__1
          >>>> ANNOTATION: Sst19
          >>>> COLUMNS: 1 20
          >>>> NO DATA
          >>>> DEVIATION: 0.01
          <<<<

     >>> ELEMENT: BS__1
          >>>> ANNOTATION: Sst20
          >>>> COLUMNS: 1 21
          >>>> NO DATA
          >>>> DEVIATION: 0.01
          <<<<

     >>> ELEMENT: BQ__1
          >>>> ANNOTATION: Sst21
          >>>> COLUMNS: 1 22
          >>>> NO DATA
          >>>> DEVIATION: 0.02
          >>>> WINDOW: 5.00  8.00 [DAYS}
          <<<<

     >>> ELEMENT: BO__1
          >>>> ANNOTATION: Sst22
          >>>> COLUMNS: 1 23
          >>>> NO DATA
          >>>> DEVIATION: 0.01
          <<<<

     >>> ELEMENT: BM__1
          >>>> ANNOTATION: Sst23
          >>>> COLUMNS: 1 24
          >>>> NO DATA
          >>>> DEVIATION: 0.01
          <<<<

     >>> ELEMENT: BK__1
          >>>> ANNOTATION: Sst24
          >>>> COLUMNS: 1 25
          >>>> NO DATA
          >>>> DEVIATION: 0.01
          <<<<

     >>> ELEMENT: BI__1
          >>>> ANNOTATION: Sst25
          >>>> COLUMNS: 1 26
          >>>> NO DATA
          >>>> DEVIATION: 0.01
          <<<<
     <<<
  <<

> COMPUTATION
 >> STOPPING criteria
     >>> IGNORE WARNINGS
     >>> max. no. of ITERATIONS: 20
     >>> IQIT=3: 50
     >>> CONSECUTIVE: 100
     >>> INCOMPLETE: 20
     >>> LEVENBERG: 0.1
     >>> STEP : 1.0
     <<<
  >> JACOBIAN
     >>> FORWARD: 8
     >>> PERTURB: 0.01
     <<<
  >> OPTIONS
#    >>> QUADRATIC-LINEAR: 3.0
#    >>> perform a SENSITIVITY analysis
     >>> DIRECT
     <<<
  >> OUTPUT
```

```
      >>> PLOTFILE: COLUMNS
      >>> DAYS
      >>> generate file with CHARACTERISTIC curves
      <<<
  <<
<
```

Appendix B

B. TOUGH2 Input File for Geysers Geothermal Rock Boiling Experiment Simulation

```
*Forward Calculations*
ROCKS----1----*----2----*----3----*----4----*----5----*----6----*----7----*----8
GEYSR    2     2600.     0.050   0.0E-20   0.0E-20 1.000E-14     2.430      485.
0.0000E+000.0000E+09     2.430       0.0
    1          0.500     0.000     1.000     0.500
    6         1.0E05     0.500
HEATE    0     2200.     0.010   0.0E-15   0.0E-15   0.0E-15     2.885     246.6
HEATB    0      240.     0.010   0.0E-15   0.0E-15   0.0E-15     0.163    1046.6
EPOXY    0     1200.     0.010   0.0E-15   0.0E-15   0.0E-15     0.577    1046.6
INSUL    0      192.     0.010   0.0E-15   0.0E-15   0.0E-15     0.115     104.7
BOUND    2     2163.     0.990   0.0E-15   0.0E-15   0.0E-15     0.642   -1611.0

   10          0.200     0.200     0.000
   10         0.5000  1000.000     0.050    0.0000                0.0
AMBIE          1.293     0.990   0.0E-20   0.0E-20   1.0E-10     0.055   -1611.0

START----1----*----2----*----3----*----4----*----5----*----6----*----7----*----8
PARAM           12345678901234567890123 4
  -31500    15001000001001010004000010 00 2.130E-05                1.0
            6.1020E5  1.00E+03                        9.8100
     1.E-5
            1.0065E5                24.                 0.0

mESHMAKER1----*----2----*----3----*----4----*----5----*----6----*----7----*----8
RZ2D
RADII
    5
         0    0.0254    0.0304    0.0812    5.0812
LAYER----1----*----2----*----3----*----4----*----5----*----6----*----7----*----8
   99
    0.0100    0.0100    0.0100    0.0100    0.0100    0.0100    0.0100    0.0100
    0.0100    0.0100    0.0100    0.0100    0.0100    0.0100    0.0100    0.0100
    0.0100    0.0100    0.0100    0.0100    0.0100    0.0100    0.0100    0.0100
    0.0100    0.0100    0.0100    0.0100    0.0100    0.0100    0.0100    0.0100
    0.0020    0.0020    0.0020    0.0020    0.0020    0.0020    0.0020    0.0020
    0.0020    0.0020    0.0020    0.0020    0.0020    0.0020    0.0020    0.0020
    0.0020    0.0020    0.0020    0.0020    0.0020    0.0020    0.0020    0.0020
    0.0020    0.0020    0.0020    0.0020    0.0020    0.0020    0.0020    0.0020
    0.0020    0.0020    0.0020    0.0020    0.0020    0.0020    0.0020    0.0020
    0.0020    0.0020    0.0020    0.0020    0.0020    0.0020    0.0020    0.0020
    0.0020    0.0020    0.0020    0.0020    0.0020    0.0020    0.0020    0.0020
    0.0020    0.0020    0.0020    0.0020    0.0500    0.0100    0.0100    0.0100
    0.0100    0.0100    5.0000
```

Appendix C

C. TOUGH2 and iTOUGH2 Input Files for Two-Phase Radial Flow Simulation

```
*Forward Calculations*
ROCKS----1----*----2----*----3----*----4----*----5----*----6----*----7----*----8
GEYSR    2    2600.0      0.05   1.0E-14       0.0       0.0      2.43     485.0
       0.0       0.0      2.43       0.0
    1          0.200     0.000     1.000     0.800
    6          0.000     0.200

START----1----*----2----*----3----*----4----*----5----*----6----*----7----*----8
PARAM           12345678901234567890123456789012345
   29999    99991000301001010004000010000 2.130E-05                1.0
              1.0E12  1.00E-01                          9.81
     1.E-5
            6420.2E3               10.70               280.0

MESHMAKER1----*----2----*----3----*----4----*----5----*----6----*----7----*----8
RZ2D
RADII
  101
       0.0      0.25     0.523     0.822     1.131     1.458     1.802     2.166
     2.549     2.953     3.380     3.830     4.304     4.805     5.333     5.890
     6.478     7.098     7.752     8.442     9.170     9.938    10.747    11.601
    12.503    13.453    14.456    15.514    16.629    17.807    19.048    20.358
    21.740    23.198    24.735    26.357    28.068    29.873    31.776    33.784
    35.903    38.138    40.495    42.982    45.605    48.373    51.292    54.371
    57.619    61.046    64.660    68.473    72.495    76.738    81.214    85.935
    90.916    96.170   101.712   107.558   113.725   120.230   127.093   134.332
   141.969   150.024   158.522   167.485   176.941   186.916   197.438   208.538
   220.246   232.598   245.626   259.370   273.869   289.163   305.296   322.314
   340.267   359.205   379.182   400.255   422.485   445.934   470.671   496.765
   524.291   553.328   583.958   616.269   650.353   686.308   724.235   764.244
   806.449   850.970   897.934   947.476    1000.0
LAYER----1----*----2----*----3----*----4----*----5----*----6----*----7----*----8
    1
      10.0

ELEME ---   100  101    0    0   0.00000  1000.000
A1  1          GEYSR .1963E+010.3927E+00          0.1250E+00          -.5000E+01
A1  2          GEYSR .6630E+010.1326E+01          0.3865E+00          -.5000E+01
A1  3          GEYSR .1263E+020.2527E+01          0.6725E+00          -.5000E+01
A1  4          GEYSR .1896E+020.3792E+01          0.9765E+00          -.5000E+01
A1  5          GEYSR .2660E+020.5319E+01          0.1294E+01          -.5000E+01
A1  6          GEYSR .3523E+020.7046E+01          0.1630E+01          -.5000E+01
A1  7          GEYSR .4538E+020.9075E+01          0.1984E+01          -.5000E+01
A1  8          GEYSR .5673E+020.1135E+02          0.2357E+01          -.5000E+01
A1  9          GEYSR .6983E+020.1397E+02          0.2751E+01          -.5000E+01
A1 10          GEYSR .8495E+020.1699E+02          0.3167E+01          -.5000E+01
A1 11          GEYSR .1019E+030.2039E+02          0.3605E+01          -.5000E+01
A1 12          GEYSR .1211E+030.2422E+02          0.4067E+01          -.5000E+01
A1 13          GEYSR .1434E+030.2867E+02          0.4554E+01          -.5000E+01
A1 14          GEYSR .1682E+030.3363E+02          0.5069E+01          -.5000E+01
A1 15          GEYSR .1964E+030.3928E+02          0.5611E+01          -.5000E+01
A1 16          GEYSR .2285E+030.4569E+02          0.6184E+01          -.5000E+01
A1 17          GEYSR .2644E+030.5289E+02          0.6788E+01          -.5000E+01
A1 18          GEYSR .3051E+030.6102E+02          0.7425E+01          -.5000E+01
A1 19          GEYSR .3510E+030.7021E+02          0.8097E+01          -.5000E+01
A1 20          GEYSR .4028E+030.8056E+02          0.8806E+01          -.5000E+01
A1 21          GEYSR .4610E+030.9221E+02          0.9554E+01          -.5000E+01
A1 22          GEYSR .5257E+030.1051E+03          0.1034E+02          -.5000E+01
```

```
A1 23          GEYSR .5996E+030.1199E+03          0.1117E+02          -.5000E+01
A1 24          GEYSR .6830E+030.1366E+03          0.1205E+02          -.5000E+01
A1 25          GEYSR .7747E+030.1549E+03          0.1298E+02          -.5000E+01
A1 26          GEYSR .8794E+030.1759E+03          0.1395E+02          -.5000E+01
A1 27          GEYSR .9961E+030.1992E+03          0.1498E+02          -.5000E+01
A1 28          GEYSR .1126E+040.2252E+03          0.1607E+02          -.5000E+01
A1 29          GEYSR .1274E+040.2549E+03          0.1722E+02          -.5000E+01
A1 30          GEYSR .1437E+040.2874E+03          0.1843E+02          -.5000E+01
A1 31          GEYSR .1622E+040.3243E+03          0.1970E+02          -.5000E+01
A1 32          GEYSR .1828E+040.3656E+03          0.2105E+02          -.5000E+01
A1 33          GEYSR .2058E+040.4117E+03          0.2247E+02          -.5000E+01
A1 34          GEYSR .2315E+040.4629E+03          0.2397E+02          -.5000E+01
A1 35          GEYSR .2603E+040.5207E+03          0.2555E+02          -.5000E+01
A1 36          GEYSR .2925E+040.5851E+03          0.2721E+02          -.5000E+01
A1 37          GEYSR .3286E+040.6571E+03          0.2897E+02          -.5000E+01
A1 38          GEYSR .3686E+040.7371E+03          0.3082E+02          -.5000E+01
A1 39          GEYSR .4136E+040.8271E+03          0.3278E+02          -.5000E+01
A1 40          GEYSR .4639E+040.9278E+03          0.3484E+02          -.5000E+01
A1 41          GEYSR .5199E+040.1040E+04          0.3702E+02          -.5000E+01
A1 42          GEYSR .5823E+040.1165E+04          0.3932E+02          -.5000E+01
A1 43          GEYSR .6522E+040.1304E+04          0.4174E+02          -.5000E+01
A1 44          GEYSR .7300E+040.1460E+04          0.4429E+02          -.5000E+01
A1 45          GEYSR .8172E+040.1634E+04          0.4699E+02          -.5000E+01
A1 46          GEYSR .9140E+040.1828E+04          0.4983E+02          -.5000E+01
A1 47          GEYSR .1022E+050.2044E+04          0.5283E+02          -.5000E+01
A1 48          GEYSR .1143E+050.2285E+04          0.5600E+02          -.5000E+01
A1 49          GEYSR .1278E+050.2555E+04          0.5933E+02          -.5000E+01
A1 50          GEYSR .1427E+050.2854E+04          0.6285E+02          -.5000E+01
A1 51          GEYSR .1595E+050.3190E+04          0.6657E+02          -.5000E+01
A1 52          GEYSR .1781E+050.3562E+04          0.7048E+02          -.5000E+01
A1 53          GEYSR .1989E+050.3978E+04          0.7462E+02          -.5000E+01
A1 54          GEYSR .2221E+050.4442E+04          0.7898E+02          -.5000E+01
A1 55          GEYSR .2479E+050.4958E+04          0.8357E+02          -.5000E+01
A1 56          GEYSR .2767E+050.5535E+04          0.8843E+02          -.5000E+01
A1 57          GEYSR .3088E+050.6176E+04          0.9354E+02          -.5000E+01
A1 58          GEYSR .3445E+050.6891E+04          0.9894E+02          -.5000E+01
A1 59          GEYSR .3843E+050.7687E+04          0.1046E+03          -.5000E+01
A1 60          GEYSR .4287E+050.8574E+04          0.1106E+03          -.5000E+01
A1 61          GEYSR .4781E+050.9562E+04          0.1170E+03          -.5000E+01
A1 62          GEYSR .5332E+050.1066E+05          0.1237E+03          -.5000E+01
A1 63          GEYSR .5945E+050.1189E+05          0.1307E+03          -.5000E+01
A1 64          GEYSR .6629E+050.1326E+05          0.1382E+03          -.5000E+01
A1 65          GEYSR .7389E+050.1478E+05          0.1460E+03          -.5000E+01
A1 66          GEYSR .8237E+050.1647E+05          0.1543E+03          -.5000E+01
A1 67          GEYSR .9180E+050.1836E+05          0.1630E+03          -.5000E+01
A1 68          GEYSR .1023E+060.2046E+05          0.1722E+03          -.5000E+01
A1 69          GEYSR .1140E+060.2280E+05          0.1819E+03          -.5000E+01
A1 70          GEYSR .1271E+060.2541E+05          0.1922E+03          -.5000E+01
A1 71          GEYSR .1416E+060.2831E+05          0.2030E+03          -.5000E+01
A1 72          GEYSR .1577E+060.3154E+05          0.2144E+03          -.5000E+01
A1 73          GEYSR .1757E+060.3515E+05          0.2264E+03          -.5000E+01
A1 74          GEYSR .1957E+060.3915E+05          0.2391E+03          -.5000E+01
A1 75          GEYSR .2180E+060.4361E+05          0.2525E+03          -.5000E+01
A1 76          GEYSR .2429E+060.4858E+05          0.2666E+03          -.5000E+01
A1 77          GEYSR .2705E+060.5410E+05          0.2815E+03          -.5000E+01
A1 78          GEYSR .3013E+060.6026E+05          0.2972E+03          -.5000E+01
A1 79          GEYSR .3355E+060.6711E+05          0.3138E+03          -.5000E+01
A1 80          GEYSR .3737E+060.7474E+05          0.3313E+03          -.5000E+01
A1 81          GEYSR .4162E+060.8323E+05          0.3497E+03          -.5000E+01
A1 82          GEYSR .4634E+060.9268E+05          0.3692E+03          -.5000E+01
A1 83          GEYSR .5160E+060.1032E+06          0.3897E+03          -.5000E+01
A1 84          GEYSR .5746E+060.1149E+06          0.4114E+03          -.5000E+01
A1 85          GEYSR .6397E+060.1279E+06          0.4342E+03          -.5000E+01
A1 86          GEYSR .7123E+060.1425E+06          0.4583E+03          -.5000E+01
A1 87          GEYSR .7931E+060.1586E+06          0.4837E+03          -.5000E+01
A1 88          GEYSR .8830E+060.1766E+06          0.5105E+03          -.5000E+01
A1 89          GEYSR .9830E+060.1966E+06          0.5388E+03          -.5000E+01
A1 90          GEYSR .1094E+070.2189E+06          0.5686E+03          -.5000E+01
A1 91          GEYSR .1218E+070.2437E+06          0.6001E+03          -.5000E+01
A1 92          GEYSR .1356E+070.2713E+06          0.6333E+03          -.5000E+01
A1 93          GEYSR .1510E+070.3020E+06          0.6683E+03          -.5000E+01
A1 94          GEYSR .1681E+070.3361E+06          0.7053E+03          -.5000E+01
A1 95          GEYSR .1871E+070.3742E+06          0.7442E+03          -.5000E+01
A1 96          GEYSR .2083E+070.4165E+06          0.7853E+03          -.5000E+01
A1 97          GEYSR .2318E+070.4636E+06          0.8287E+03          -.5000E+01
A1 98          GEYSR .2580E+070.5161E+06          0.8745E+03          -.5000E+01
```

```
A1 99          GEYSR .2872E+070.5744E+06          0.9227E+03          -.5000E+01
A11 0          GEYSR .3214E+070.6427E+06          0.9737E+03          -.5000E+01

CONNE
A1  1A1  2                  10.1250E+000.1365E+000.1571E+02
A1  2A1  3                  10.1365E+000.1495E+000.3286E+02
A1  3A1  4                  10.1495E+000.1545E+000.5165E+02
A1  4A1  5                  10.1545E+000.1635E+000.7106E+02
A1  5A1  6                  10.1635E+000.1720E+000.9161E+02
A1  6A1  7                  10.1720E+000.1820E+000.1132E+03
A1  7A1  8                  10.1820E+000.1915E+000.1361E+03
A1  8A1  9                  10.1915E+000.2020E+000.1602E+03
A1  9A1 10                  10.2020E+000.2135E+000.1855E+03
A1 10A1 11                  10.2135E+000.2250E+000.2124E+03
A1 11A1 12                  10.2250E+000.2370E+000.2406E+03
A1 12A1 13                  10.2370E+000.2505E+000.2704E+03
A1 13A1 14                  10.2505E+000.2640E+000.3019E+03
A1 14A1 15                  10.2640E+000.2785E+000.3351E+03
A1 15A1 16                  10.2785E+000.2940E+000.3701E+03
A1 16A1 17                  10.2940E+000.3100E+000.4070E+03
A1 17A1 18                  10.3100E+000.3270E+000.4460E+03
A1 18A1 19                  10.3270E+000.3450E+000.4871E+03
A1 19A1 20                  10.3450E+000.3640E+000.5304E+03
A1 20A1 21                  10.3640E+000.3840E+000.5762E+03
A1 21A1 22                  10.3840E+000.4045E+000.6244E+03
A1 22A1 23                  10.4045E+000.4270E+000.6753E+03
A1 23A1 24                  10.4270E+000.4510E+000.7289E+03
A1 24A1 25                  10.4510E+000.4750E+000.7856E+03
A1 25A1 26                  10.4750E+000.5015E+000.8453E+03
A1 26A1 27                  10.5015E+000.5290E+000.9083E+03
A1 27A1 28                  10.5290E+000.5575E+000.9748E+03
A1 28A1 29                  10.5575E+000.5890E+000.1045E+04
A1 29A1 30                  10.5890E+000.6205E+000.1119E+04
A1 30A1 31                  10.6205E+000.6550E+000.1197E+04
A1 31A1 32                  10.6550E+000.6910E+000.1279E+04
A1 32A1 33                  10.6910E+000.7290E+000.1366E+04
A1 33A1 34                  10.7290E+000.7685E+000.1458E+04
A1 34A1 35                  10.7685E+000.8110E+000.1554E+04
A1 35A1 36                  10.8110E+000.8555E+000.1656E+04
A1 36A1 37                  10.8555E+000.9025E+000.1764E+04
A1 37A1 38                  10.9025E+000.9515E+000.1877E+04
A1 38A1 39                  10.9515E+000.1004E+010.1997E+04
A1 39A1 40                  10.1004E+010.1059E+010.2123E+04
A1 40A1 41                  10.1059E+010.1117E+010.2256E+04
A1 41A1 42                  10.1117E+010.1178E+010.2396E+04
A1 42A1 43                  10.1178E+010.1244E+010.2544E+04
A1 43A1 44                  10.1244E+010.1311E+010.2701E+04
A1 44A1 45                  10.1311E+010.1384E+010.2865E+04
A1 45A1 46                  10.1384E+010.1460E+010.3039E+04
A1 46A1 47                  10.1460E+010.1540E+010.3223E+04
A1 47A1 48                  10.1540E+010.1624E+010.3416E+04
A1 48A1 49                  10.1624E+010.1713E+010.3620E+04
A1 49A1 50                  10.1713E+010.1807E+010.3836E+04
A1 50A1 51                  10.1807E+010.1907E+010.4063E+04
A1 51A1 52                  10.1907E+010.2011E+010.4302E+04
A1 52A1 53                  10.2011E+010.2121E+010.4555E+04
A1 53A1 54                  10.2121E+010.2238E+010.4822E+04
A1 54A1 55                  10.2238E+010.2361E+010.5103E+04
A1 55A1 56                  10.2361E+010.2490E+010.5399E+04
A1 56A1 57                  10.2490E+010.2627E+010.5712E+04
A1 57A1 58                  10.2627E+010.2771E+010.6043E+04
A1 58A1 59                  10.2771E+010.2923E+010.6391E+04
A1 59A1 60                  10.2923E+010.3083E+010.6758E+04
A1 60A1 61                  10.3083E+010.3253E+010.7146E+04
A1 61A1 62                  10.3253E+010.3431E+010.7554E+04
A1 62A1 63                  10.3431E+010.3619E+010.7985E+04
A1 63A1 64                  10.3619E+010.3819E+010.8440E+04
A1 64A1 65                  10.3819E+010.4028E+010.8920E+04
A1 65A1 66                  10.4028E+010.4249E+010.9426E+04
A1 66A1 67                  10.4249E+010.4482E+010.9960E+04
A1 67A1 68                  10.4482E+010.4728E+010.1052E+05
A1 68A1 69                  10.4728E+010.4987E+010.1112E+05
A1 69A1 70                  10.4987E+010.5261E+010.1174E+05
A1 70A1 71                  10.5261E+010.5550E+010.1241E+05
A1 71A1 72                  10.5550E+010.5854E+010.1310E+05
A1 72A1 73                  10.5854E+010.6176E+010.1384E+05
```

```
A1 73A1 74                  10.6176E+010.6514E+010.1461E+05
A1 74A1 75                  10.6514E+010.6872E+010.1543E+05
A1 75A1 76                  10.6872E+010.7250E+010.1630E+05
A1 76A1 77                  10.7250E+010.7647E+010.1721E+05
A1 77A1 78                  10.7647E+010.8066E+010.1817E+05
A1 78A1 79                  10.8066E+010.8509E+010.1918E+05
A1 79A1 80                  10.8509E+010.8976E+010.2025E+05
A1 80A1 81                  10.8976E+010.9469E+010.2138E+05
A1 81A1 82                  10.9469E+010.9989E+010.2257E+05
A1 82A1 83                  10.9989E+010.1054E+020.2382E+05
A1 83A1 84                  10.1054E+020.1112E+020.2515E+05
A1 84A1 85                  10.1112E+020.1172E+020.2655E+05
A1 85A1 86                  10.1172E+020.1237E+020.2802E+05
A1 86A1 87                  10.1237E+020.1305E+020.2957E+05
A1 87A1 88                  10.1305E+020.1376E+020.3121E+05
A1 88A1 89                  10.1376E+020.1452E+020.3294E+05
A1 89A1 90                  10.1452E+020.1531E+020.3477E+05
A1 90A1 91                  10.1531E+020.1616E+020.3669E+05
A1 91A1 92                  10.1616E+020.1704E+020.3872E+05
A1 92A1 93                  10.1704E+020.1798E+020.4086E+05
A1 93A1 94                  10.1798E+020.1896E+020.4312E+05
A1 94A1 95                  10.1896E+020.2000E+020.4551E+05
A1 95A1 96                  10.2000E+020.2110E+020.4802E+05
A1 96A1 97                  10.2110E+020.2226E+020.5067E+05
A1 97A1 98                  10.2226E+020.2348E+020.5347E+05
A1 98A1 99                  10.2348E+020.2477E+020.5642E+05
A1 99A11 0                  10.2477E+020.2626E+020.5953E+05

GENER----1----*----2----*----3----*----4----*----5----*----6----*----7----*----8
A1  1                           DELV    1.0E-13  1378.6E3      10.0

ENDCY----1----*----2----*----3----*----4----*----5----*----6----*----7----*----8

#Linear RP / Leverett CP ITOUGH2 input file
> PARAMETERS
  >> ABSOLUTE permeability
     >>> MATERIAL: GEYSR
         >>>> LOGARITHM
         >>>> INDEX: 1
         >>>> DEVIATION: 0.2
         <<<<
     <<<

  >> RELATIVE permeability function
     >>> MATERIAL: GEYSR
         >>>> PARAMETER No.: 1
         >>>> ANNOTATION   : Slr (RP)
         >>>> standard DEVIATION : 0.05
         >>>> max STEP : 0.05
         >>>> PERTURB : -0.001
         >>>> estimate VALUE
         >>>> RANGE  : 0.00 0.50
         <<<<
     >>> MATERIAL: GEYSR
         >>>> PARAMETER No.: 2
         >>>> ANNOTATION   : Sgr
         >>>> standard DEVIATION : 0.05
         >>>> max STEP : 0.05
         >>>> PERTURB : -0.001
         >>>> estimate VALUE
         >>>> RANGE  : 0.00 0.50
         <<<<
     >>> MATERIAL: GEYSR
         >>>> PARAMETER No.: 3
         >>>> ANNOTATION   : Sls
         >>>> standard DEVIATION : 0.05
         >>>> max STEP : 0.05
         >>>> PERTURB : -0.001
         >>>> estimate VALUE
         >>>> RANGE  : 0.51 1.00
         <<<<
     >>> MATERIAL: GEYSR
         >>>> PARAMETER No.: 4
         >>>> ANNOTATION   : Sgs
         >>>> standard DEVIATION : 0.05
         >>>> max STEP : 0.02
```

```
          >>>> estimate VALUE
          >>>> RANGE  : 0.51 1.00
          >>>> PERTURB : -0.001
          <<<<

       <<<

    >> parameters of the CAPILLARY pressure function
       >>> MATERIAL: GEYSR
          >>>> PARAMETER No.:  1
          >>>> ANNOTATION  :  Po
          >>>> standard DEVIATION : 0.50
          >>>> max STEP: 0.2
          <<<<
       >>> MATERIAL: GEYSR
          >>>> PARAMETER No.: 2
          >>>> ANNOTATION   : Slr
          >>>> standard DEVIATION : 0.05
          >>>> max STEP : 0.05
          >>>> PERTURB : -0.001
          >>>> estimate VALUE
          >>>> RANGE  : 0.00 1.00
          <<<<
       <<<
    <<

  > OBSERVATIONS
    >> : 100 LOGARITHMICALLY spaced TIMES in SECONDS between
       1.0   1.0E10

    >> TEMPERATURE
       >>> ELEMENT: A1__1
          >>>> ANNOTATION: T1
          >>>> COLUMNS: 1 2
          >>>> PICK : 10
          >>>> NO DATA
          >>>> DEVIATION: 2.0 deg C
          <<<<

       >>> ELEMENT: A1_87
          >>>> ANNOTATION: T2
          >>>> COLUMNS: 1 3
          >>>> PICK : 10
          >>>> NO DATA
          >>>> DEVIATION: 1.0 deg C
          <<<<

       >>> ELEMENT: A11_0
          >>>> ANNOTATION: T3
          >>>> COLUMNS: 1 4
          >>>> PICK : 10
          >>>> NO DATA
          >>>> DEVIATION: 1.0 deg C
          <<<<
       <<<

    >> PRESSURE
       >>> ELEMENT: A1__1
          >>>> ANNOTATION: P1
          >>>> COLUMNS: 1 2
          >>>> FACTOR: 1E6
          >>>> PICK : 10
          >>>> NO DATA
          <<<<

       >>> ELEMENT: A1_87
          >>>> ANNOTATION: P2
          >>>> COLUMNS: 1 3
          >>>> FACTOR: 1E6
          >>>> PICK : 10
          >>>> NO DATA
          <<<<

       >>> ELEMENT: A11_0
          >>>> ANNOTATION: P3
          >>>> COLUMNS: 1 4
```

```
        >>>> FACTOR: 1E6
        >>>> PICK : 10
        >>>> NO DATA
        <<<<
    <<<

  >> LIQUID SATURATION
    >>> ELEMENT: A1__1
        >>>> ANNOTATION: Sw1
        >>>> COLUMNS: 1 2
        >>>> NO DATA
        >>>> DEVIATION: 0.02
        <<<<

    >>> ELEMENT: A1_87
        >>>> ANNOTATION: Sw2
        >>>> COLUMNS: 1 3
        >>>> NO DATA
        >>>> DEVIATION: 0.01
        <<<<

    >>> ELEMENT: A11_0
        >>>> ANNOTATION: Sw3
        >>>> COLUMNS: 1 4
        >>>> NO DATA
        >>>> DEVIATION: 0.01
        <<<<

    <<<

  >> VAPOR GENERATION

    >>> SINK: A1__1
        >>>> ANNOTATION: Steam
        >>>> NO DATA
        <<<<
    <<<

  >> LIQUID GENERATION

    >>> SINK: A1__1
        >>>> ANNOTATION: Water
        >>>> NO DATA
        <<<<
    <<<

  >> ENTHALPY

    >>> SINK: A1__1
        >>>> ANNOTATION: Enthalpy
        >>>> FACTOR: 1000.0
        >>>> NO DATA
        <<<<
    <<<

  >> CUMULATIVE VAPOR

    >>> SINK: A1__1
        >>>> ANNOTATION: SteamCum
        >>>> NO DATA
        <<<<
    <<<


  >> CUMULATIVE LIQUID

    >>> SINK: A1__1
        >>>> ANNOTATION: WaterCum
        >>>> NO DATA
        <<<<
    <<<

  <<

> COMPUTATION
  >> STOPPING criteria
```

```
     >>> IGNORE WARNINGS
     >>> max. no. of ITERATIONS: 20
     >>> CONSECUTIVE: 100
     >>> INCOMPLETE: 20
     >>> LEVENBERG: 0.1
     >>> STEP : 1.0
     <<<
  >> JACOBIAN
     >>> FORWARD: 8
     >>> PERTURB: 0.01
     <<<
  >> OPTIONS
#    >>> QUADRATIC-LINEAR: 3.0
#    >>> perform a SENSITIVITY analysis
     >>> DIRECT
     <<<
  >> OUTPUT
     >>> PLOTFILE: COLUMNS
     >>> DAYS
     >>> generate file with CHARACTERISTIC curves
     <<<
  <<
<
```